UNIVERSITY OF LONDON
IMPERIAL COLLEGE OF SCIENCE AND TECHNOLOGY
Department of Electrical Engineering

THE EFFECT OF LOAD CHARACTERISTICS ON MULTI-MACHINE ELECTRIC POWER SYSTEM DYNAMIC STABILITY

by

Daniel Olguin Salinas
Ing. Elec., M.en C. en Ing. Elec.
(Instituto Politecnico Nacional, Mexico City)

Thesis submitted for the degree of
Doctor of Philosophy and for the
Diploma of Imperial College in the
Faculty of Engineering.

London
June 1979

To my beloved wife and daughter,

Amparo and Marisol,

(pnav)

ABSTRACT

The small perturbation analysis of interconnected systems using eigenvalue methods and multi-state feedback controllers design in order to stabilize the generators has been calculated without simplifying assumptions. A method of general multi-machine analysis considering the effect of load characteristics has been devised.

It is shown here in a number of studies of single-machine infinite busbar and multi-machine systems that the effect of load characteristics is considerable. Dynamic stability of a multi-machine system when the effect of load characteristics is included has been analysed. A new approach for obtaining the state space formulation of the linearized system equations is given. This is convenient for the evaluation of the open loop system performance and also enables the design of a closed loop multi-input controller. The analysis is realised by checking the eigenvalues of the free response system in order to determine the asymptotic stability of the system when different load characteristics are included.

Modal control theory is used to improve the steady-state performance of the generators by the addition of multiple feedback paths. The critical eigenvalues are moved towards the left in the complex plane, sequentially in groups using the dominant input for each group. It is shown that the nature of the load can change the design of the controllers. The effect of network representation has also been explored.

In a multi-machine system a local modal controller is derived for each machine from the global control design, where feedback to each machine comes from its individual state variables.

ACKNOWLEDGEMENTS

The work in this thesis was carried out under the supervision of Dr. D.C. Macdonald, B.Sc. (Eng.), Ph.D., M.I.E.E., C. Eng., Lecturer in Electrical Engineering Department, Imperial College of Science and Technology, London. I wish to express my sincere gratitude to Dr. Macdonald for his helpful guidance, constant encouragement and keen interest during the preparation and completion of this project.

I also wish to express my sincere thanks to Mr. Waldyr Mauricio, Light-Servicos de Electricidade S.A., Sao Paulo, Brazil for his assistance during the early stages of this project.

I wish to acknowledge the valuable discussions I have had with the late Dr. L. Angerer throughout this work.

I would like to express my appreciation to my colleagues of the Power System Laboratory for their advice and assistance, in particular Dr. E. Arriola, Dr. C.K. Gharban, Dr. S.A. Molina, Dr. A. Nava and Mr. E. Vaahedi.

I wish to express my gratitude to Consejo Nacional de Ciencia y Tecnologia (CONACYT) and Instituto Politecnico Nacional (ESIME) for the leave permit and financial support which made this work possible.

Lastly, I would like to express my gratitude to Mrs Shelagh Murdock who patiently typed the manuscript.

TABLE OF CONTENTS

NOTATIONS

v_d, v_q, i_d, i_q	direct and quadrature axis voltages and currents of a synchronous machine
$V = \|V\| \angle\delta$	busbar voltage
i_{fd}, i_{kd}, i_{kq}	rotor circuit currents of a synchronous machine
P, Q	active and reactive powers
G, B	conductance and susceptance
r_s, r_{fd}, r_{kd}, r_{kq}	stator and rotor circuit resistances of a synchronous machine
X_{ffd}, X_{afd}, X_{fkd}, X_d, X_{akd}, X_{kkd}, X_{akq}, X_{kkq}	coupling and self reactances of a synchronous machine
ω_o	rated angular frequency, electrical radians per second
ω_s	instantaneous angular frequency of bus voltage, electrical radians per second
ω_r	instantaneous angular frequency of machine rotor, electrical radians per second
$n = \omega_r/\omega_o$	per unit instantaneous angular frequency
δ_r	rotor angle of synchronous machine, with respect to infinite busbar, or reference machine
H	machine inertia constant, kW.sec/kVA
$M = 2H/\omega_o$	moment of inertia, sec^2/elec.radian
$T_m = 2H$	inertia time constant, seconds
$p = d/dt$	differential operator
v_{sd}, v_{sq}, i_{sd}, i_{sq}	direct and quadrature stator circuit voltages and currents of an induction machine
i_{rd}, i_{rq}	rotor circuit currents of an induction machine
R_s	stator circuit resistance of an induction motor
R_r	rotor circuit resistance of an induction machine
X_m, X_s, X_r	coupling and self reactances of an induction machine

X_{ℓ_1}, X_{ℓ_2}	stator and rotor leakage reactances of induction machine
$S = \frac{\omega_s - \omega_r}{\omega_s}$	induction motor slip
S_{cr}	induction motor critical slip (corresponding to maximum torque)
T_g	air gap torque of a synchronous or an induction machine
T_{mech}	mechanical torque
$\hat{T}_{max}$	pull-out torque or maximum torque
K_r	voltage regulator gain
T_{rg}	excitation system time constant, seconds
$E_{fd} = X_{afd} v_{fd} / r_{fd}$	air gap line open circuit voltage; excitation voltage
A_t	turbine gain
B	equilibrium real gate position
C	input signal to governor servo-valve
D_{nom}	turbine damping coefficient
g	per unit real gate position deviation
h	per unit head deviation
Q_g	servo-valve gain of governor
W_s	relative derivative gain of governor
T_R	dashpot time constant, seconds
T_w	water inertia time constant, seconds
δ_t	governor temporary droop
δ_p	governor permanent droop
g_1	real no-load gate position
D	instantaneous turbine damping coefficient
$X_{\ell_{fd}}$	field winding leakage reactance
X_{ℓ_a}, $X_{\ell_{kd}}$, $X_{\ell_{kq}}$	leakage reactances of a synchronous generator
X_t	transmission line reactance

r_t	transmission line resistance
V_B	voltage magnitude at infinite bus bar
V_{qB}	quadrature axis infinite bus bar voltage
V_{qd}	direct axis infinite bus bar voltage
$X_{md}=X_{afd}=X_{akd}=X_{fkd}$	direct axis magnetizing reactance of a synchronous machine
$X_{mq}=X_{akq}$	quadrature axis magnetizing reactance of a synchronous machine
$[A]$	system matrix
$[B]$	control input matrix
$u(t)$	control vector
$y(t)$	state vector
$\dot{y}(t)$	time derivative of $y(t)$
Δ	prefix denoting a linearized variable
$\lambda_i = \alpha_i + j\beta_i$	eigenvalues, $i = 1,2,\ldots,n$

The remaining variables are defined where they are used.

CHAPTER 1

INTRODUCTION

1.1 GENERAL

Since the industrial revolution man's consumption of energy has increased steadily. A major proportion of the power requirements of modern society is supplied in the form of electrical energy. Industrially developed societies need an ever-increasing supply of electrical power. Very complex power systems have been built to satisfy this increasing demand. The trend in electric power production is toward an interconnected network of transmission lines linking generators and loads into large integrated systems. This vast enterprise for supplying electrical energy presents many engineering problems that provide the engineer with a variety of challenges. The planning, construction and operation of such systems is exceedingly complex. To be able to predict the performance of such systems, the engineer is forced to seek the most powerful tools of analysis and synthesis. Successful operation of a power system depends largely on the engineer's ability to provide reliable and uninterrupted service to the loads. The reliability of the power supply implies much more than merely power being available. Ideally, the loads must be fed at constant voltage and frequency at all times. In practical terms this means that both voltage and frequency must be held within close tolerances so that the consumer's equipment may operate satisfactorily, and while it is frequently convenient to talk about the power system in the steady state, such a state never exists in the true sense.

Random changes in loads are taking place at all times, with subsequent adjustments of generation. Furthermore, major changes do take place, e.g. a fault on the network, failure of a piece of equipment, sudden application of a major load, or loss of a line or generating unit. It might be tempting to say that successful operation requires only that the new state be a stable state. Unfortunately, synchronism is frequently lost in the transition period from one equilibrium state to another, or growing oscillations may occur over a transmission line, eventually leading to its overload and tripping. These problems must be studied by the power system engineer and fall in the area of power system stability.

1.2 POWER SYSTEM STABILITY

Power system stability is normally considered in two forms, dynamic and transient stability. Dynamic stability implies that if the system is disturbed in a minor way, such as a slight missmatch of load and generation, it immediately returns to a steady operating point near to the original, restoring "forces" existing to maintain a steady operating condition. Dynamic instability implies that any operating condition is not maintained, any slight disturbance causing mounting oscillation, or a steady drift occurring, each of which results eventually in pole slipping.

A system may be dynamically stable but unable to withstand a major disturbance, and is then considered to be transiently unstable. Transient stability is a relative quality (unlike dynamic stability, which is absolute), for all synchronous machines will lose

synchronism if subjected to a long enough fault. The ability to withstand a fault of given duration is expressed as the critical fault clearance time (c.f.c.t.). If a fault longer than the c.f.c.t. occurs, the generator will slip poles and is then normally lost to the system, being tripped to prevent the associated large swings of voltage, current and power.

Any system operating condition must be dynamically stable and have an adequate transient stability margin. For many years attention was directed at the latter but with the growth of power systems and some unfortunate occurrences (islanding) it has been realised that both require careful consideration.

The number of power system components included in any study and the complexity of the mathematical description is variable, but in general differential equations are used to describe the various components. Study of the dynamic behaviour of the system depends upon the nature of these differential equations. The system equations for transient stability are usually nonlinear. Here the system is described by a large set of coupled nonlinear differential equations. In considering the response to a particular fault or disturbance, a solution of the nonlinear differential equations is obtained by numerical methods with the aid of digital computers. When the dynamic stability of the system is investigated it is convenient to assume that the disturbances causing the changes disappear and the motion of the system is then free. Stability is assured if the system returns to its original state. If the system equations are linear or have been linearized, the techniques of linear system analysis may be used to study the dynamic behaviour. The most common

method is to simulate each component by its function transfer equation. The system performance may then be analyzed by such methods as root-locus plots, frequency domain analysis, Nyquist criterion and Routh's criterion. These methods have been frequently used in studies of small systems. For larger systems the state space model is more common, stability characteristics being determined by examining the eigenvalues of the $[A]$ matrix, where $[A]$ is defined by the equation:

$$\dot{y}(t) = [A]\, y(t) + [B]\, u(t)$$

Up to the present, the efforts of power system analysts engaged in the study of the dynamics of power systems have been mainly devoted to a better understanding of the modelling of generators, and, in more recent times, to seeking reliable and accurate data for use in generator models. The performance of the loads in power systems, which are equal in magnitude to the generation, has received scant attention. Recently this situation has changed, and much more attention has been devoted to load behaviour as a function of both voltage and frequency variation. There are several reasons for this:

1. There is a need to improve the quantitative accuracy of system simulation.

2. Digital computers are almost universally used and it has become possible to employ more refined representations of all the elements.

3. Methods of control are becoming more complicated and their success depends on a full evaluation of the stability of the system, including the contribution of the loads.

There are two aspects to the load problem. One is the examination of system data to determine the most appropriate model to use in subsequent studies; the other, the subject of this thesis, is the examination of the effect of a range of models on system stability.

The primary aim of this thesis is to devise a method of digital computation by which the dynamic stability of a multimachine power system including the effect of load characteristics may be calculated accurately and reliably.

In addition, the effect of load characteristics in the design of feedback controllers in a single machine and in a multimachine system have been studied.

1.3 REVIEW OF PREVIOUS WORK

The effect of load characteristics is only one aspect of the current interest in dynamic stability calculations. Because developments have already occurred in the representation and analysis of generation and transmission systems, attention is now being focussed on the adequacy of load representation and elaborate load models have been included in analysis programs.

A number of studies have been made of the contribution of different forms of load to stability (8, 10, 11, 12, 19, 23). Brereton et al.[8] considered that it is of the utmost importance in transient stability studies to represent the loads not just as shunt impedances but in a more accurate manner. Particular attention has

been paid to the load inertia of induction machines. Several methods of simulating the behaviour of induction motors have been presented. The system studied has usually been a single motor connected to an infinite busbar. Kalsi[10,11] gave a method for obtaining the fault contribution made by induction motors in a system. His study included the transient stability of a composite system including a large induction motor and a synchronous generator. The deep bar effect in the squirrel cage motors was simulated by two equivalent rotor windings. Alford[12] proposed a common method of representation for synchronous and asynchronous machines; practical tests were also carried out on a model system. The accurate representation of induction motor loads located close to the synchronous generator was shown to be important in a stability study. Dandeno and Kundur[19] presented a novel simulation technique to achieve a direct or non-iterative solution of algebraic equations while retaining the ability to represent loads so that the real and reactive power components at each bus bar could vary as any power of the voltage magnitude. Results of computer tests on a complex multi-machine system demonstrating the importance of load modelling were presented. Shanckle et al.[23] have presented a method for determining the transient stability of a system including synchronous and induction machines.

The area of small signal stability did not receive much attention until recently, although Crary[27] pointed out the importance of the load characteristics on the composite system performance as early as 1934. In his calculations of synchronising power coefficients he included the effect of composite loads and induction machines. Heffron[26] presented a numerical study that shows the effect of shunt loads on the steady state stability limit. He concluded that shunt

loads have a stabilizing effect on the system except when the load is heavy. In the past decade a number of workers have continued this study.

Mauricio and Semlyen[14] have shown that the dynamic stability limit of a power system is affected significantly by the nature of the system load. They showed that the dynamic behaviour of loads can have a decisive influence on the stability limit of a power system. Alden and Zein El-Din[34] showed that the stability calculated for a test system was dependent on the load model, load being modelled as several non-linear functions of voltages. Rao and Tripathy[35] concluded that the gain associated with the speed stabilizing signal in the excitation system of a generator should be set to match the power-voltage characteristics of the load to maximise the damping effect. Subramanian and Berg[36] discussed the effects of electric load on optimal excitation control in a power system. They concluded that the state feedback gains for optimal excitation control vary significantly with the type of load present in the system. Several authors have represented experimental results which have been compared with calculated values in order to find the most appropriate load model[37-41]. Induction motor representation and behaviour has been considered in detail[42-45] including the equivalence of induction motors[46]. A summary of work in this area is given in reference 18.

1.4 CONTENTS OF THE THESIS

In Chapter 2 the effect of load characteristics on the assessment of dynamic stability of a single machine system with the load at an intermediate bus-bar is studied. The load is assumed to be static with exponential power-voltage dependence, dynamic in nature or a combined load composed of a constant impedance and induction motors. The equations for the system are linearized about an operating point, the computer being used to reduce the whole set of differential and algebraic equations to the state space form - $\dot{y}(t) = [A]\, y(t)$; and the eigenvalues of $[A]$ are obtained. The stability limit is obtained as the eigenvalues become positive. Results are compared for each load representation. When there are many eigenvalues, the results are not easy to interpret. A method of finding the rates of change or sensitivities of the critical eigenvalues is applied and this analysis can lead to the identification of some of the sources of oscillation. State variable reduction techniques to identify states or loops associated with each oscillatory mode have also been studied.

In Chapter 3 a digital simulation of the small signal dynamics model of an arbitrary number of interconnected power generating units including the effect of load characteristics is presented in state space form. Load is represented in two ways: as a static non-linear form, being dependent on voltage, and as a combined load. Sparsity techniques were used to minimize the computer storage requirements. The machine model is 11^{th} order, a.v.r. and speed governor equations being included. The analysis is based on calculating the eigenvalues of the characteristic matrix in order to to determine the asymptotic stability of the system.

In Chapter 4, modal control theory has been applied to the design of a controller with linear feedback for a single machine-infinite bus-bar system which represents a pumped storage plant. The effect of different load characteristics on the design of the feedback controller has been studied, load being added at the machine bus-bar in a non-linear passive form and as a combined load. The effect of representing the network of this system in different ways on the design of the feedback controller has also been explored. The eigenvalues of the system are relocated to satisfactory positions during the design process. It is well known that it is possible to achieve any closed loop eigenvalue if the open loop is controllable. Here it has only been found necessary to re-locate the critical eigenvalues.

Lastly, in Chapter 5 a study of the effect of load characteristics in the design of feedback controllers for a multi-machine system is presented. Global and local modal controllers were designed and their performance was compared. Local control is derived from the global controller by disconnecting the feedback paths into a machine from the state variables that come from other machines.

1.5 THE CONTRIBUTION OF THE THESIS

It is thought that the original contributions of the thesis are:

(i) Comparison between two methods for assessing the dynamic stability limits and identification of all the eigenvalues of a power system by systematically isolating the state variables. Thus the modes of oscillation are fully understood.

(ii) A systematic formulation for the dynamic stability of multi-machine power systems in order to study the interaction between machines, including the effect of different load representation, which is developed and implemented in a digital simulation.

(iii) An assessment of the importance of load characteristics and the transient network terms in the design of feedback controllers in power systems.

(iv) A method for the design of a local controller for use in multi-machine models. The local controller is obtained by removing inter-machine feedback paths. Where this caused instability it was found that one path between machines could be used to give satisfactory performance.

CHAPTER 2

THE EFFECT OF LOAD CHARACTERISTICS IN SINGLE MACHINE SYSTEM ANALYSIS

2.1 INTRODUCTION

Several papers contain the analysis of dynamic stability of a power system including the effect of load characteristics[14,26,27,34,35,36]. Here a single-machine infinite busbar system has been considered with an intermediate load bus-bar, as shown in Figure 2.1. The method is largely that of Mauricio and Semlyen[14].

The conditions for each operating point are determined by a load flow analysis in polar form using the method of Arriola[15]. The equations of the system are linearised about the operating point and obtained in the form:

$$\dot{y}(t) = [A]\, y(t)$$

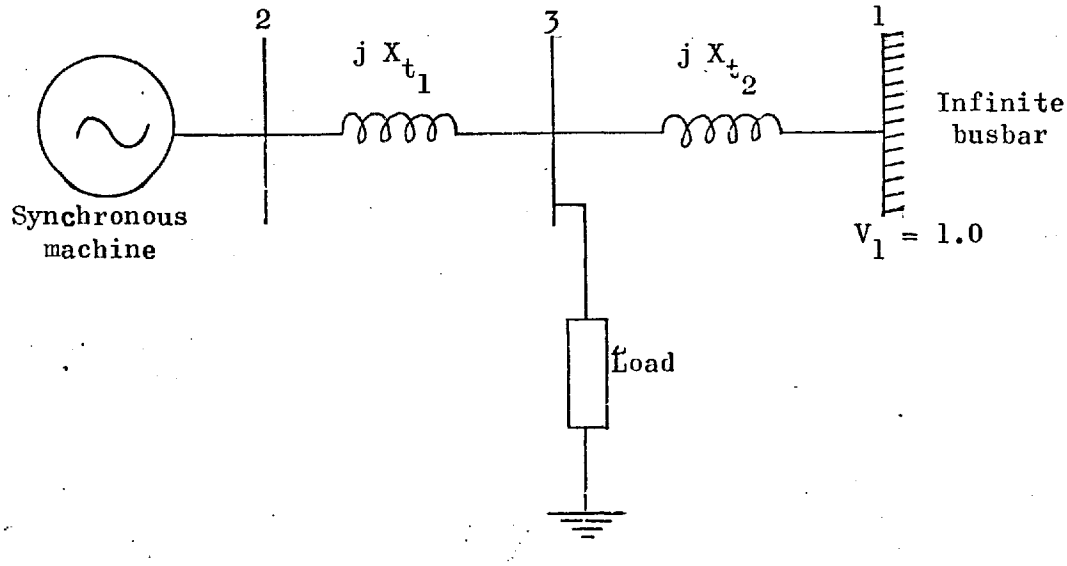

Figure 2.1 Single-machine infinite busbar system.

The dynamic stability is assessed by considering the eigenvalues of $[A]$, stability being lost when any eigenvalue has a positive real part. The boundaries to stable operation of the system are found by considering a succession of operating points. The effect of load in different representations[14,38,39] has been explored. Two generator AVRs have been considered, the generator being a hydroelectric machine.

Sensitivity analysis of the eigenvalues with respect to system parameters and a state variable reduction technique to identify the states and paths associated with each oscillating mode have been used.

2.2 METHOD OF ANALYSIS

Every stability study requires a load flow calculation in order to determine the equilibrium point about which stability is to be investigated. The Newton-Raphson method may be used to obtain load flow very efficiently. In the iterative solution the method uses the linearized power flow equations (2.1) which may also represent the network in a small-signal stability study:

$$\begin{bmatrix} \Delta P \\ \Delta Q \end{bmatrix} = \begin{bmatrix} J_1 & J_2 \\ J_3 & J_4 \end{bmatrix} \begin{bmatrix} \Delta \delta \\ \Delta V \end{bmatrix} \qquad (2.1)$$

The synchronous machine representation, described in detail in Section 2.2.1, is referred to a d.q. frame fixed to the machine rotor and for which the terminal quantities are v_d, V_q, i_d, i_q.

However, the network is represented on the basis of a steady state representation and this assumption implies that the transient components in the network are ignored. Attention is concentrated on the steady state behaviour of the network in a polar frame of reference, rather than the rectangular DQ frame adopted in several works[3,5,29]. In this polar frame the terminal (bus) quantities are P, Q, δ, V. This also eases the representation of many types of loads whose behaviour is defined by relations of active and reactive power as functions of voltage.

In order to investigate how the load characteristics affect the system stability, several types of loads have been considered in the computations, and the stability limit has been determined for each.

2.2.1 Description of Synchronous Machine

A complete description of the dynamic behaviour of the synchronous machine requires consideration of its electrical and mechanical characteristics as well as the associated control systems. Park's model describing the dynamic characteristics of a synchronous machine in per-unit[3,5,47,63], with the sign convention for currents adopted by the IEEE Rotating Machinery Committee[13], is given by the following equations. In the per-unit system, each voltage, flux, current and impedance is expressed as the ratio of its actual value to a selected base value. The equations are:

for the direct axis flux linkages:

$$\psi_{fd} = X_{ffd} i_{fd} + X_{afd} i_d + X_{fkd} i_{kd} \tag{2.2}$$

$$\psi_d = X_{afd} i_{fd} + X_d i_d + X_{akd} i_{kd} \tag{2.3}$$

$$\psi_{kd} = X_{fkd} i_{fd} + X_{akd} i_d + X_{kkd} i_{kd} \tag{2.4}$$

for the quadrature axis flux linkages:

$$\psi_q = X_q i_q + X_{akq} i_{kq} \tag{2.5}$$

$$\psi_{kq} = X_{akq} i_q + X_{kkq} i_{kq} \tag{2.6}$$

and the direct axis voltages:

$$v_{fd} = r_{fd} i_{fd} + \frac{1}{\omega_o} p \psi_{fd} \tag{2.7}$$

The exciter voltage referred to the armature circuit is defined[4] by:

$$E_{fd} = \frac{X_{afd}}{r_{fd}} v_{fd} \tag{2.8}$$

Then the field circuit equation can be written as:

$$\frac{r_{fd}}{X_{afd}} E_{fd} = r_{fd} i_{fd} + \frac{1}{\omega_o} p \psi_{fd} \tag{2.9}$$

$$v_d = - \frac{1}{\omega_o} p \psi_d - n \psi_q - r_s i_d \tag{2.10}$$

$$0 = \frac{1}{\omega_o} p \psi_{kd} + r_{kd} i_{kd} \tag{2.11}$$

The quadrature axis voltages are:

$$v_q = -\frac{1}{\omega_o} p\psi_q + n\psi_d - r_s i_q \tag{2.12}$$

$$0 = \frac{1}{\omega_o} p\psi_{kq} + r_{kq} i_{kq} \tag{2.13}$$

These equations have been derived neglecting the effects of saturation and assuming that all p.u. mutual inductances between rotor and stator circuits in each axis are equal to one another. On this basis, the following relations between self-mutual and leakage reactances pertain:

$$X_{ffd} = X_{md} + X_{\ell fd} \tag{2.14}$$

$$X_d = X_{md} + X_{\ell a} \tag{2.15}$$

$$X_{kkd} = X_{md} + X_{\ell kd} \tag{2.16}$$

$$X_q = X_{mq} + X_{\ell a} \tag{2.17}$$

$$X_{kkq} = X_{mq} + X_{\ell kq} \tag{2.18}$$

In order to complete the description of the synchronous machine, the following equations of motion are necessary:

$$T_m pn = T_{mech} - T_g \tag{2.19}$$

$$p\delta_r = \omega_o n \tag{2.20}$$

The air gap torque is given by:

$$T_g = \psi_d i_q - \psi_q i_d \tag{2.21}$$

A widely used model for the automatic voltage regulator[1,2,3,14] is given by the single delay equation:

$$E_{fd} = \frac{K_r}{1 + T_E p} (V_{ref} - V_t) \qquad (2.22)$$

The conventional dashpot hydrospeed governor is represented in the following equations for the turbine, the governor, the gate servomotor and the water column:

$$T_{mech} = (A_t B + A_t g - Dn)(1 + h)^{3/2} - A_t B \qquad (2.23)$$

$$pC = - pn - \delta_t pg - \frac{1}{T_R}(C - n) \qquad (2.24)$$

$$pg = Q_g(C - \delta p\, g - W_s pn) \qquad (2.25)$$

$$ph = - 2pg - \frac{2}{T_w} h \qquad (2.26)$$

These equations are similar to those used in other papers[4,5,14]. Any other models for the voltage regulator and speed governor could be easily introduced.

2.2.2 Transformation Equations

A set of transformation equations is necessary in order to establish the interconnection between the machine dq frame and the network polar frame. The active and reactive powers at the machine terminals are referred to the dq frame fixed to the machine rotor. In order to relate v_d, v_q, i_d, i_q to the polar network frame the angles in the phasor diagram shown in Figure 2.2 have to be taken into account.

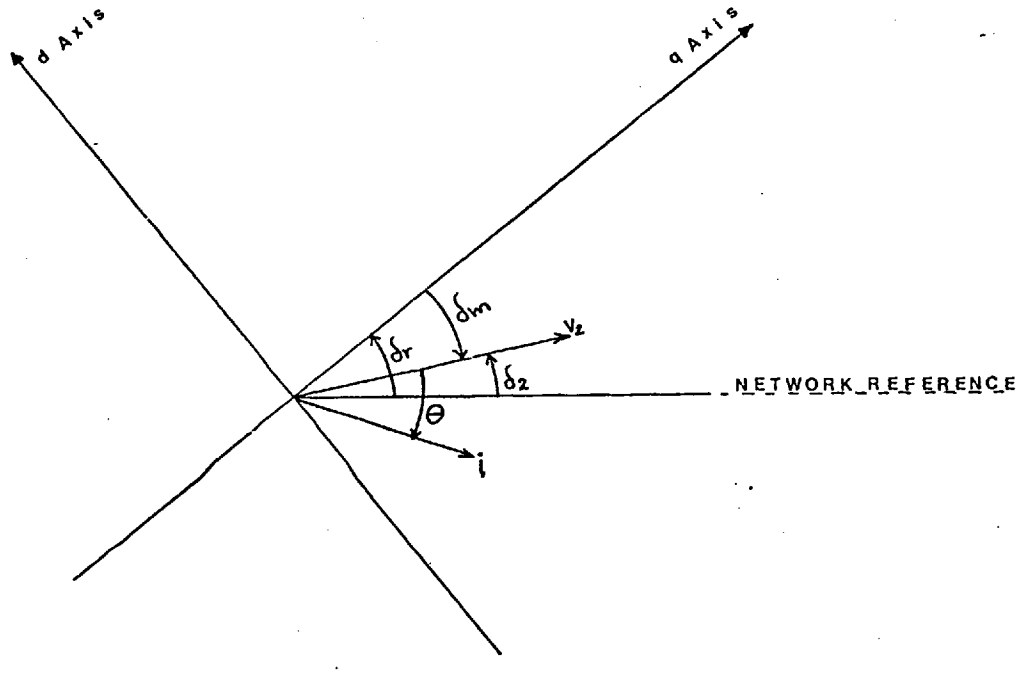

Figure 2.2 Relation between the dq and network reference frames.

From the phasor diagram in Figure 2.2:

$$V_2 = v_q + jv_d \tag{2.27}$$

$$i = i_q + ji_d \tag{2.28}$$

then:

$$P_2 = v_d i_d + v_q i_q \tag{2.29}$$

$$Q_2 = v_d i_q - v_q i_d \tag{2.30}$$

$$V_2 = v_d^2 + v_q^2 \tag{2.31}$$

$$\delta_m = t_g^{-1} \frac{v_d}{v_q} \tag{2.32}$$

$$\delta_r = \delta_2 - \delta_m \tag{2.33}$$

2.2.3 Linear Power System Model

If the power system is perturbed, it will acquire a new operating state. If the perturbation is small, the new operating state will not be appreciably different from the initial one. In other words, the state variables or the system parameters will usually not change appreciably. Thus the operation is in the neighbourhood of a certain quiescent state y_o. In this limited range of operation a non-linear system can be described mathematically by linearized equations. The method of analysis used to linearize the differential equations describing the system behaviour is to assume small changes in system quantities such as $\Delta\delta_r$, ΔV, ΔP, change in rotor angle, voltage, and power respectively. Equations for these variables are found by making a Taylor series expansion about y_o and neglecting higher order terms[1,5,14].

If the state space vector y has an initial state y_o at time $t = t_o$, on the occurrence of a small disturbance, i.e. after $t = t_o^+$, the state will change slightly from their previous positions or values. Thus:

$$y = y_o + \Delta y \tag{2.34}$$

If the state space model is in the form:

$$\dot{y} = f(y, t) \tag{2.35}$$

the A matrix may be computed by finding the total differential dy at y_o with respect to all variables, i.e. with $dy = \Delta y$:

$$y = y_o + \Delta y \tag{2.36}$$

$$\Delta\dot{y} = \left.\frac{\partial f}{\partial y_1}\right]_{y_o} \Delta y_1 + \left.\frac{\partial f}{\partial y_2}\right]_{y_o} \Delta y_2 + \ldots + \left.\frac{\partial f}{\partial y_n}\right]_{y_o} \Delta y_n \quad (2.37)$$

$$\Delta\dot{y} = \left[\frac{\partial f}{\partial y_1}\frac{\partial f}{\partial y_2}\ldots\frac{\partial f}{\partial y_n}\right]_{y_o} \Delta t = A\Delta y \quad (2.38)$$

The elements of the A matrix depend upon the initial value of the state vector y_o. For a specific dynamic study the A matrix is considered constant. The dynamic properties of the system described by equation (2.38) are determined from the nature of the eigenvalues of the A matrix. The general form of the above equations has been used to linearize the power system equations.

The linearized machine model is given below in a compact form, detailed derivations being given in Appendix A.1:

$$[\Delta\psi_g] = [X][\Delta i_g] \quad (2.39)$$

$$[\Delta V] = [R][\Delta i_g] + \left\{\frac{p}{\omega_o}[I] + [I^*]\right\}[\Delta\psi_g] + [\psi_g^*]\Delta n \quad (2.40)$$

$$T_m\, p\Delta n = \Delta T_{mech} - \Delta T_g \quad (2.41)$$

$$p\Delta\delta_r = \omega_o\, \Delta n \quad (2.42)$$

For the automatic voltage regulator:

$$\Delta E_{fd} = \frac{K_r}{1 + T_{rg}p}\,\Delta V \quad (2.43)$$

The speed governor and associated equations are:

$$\Delta T_{mech} = A_t \Delta g - BD_{nom}\Delta n + 1.5\, BA_t\, \Delta h \quad (2.44)$$

$$p\Delta C = -p\Delta n - \delta_t p\Delta g - \frac{1}{T_R}(\Delta C + \Delta n) \quad (2.45)$$

$$p\Delta g = Q_g(\Delta C - \delta_p \Delta g - W_s p \Delta n) \tag{2.46}$$

$$p\Delta h = -2p\Delta g - \frac{2}{T_W}\Delta h \tag{2.47}$$

As mentioned earlier, the short-lived transients in the transmission system are neglected and the network equations (2.1) can be used, which are directly in linear form. In Chapter 4, Section 4.4.1, the significance of these transient network terms is examined.

Equations (2.29)-(2.33) can be rearranged in a matrix form as:

$$\begin{bmatrix} \Delta P_2 \\ \Delta Q_2 \\ \Delta V_2 \\ \Delta \delta_2 \end{bmatrix} = \begin{bmatrix} i_d & i_q & v_d & v_q & 0 \\ i_q & -i_d & -v_q & v_d & 0 \\ \frac{v_d}{V_2} & \frac{v_q}{V_2} & 0 & 0 & 0 \\ \frac{v_q}{V_2^2} & -\frac{v_d}{V_2^2} & 0 & 0 & 1 \end{bmatrix} \begin{bmatrix} \Delta v_d \\ \Delta v_q \\ \Delta i_d \\ \Delta i_q \\ \Delta \delta_r \end{bmatrix} \tag{2.48}$$

2.2.4 Nonsynchronous Loads Representation

Several types of loads were considered in the present analysis; a non-linear passive load recommended by the IEEE group[38], an induction motor represented by Mauricio and Semlyen[14] and a combined load recommended by Shackshaft et al.[39] that includes a constant impedance load in parallel with an equivalent induction motor.

Neglecting the frequency dependence of the non-linear load and representing it by a static model of exponential form,

the load-voltage dependence can be expressed in linearised form as follows, details of derivation being given in Appendix A.1:

$$\Delta P_L = K_p \frac{P_L}{V} \Delta V \tag{2.49}$$

$$\Delta Q_L = K_q \frac{Q_L}{V} \Delta V \tag{2.50}$$

The representation of an induction motor is desirable in a stability study, when appreciable system load is known to be induction motors and representational accuracy is of great importance.

Basically the same set of equations that describes a synchronous machine can be used. However, several simplifications can be made, as shown in Appendix A.1. Thus:

$$[\Delta\psi_{mot}] = [X_{mot}][i_{mot}] \tag{2.51}$$

$$[\Delta V] = [R][\Delta i_{mot}] + \left\{\frac{p}{\omega_o}[I] + [S]\right\}\Delta\psi_{mot} + [\psi^*_{mot}]\Delta n \tag{2.52}$$

$$T_m p \Delta n = \Delta T_{mech} - \Delta T_g \tag{2.53}$$

The transformation equation is:

$$\begin{bmatrix} \Delta P_L \\ \Delta Q_L \\ \Delta V_L \\ \Delta\delta \end{bmatrix} = \begin{bmatrix} i_d & i_q & v_d & v_q \\ i_q & -i_d & -v_q & v_d \\ v_d/V & v_q/V & 0 & 0 \\ v_q/V^2 & -v_d/V^2 & 0 & 0 \end{bmatrix} \begin{bmatrix} \Delta v_d \\ \Delta v_q \\ \Delta i_d \\ \Delta i_q \end{bmatrix} \tag{2.54}$$

The equivalent combined load model[39] consists of an induction motor taking powers P_m and Q_m, a constant impedance static load model P_s and Q_s, and a saturation characteristic Q_{sat} to represent the magnetic saturation of transformer and motor steel.

The active and reactive power of the group in a linearized form responds to small changes in both the magnitude and phase angle of the supply voltage and the following equations apply:

$$\Delta P_L = [2V(G_m+G_s)-V_m Y_m \cos(\theta_m+\delta)]\Delta V+[VV_m Y_m \sin(\theta_m+\delta)]\Delta\delta \quad (2.55)$$

$$\Delta Q_L = [2V(B_m+B_s)-V_m Y_m \sin(\theta_m+\delta)]\Delta V-[VV_m Y_m \cos(\theta_m+\delta)]\Delta\delta \quad (2.56)$$

Derivation of these equations is given in Appendix A.1.

2.2.5 Basic State Space Formulation Approach

When the load flow has been obtained for the system and the equations have been linearised as explained before, the equations are transformed into a form in which small signal analysis can be implemented in a digital computer program.

The small signal form of equation (2.1) may be used to represent the network, if:

$$[\sigma_N]^T = [\Delta P \ \Delta Q \ \Delta\delta \ \Delta V] \quad (2.57)$$

Equation (2.1) may be rewritten as:

$$[K_N][\sigma_N] = 0 \quad (2.58)$$

where: $$[K_N] = [-I \mid J] \quad (2.59)$$

$[I]$ = unit matrix

and: $[J]$ = Jacobian matrix as defined by equation (2.1).

The terminal quantities of the network can then be matched with the small-signal variables of the generators or loads:

$$[K_R][\sigma_R] = [0] \tag{2.60}$$

Equations (2.58) and (2.60) completely describe the small signal behaviour of the system:

$$[K][\sigma_z] = [0] \quad * \tag{2.61}$$

or rearranged as:

$$[K_1]\,\dot{y}(t) + [K_2]\,y(t) + [K_3]\,z = [0] \tag{2.62}$$

and:
$$[K_4]\,y(t) + [K_5]\,z = [0] \tag{2.63}$$

where $y(t)$ are the state variables and z are the algebraic variables. Equations (2.62) and (2.63) are developed in Appendix A.2. The state equations of the system are obtained in the normal form:

$$\dot{y}(t) = [A]\,y(t) \tag{2.64}$$

where:
$$[A] = [K_1]^{-1}\left\{[K_3][K_5]^{-1}[K_4] - [K_2]\right\} \tag{2.65}$$

$[A]$ is asymmetric and ill-conditioned. The eigenvalues are obtained using a standard subroutine and the system is stable so long as none has a positive real part.

---

* Eqn (2.61) defined as in reference 14

$$\begin{bmatrix} K_1 & K_2 & K_3 \\ 0 & K_4 & K_5 \end{bmatrix} \begin{bmatrix} \dot{y}(t) \\ y(t) \\ z \end{bmatrix} = \begin{bmatrix} 0 \end{bmatrix}$$

2.3 APPLICATION OF THE TECHNIQUE

In this chapter the effect of load characteristics is studied in a single-machine system, as shown in Figure 2.1. In this section the technique presented in the previous section is applied. Several types of load representation were considered:

1. Non-linear passive load,
2. Induction motor load,
3. Combined load.

In Appendix A.2 the system equations are given for each case. They have been arranged in such a way that the $[K]$ matrix in equation (2.61) can be formed easily by the computer program. This section shows how the linear equations that represent the system are arranged in a matrix form for each load representation. The flow chart of the program is shown in Figure 2.2. For the non-linear passive load any type or combination of exponential forms of load equations (2.49) and (2.50) can be represented very easily by merely changing the value of the constants K_p and K_q. For example, for constant impedance representation, $K_p = K_q = 2$. The $[K]$ matrix does not change its structure when the values of the Ks change.

The states of the system are:

$$y(0) = [\ \Delta\psi_g,\ \Delta E_{fd},\ \Delta\delta r,\ \Delta n,\ \Delta g,\ \Delta c,\ \Delta h]^t \qquad (2.66)$$

where:

$$\Delta\psi_g = [\ \Delta\psi_{fd},\ \Delta\psi_d,\ \Delta\psi_{kd},\ \Delta\psi_q,\ \Delta\psi_{kq}] \qquad (2.67)$$

and the algebraic variables:

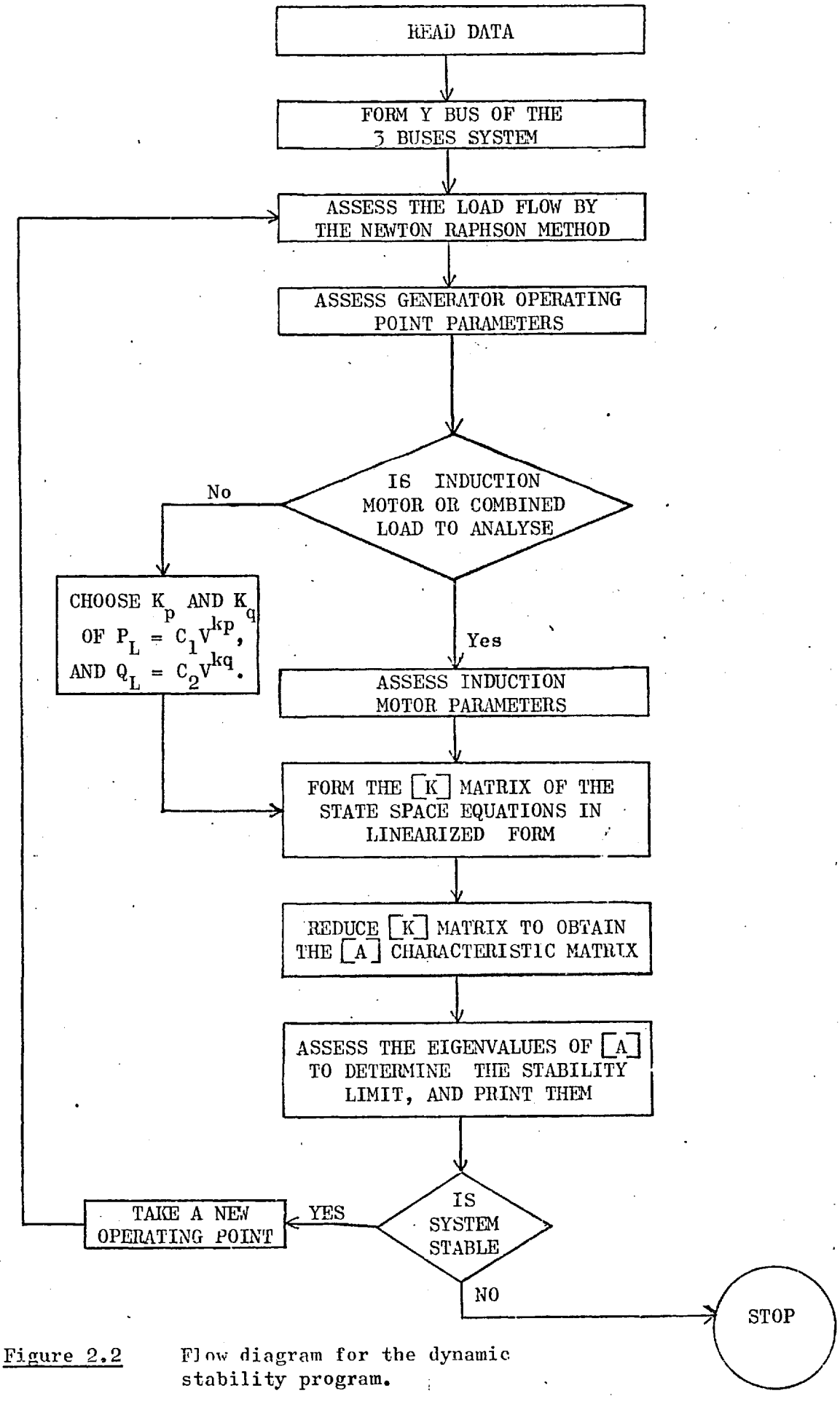

Figure 2.2 Flow diagram for the dynamic stability program.

$$z = [\Delta P_2, \Delta Q_2, \Delta\delta_2, \Delta V_2, \Delta v_d, \Delta v_q, \Delta i_g, \Delta P_3, \Delta Q_3, \Delta\delta_3, \Delta V_3]^t \quad (2.68)$$

where:

$$\Delta i_g = [i_{fd}, \Delta i_d, \Delta i_{kd}, \Delta i_q, \Delta i_{kq}] \quad (2.69)$$

The $[K]$ matrix for this case is shown in Figure 2.3.

For an induction motor load, the state vector $[y]$ has the form:

$$y(t) = [\Delta\psi_g, \Delta E_{fd}, \Delta\delta_r, \Delta n, \Delta g, \Delta C, \Delta h, \Delta\psi_m, \Delta n]^t \quad (2.70)$$

where:

$$\Delta\psi_m = [\Delta\psi_{sd}, \Delta\psi_{rd}, \Delta\psi_{sq}, \Delta\psi_{rq}] \quad (2.71)$$

The algebraic variables are:

$$z = [\Delta P_2, \Delta Q_2, \Delta\delta_2, \Delta V_2, \Delta v_d, \Delta v_q, \Delta i_g, \Delta P_3, \Delta Q_3, \Delta\delta_3, \Delta V_3, \Delta v_{sd}, \Delta v_{sq}, \Delta i_m]^t \quad (2.72)$$

where:

$$i_m = [\Delta i_{sd}, \Delta i_{rd}, \Delta i_{sq}, \Delta i_{rq}] \quad (2.73)$$

The numerical subscripts are related to the respective nodes of the system in Figure 2.1. The $[K]$ matrix for this case is shown in Figure 2.4.

For a combined load the structure of the $[K]$ matrix is similar to that in the non-linear passive load representation. Only the load equations are changed, equations (2.55) and (2.56) being substituted for equations (2.49) and (2.50) in the system equations. These are shown in Appendix A.2 and identified in the computer program as:

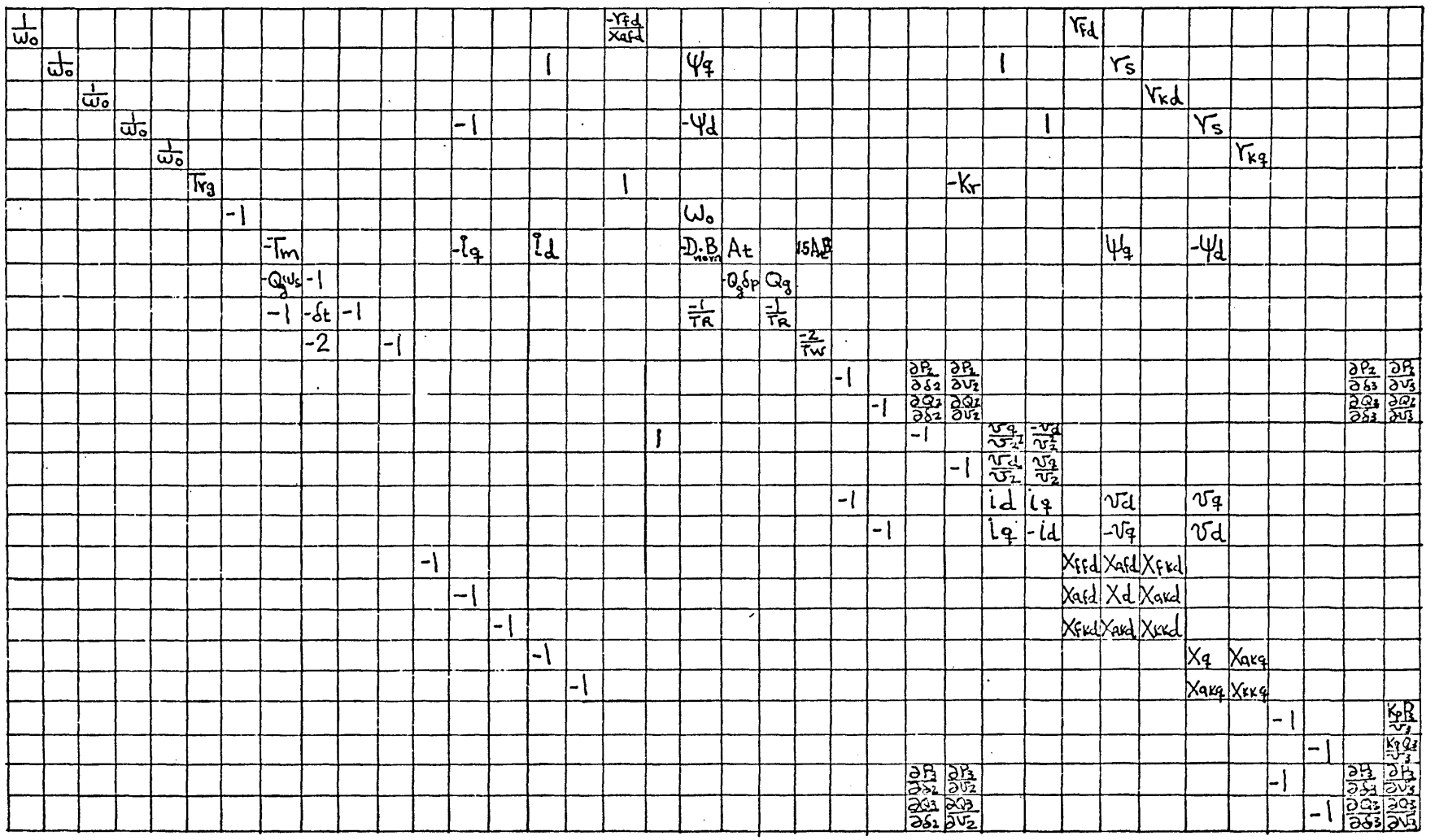

Figure 2.3: Matrix [K] for the system, considering the load as non-linear, P or Q = CV^k.

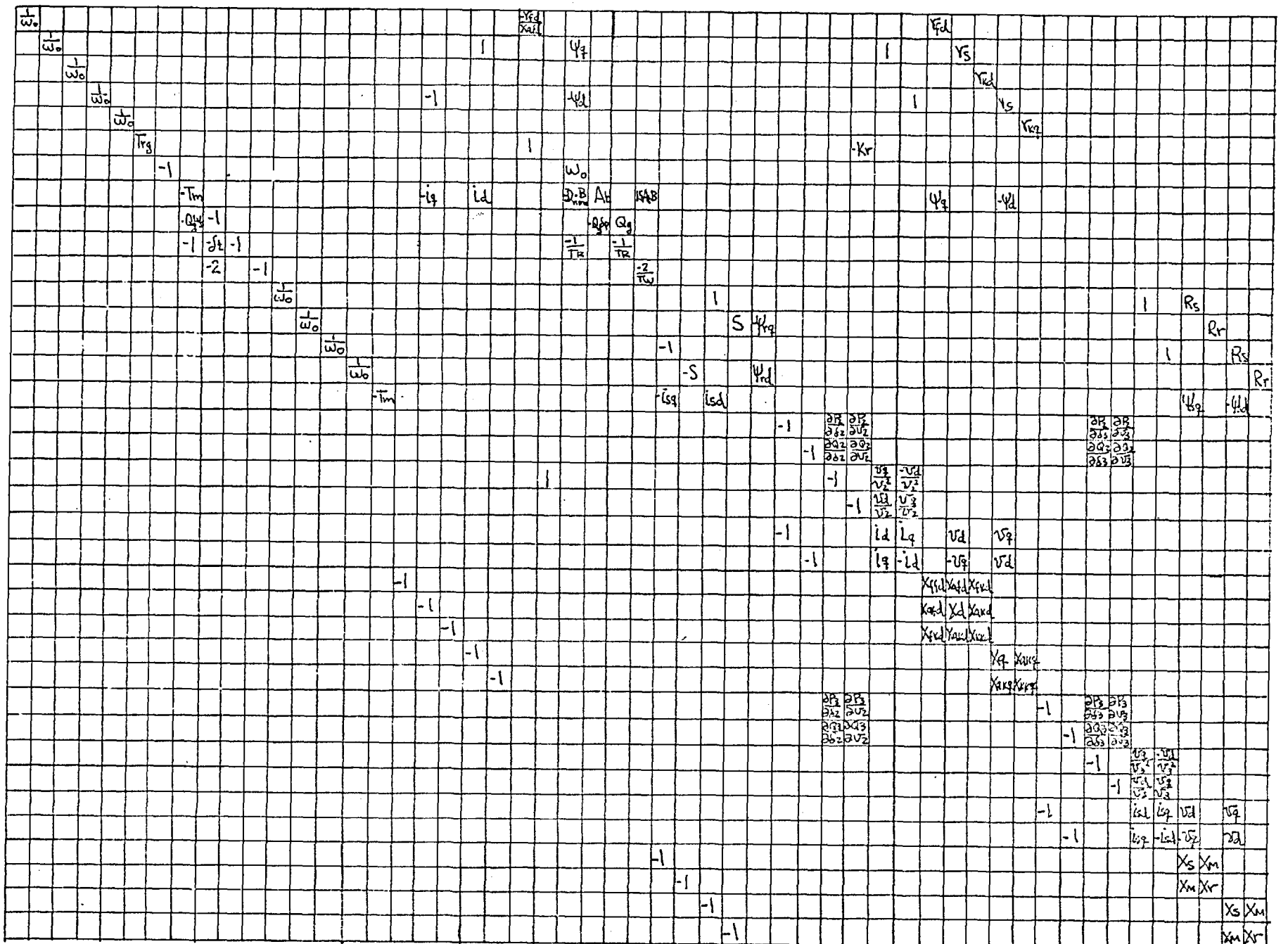

Figure 2.4: Matrix [K] for the system, considering the load as induction motor.

$$\Delta P_L = (PART_3)\,\Delta V + (PART_4)\,\Delta\delta \qquad (2.74)$$

$$\Delta Q_L = (QART_3)\,\Delta V + (QART_4)\,\Delta\delta \qquad (2.75)$$

These terms appear in the $[K]$ matrix at the last two columns and the 23^{rd} and 24^{th} rows of Figure 2.3.

2.4 THE DYNAMIC STABILITY LIMIT CONSIDERING THE EFFECT OF LOAD CHARACTERISTICS

Results are presented in this section for the power system shown in Figure 2.1. The generator data is given in Table 2.1 and a variety of loads are applied at the intermediate bus-bar. Two methods are used for determining the stability limit:

1. A succession of load flows were made for ever-increasing generated power, as did Mauricio and Semlyen[14], keeping the load power constant. The eigenvalues were obtained for each operating point indicating the asymptotic stability.

2. Instead of increasing generated power, the power factor of generation was varied keeping within the feasible machine operating region.

It is shown below that the first method gives rise to operating conditions that are not feasible and that therefore the stability limits devised with it are of little consequence. The second method is more realistic as it represents actual operating conditions.

X_{ffd}	= 1.1	D_{nom}	= 1.0
X_{afd}	= 1.0	δt	= 0.33
X_{fkd}	= 1.0	δp	= 0.03
X_{d}	= 1.2	Q_{g}	= 1.0
X_{akd}	= 1.0	A_{t}	= 1.25
X_{kkd}	= 1.1	W_{s}	= 0.5
X_{q}	= 0.8	g_{1}	= 0.16
X_{akq}	= 0.6	g_{2}	= 0.96
X_{kkq}	= 0.8	T_{w}	= 1.0 sec.
K_{r}	= -20.0	T_{R}	= 4.0 sec.
T_{rg}	= 0.5 sec.		
H	= 3 kWS/kVA	$X_{t_1}+X_{t_2}$	= 0.3

Table 2.1: Typical parameters of a hydro generating set, a.v.r., dashpot hydrospeed governor and network. All values are in per unit.

Operating conditions for the computed results with method 1 are shown in Tables 2.3 and 2.4. Load is taken to consist of:

(i) Non-linear passive load with K_p and K_q in the ranges 0→3 and 2→0 and also as 0 and 6. Critical eigenvalues are shown in Figure 2.5.

(ii) An induction motor with the parameters shown in Table 2.2. The eigenvalues of the system when the induction motor is at full load are shown in Table 2.5 and critical eigenvalues are also indicated in Figure 2.5. The inertia constant (H) was varied and the mechanical load torque (T_{mech}) of the induction machine was considered in three different ways, in order to investigate the effect in the power system stability. The eigenvalues associated with transient rotor terms, and that with the mechanical oscillation of the induction machine were the most affected. Results are summarized in Table 2.6.

Speed rev/s	R_s	R_r	X_s	X_r	X_m
1800	0.032	0.034	0.443	0.388	20.15

$H = 2 - 4 \frac{kW - s}{kVA}$

$T_{mech} \propto \text{velocity}^2$

$\propto \text{velocity}$

$= \text{constant}$

Slip at full load $S = 0.016$

Table 2.2: Induction motor parameters p.u. for a 40 MW machine.

P.F. Lagging	θ	V_2	δ_2	V_1	δ_1	δ_r	i_d	i_q	v_d	v_q	ψ_d	ψ_q	P_G	Q_G
0.981	11.058	1.00	9.961	1.00	0.0	36.530	-0.435	0.568	-0.447	0.895	0.900	0.452	0.700	0.137
0.964	15.390	1.00	24.676	1.00	0.0	66.306	-1.305	0.846	-0.664	0.748	0.756	0.677	1.500	0.413
0.940	19.806	1.00	34.830	1.00	0.0	79.770	-1.922	0.907	-0.706	0.708	0.717	0.726	2.000	0.720
0.920	22.930	1.00	41.586	1.00	0.0	87.043	-2.322	0.920	-0.713	0.701	0.711	0.736	2.300	0.973
0.900	24.060	1.00	43.996	1.00	0.0	89.414	-2.462	0.921	-0.712	0.702	0.711	0.737	2.400	1.072
0.900	25.265	1.00	46.580	1.00	0.0	91.877	-2.608	0.920	-0.710	0.712	0.712	0.736	2.500	1.179

Table 2.3: Machine variables for various armature power factors. Angles are in degrees and all other variables are in per unit, using method 1.

P_L	Q_L	V_3	δ_3	i_{sd}	i_{sq}	i_{rd}	i_{rq}
-0.395	-0.201	0.983	1.778	0.193	-0.409	-0.147	0.416
-0.395	-0.201	0.965	6.573	0.161	-0.431	-0.114	0.435
-0.395	-0.201	0.945	9.781	0.139	-0.450	-0.091	0.450
-0.395	-0.201	0.927	11.853	0.125	-0.462	-0.076	0.461
-0.395	-0.201	0.920	12.579	0.120	-0.467	-0.071	0.466

v_{sd}	v_{sq}	ψ_{sd}	ψ_{sq}	ψ_{rd}	ψ_{rq}	P_{ROT}	P_{mech}
0.030	0.982	0.970	-0.036	0.832	0.294	0.378	0.371
0.110	0.959	0.946	-0.115	0.838	0.219	0.364	0.358
0.160	0.931	0.918	-0.164	0.831	0.169	0.349	0.343
0.190	0.908	0.894	-0.194	0.821	0.136	0.336	0.331
0.200	0.898	0.886	-0.203	0.817	0.125	0.331	0.326

Table 2.4: Induction motor variables for different operating points.

δ_r	λ_1, λ_2	λ_3, λ_4	λ_5, λ_6	λ_7	λ_8	λ_9	λ_{10}, λ_{11}	λ_{12}, λ_{13}	λ_{14}	λ_{15}	λ_{16}
36.530	$-20.79 \pm j780.84$	$-15.70 \pm j406.71$	$-10.11 \pm j\ 13.01$	-44.11	-31.52	- 8.02	$-0.550 \pm j\ 8.70$	$-\ 1.24 \pm j\ 2.57$	-0.596	-0.012	-2.000
66.306	$-20.82 \pm j781.55$	$-15.73 \pm j407.77$	$-10.11 \pm j\ 13.06$	-44.00	-32.12	- 7.88	$-0.452 \pm j\ 8.90$	$-\ 1.07 \pm j\ 2.87$	-0.596	-0.012	-2.000
79.770	$-20.83 \pm j782.44$	$-15.73 \pm j409.08$	$-10.11 \pm j\ 13.07$	-44.00	-32.29	- 7.71	$-0.554 \pm j\ 7.93$	$-0.893 \pm j\ 3.47$	-0.596	-0.012	-2.000
87.043	$-20.84 \pm j783.23$	$-15.81 \pm j410.25$	$-10.12 \pm j\ 13.06$	-44.00	-32.34	- 7.55	$-0.945 \pm j\ 6.52$	$-0.497 \pm j\ 4.32$	-0.596	-0.012	-2.000
89.414	$-20.84 \pm j783.56$	$-15.82 \pm j410.73$	$-10.12 \pm j\ 13.06$	-44.00	-32.35	- 7.48	$-1.580 \pm j\ 5.92$	$+0.130 \pm j\ 4.68$	-0.596	-0.012	-2.000

Table 2.5: The eigenvalues of the [A] matrix at various operating angles.
Load considered as induction motor.
S = 0.01642. H = 2 seconds, T_{mech} = constant, Method 1.

Induction Motor Oscillation	T_{mech} = constant			H = 2		Rotor Angle δr
	H = 2	H = 3	H = 4	$T_{mech} \propto vel^2$	$T_{mech} \propto vel$	
λ_5 λ_6	-10.11 ± j 13.0	-11.00 ± j 10.61	-11.69 ± j 9.44	-9.17 ± j 12.57	-10.05 ± j 12.94	36.53
λ_5 λ_6	-10.11 ± j 13.0	-10.97 ± j 10.70	-11.65 ± j 9.65	-9.82 ± j 12.62	-10.06 ± j 12.99	66.30
λ_5 λ_6	-10.11 ± j 13.0	-10.97 ± j 10.70	-11.61 ± j 9.56	-9.83 ± j 12.63	-10.06 ± j 12.99	79.77
λ_5 λ_6	-10.11 ± j 13.0	-10.96 ± j 10.76	-11.59 ± j 9.60	-9.83 ± j 12.63	-10.06 ± j 12.99	87.04
λ_5 λ_6	-10.11 ± j 13.0	-10.96 ± j 10.76	-11.58 ± j 9.60	-9.83 ± j 12.63	-10.06 ± j 12.99	89.41
λ_g	-8.02	-6.23	-4.85	-7.40	-7.91	"
λ_g	-7.88	-6.14	-4.80	-7.27	-7.77	
λ_g	-7.71	-6.04	-4.75	-7.11	-7.61	
λ_g	-7.55	-5.90	-4.69	-6.95	-7.45	
λ_g	-7.48	-5.88	-4.66	-6.88	-7.38	

Table 2.6: Eigenvalues associated with the induction motor for different operating points and different motor characteristics.

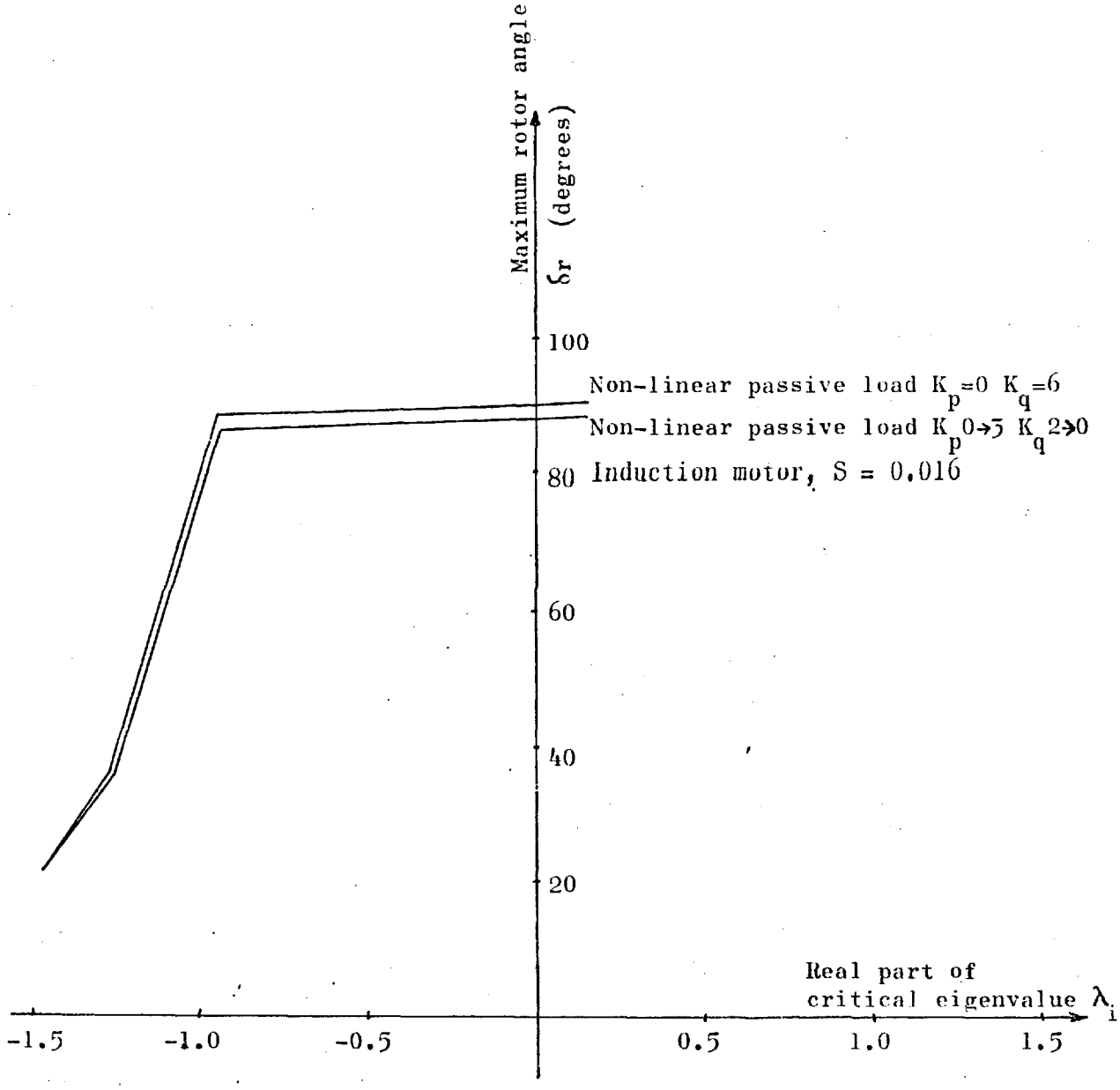

Figure 2.5: Locus of real part of the critical eigenvalues with changing rotor angle, for different types of load, using Method 1 (medium load).

Method 2 was used in order to improve the system representation, different generator power factors being considered, as shown in Table 2.8.

Three different types of load representation were analysed, the first two being, as with Method 1. For non-linear passive load with several values of K_p and K_q , critical eigenvalues are shown in Figure 2.6. Induction motor load was considered as an equivalent motor with the parameters of the largest motor shown in Table 2.7. Eigenvalues when full load operation is considered are shown in Table 2.9. Figure 2.6 shows the critical eigenvalue variations for both full load and overload induction motor operation, i.e. operating near maximum torque ($\tilde{T}_{max}$). An alternative approach suggested by Hacking and Berg[46] in which the load is a number of induction machines of different sizes is shown in Appendix A.3, but has not been used here.

Shackshaft's combined load model (described in Section 2.2.4) was used with the same power load as in previous analyses. 60% of the load was induction motor load with the parameters used earlier. The remainder was considered as constant impedance load. The eigenvalues for this type of load are shown in Table 2.10.

The significance of these results appears to be that for a medium load compared with the generated power the non-linear passive load may be either stabilizing or unstabilizing, depending on the values of K_p and K_q. Induction motor load reduces the stability limit only when it is operating near the maximum torque. Different induction motor inertias and mechanical loads were

HP	V	RATED SPEED r.p.m.	R_s Ω	R_r Ω	$L_1=L_2$ H	L_M H	J kg.m^2
3	220	1710	0.435	0.816	0.0713	0.0693	0.089
25	460	1695	0.249	0.536	0.0602	0.0587	0.554
50	460	1705	0.087	0.228	0.0355	0.0347	1.662
100	460	1700	0.031	0.134	0.0193	0.0189	4.449
250	2300	1769	0.681	0.401	0.2342	0.2277	6.918
500	2300	1773	0.262	0.187	0.1465	0.1433	11.062
800	2300	1778	0.131	0.094	0.0976	0.0957	21.262
1000	2300	1778	0.112	0.074	0.1452	0.1436	29.871
1500	2300	1783	0.056	0.037	0.0532	0.0527	44.542
2250	2300	1786	0.029	0.022	0.0352	0.0346	63.971
6000	4160	1787	0.022	0.022	0.0597	0.0589	674.971

Table 2.7: Parameters of typical induction motors[44,45].

considered for the induction motor representation. The stability limit of the power system was not affected, but the damping of the oscillations introduced by the induction machine (eigenvalues λ_5, λ_6, λ_9 of Table 2.6) were affected, with the possibility of instability due to the induction motor's undamped oscillations. Table 2.10 shows the results when a combined load model was used. These results are similar to those of the non-linear passive load and the induction motor load (at full load). However, this combined load can be considered as a static load representation because no dynamic equations are included. The combined load is sufficiently general to be a good representation in any system. It has been used in the multi-machine stability studies in the following chapters.

Mauricio and Semlyen[14] have suggested that the non-linear passive load can have a significant effect on the stability of a power system, indicating high power stability limits (P_{max}). They tried to show that the dynamic behaviour of loads can have a decisive influence on the stability limit of a power system. Their results are in contrast with the results shown in this thesis, because:

1. Different magnitudes of loads have been used in the present analysis.

2. A different approach to obtaining the operating conditions was taken.

3. Differenc induction motor parameters were used.

However, when the load at the intermediate bus bar was considered to be of high magnitude, i.e. P_L = 2.0 p.u. and Q_L =

P.F.	θ	V_2	δ_2	V_1	δ_1	δ_r	i_d	i_q	v_d	v_q	ψ_d	ψ_q	P_G	Q_G
-0.899	26.0	1.06	9.279	1.00	0.00	30.7	-0.5377	0.4945	-0.390	0.991	0.996	0.395	0.70	0.340
-0.899	25.8	1.07	12.410	1.00	0.00	37.6	-0.720	0.582	-0.582	0.976	0.825	0.466	0.90	0.436
1.000	0.0	0.93	16.510	1.00	0.00	58.5	-0.714	0.792	-0.627	0.696	0.704	0.634	1.00	0.000
+0.940	-19.0	0.77	20.500	1.00	0.00	88.0	-1.010	0.909	-0.717	0.296	0.305	0.727	1.00	-0.350
+0.920	-21.0	0.74	21.600	1.00	0.00	95.0	-1.130	0.902	-0.710	0.211	0.220	0.721	1.00	-0.400
+0.920	-22.0	0.72	22.100	1.00	0.00	98.1	-1.190	0.894	-0.703	0.175	0.184	0.715	1.00	-0.420
+0.910	-24.0	0.71	22.640	1.00	0.00	100.8	-1.250	0.886	-0.696	0.145	0.153	0.709	1.00	-0.430

Table 2.8: Machine variables for various armature power factors; angles are in degrees and all other variables are in per unit. Method 2; $P_L = 0.382$ p.u., $Q_L = 0.127$ p.u.

- Lagging P.F.
+ Leading P.F.

δ_r	λ_1, λ_2	λ_3, λ_4	λ_5, λ_6	λ_7	λ_8	λ_9	$\lambda_{10}, \lambda_{11}$	$\lambda_{12}, \lambda_{13}$	λ_{14}	λ_{15}	λ_{16}
30.7	$-20.9 \pm j802$	$-16.0 \pm j437$	$-5.35 \pm j108$	-44.1	-31.4	-11.34	$-0.615 \pm j9.23$	$-1.319 \pm j2.6$	-0.596	-0.012	-2.00
37.6	$-20.9 \pm j801$	$-16.0 \pm j436$	$-5.35 \pm j108$	-44.1	-31.5	-11.36	$-0.583 \pm j9.54$	$-1.288 \pm j2.6$	-0.596	-0.012	-2.00
58.5	$-20.9 \pm j806$	$-16.1 \pm j442$	$-5.33 \pm j107$	-44.0	-31.77	-11.25	$-0.561 \pm j8.57$	$-1.119 \pm j2.54$	-0.596	-0.012	-2.00
88.0	$-21.0 \pm j813$	$-16.3 \pm j449$	$-5.26 \pm j106$	-44.0	-31.98	-11.09	$-0.755 \pm j6.59$	$-0.78 \pm j2.97$	-0.596	-0.012	-2.00
95.0	$-21.0 \pm j815$	$-16.3 \pm j451$	$-5.23 \pm j105$	-44.0	-32.0	-11.04	$-1.030 \pm j5.55$	$-0.50 \pm j3.51$	-0.596	-0.012	-2.00
98.0	$-21.0 \pm j816$	$-16.3 \pm j452$	$-5.22 \pm j105$	-44.0	-32.0	-11.02	$-1.500 \pm j4.97$	$-0.01 \pm j3.83$	-0.596	-0.012	-2.00
100.8	$-21.0 \pm j816$	$-16.4 \pm j453$	$-5.20 \pm j105$	-44.0	-32.0	-11.00	$-2.000 \pm j4.74$	$+0.48 \pm j3.80$	-0.596	-0.012	-2.00

Table 2.9: The eigenvalues of the [A] matrix at various operating angles.
Load considered as induction-equivalent motor.
S = 0.0057, H = 5 seconds, Method 2.

δ_r	λ_1 λ_2	λ_3	λ_4	λ_5 λ_6	λ_7 λ_8	λ_9	λ_{10}	λ_{11}
30.77	$-20.9 \pm j745$	-44.1	-31.3	$-0.56 \pm j9.31$	$-1.32 \pm j2.58$	-0.596	-0.012	-2.0
37.6	$-21.0 \pm j745$	-44.0	-31.5	$-0.52 \pm j9.6$	$-1.29 \pm j2.59$	-0.596	-0.012	-2.0
58.53	$-21.2 \pm j743$	-44.0	-31.9	$-0.51 \pm j8.6$	$-1.12 \pm j2.50$	-0.596	-0.012	-2.0
88.00	$-21.2 \pm j741$	-43.9	-32.2	$-0.717 \pm j6.8$	$-0.80 \pm j2.85$	-0.596	-0.012	-2.0
95.00	$-21.2 \pm j741$	-43.9	-32.2	$-0.94 \pm j5.85$	$-0.59 \pm j3.31$	-0.596	-0.012	-2.0
98.16	$-21.2 \pm j740$	-43.9	-32.2	$-1.25 \pm j5.25$	$-0.28 \pm j3.60$	-0.596	-0.012	-2.0
100.88	$-21.1 \pm j740$	-43.9	-32.2	$-1.70 \pm j4.88$	$+0.23 \pm j3.80$	-0.596	-0.012	-2.0

Table 2.10: Eigenvalues of the [A] matrix for the different operating points. Load considered as combined load CEGB model 60% induction motor load and the rest as constant impedance. Method 2.

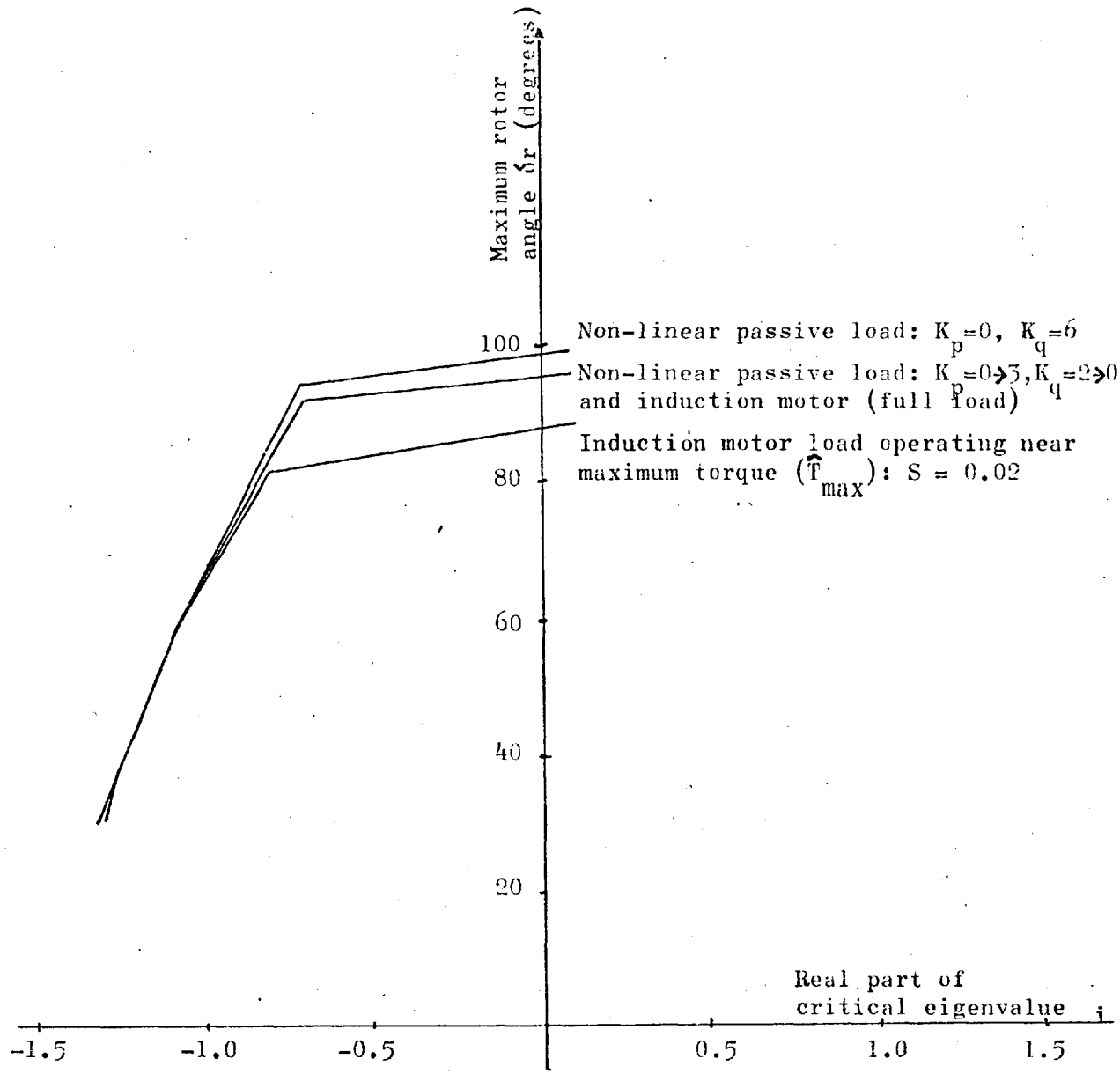

Figure 2.6: Locus of real part of the critical eigenvalues with change in the rotor angle; for non-linear passive load and induction motor load, using Method 2 (medium load).

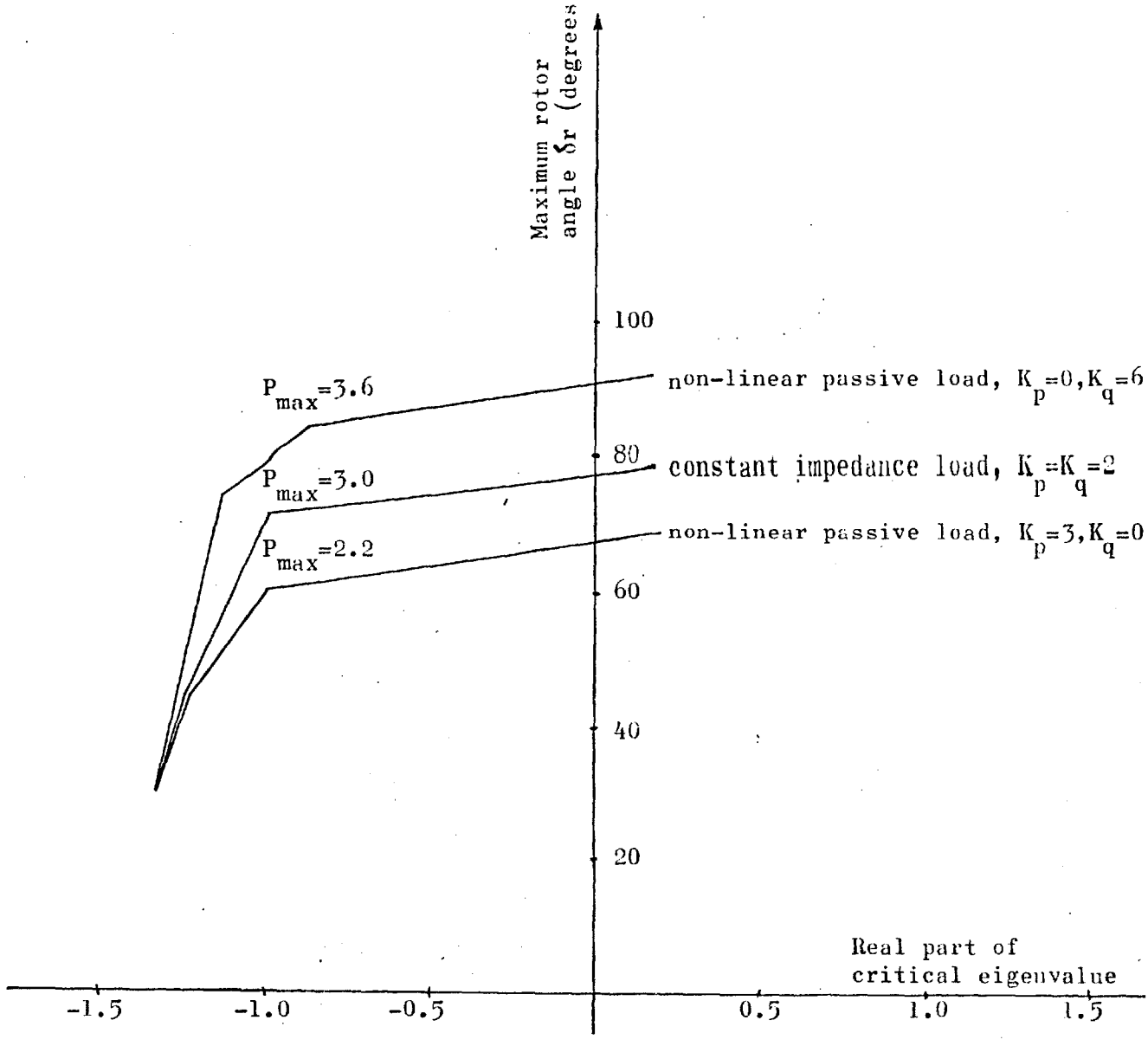

Figure 2.7: Locus of real part of the critical eigenvalues with change in the rotor angle; for non-linear passive load and constant impedance load, using Method 1 (high load).

1.0 p.u., and the operating conditions assessed by Method 1, as shown in Figure 2.7, the stability limits are very near to those presented in Reference 14.

2.5 OSCILLATING MODES IDENTIFICATION

In the simulation of complex systems, eigenvalue analysis is difficult to interpret, i.e. the location of the principal causes of the oscillating modes is not easy to find. Mauricio and Semlyen[14] comment that it is not very easy to directly associate an eigenvalue to one particular loop, unless the respective eigenvector indicates this. Here, two methods of locating the source of oscillations have been tried.

Firstly, the sensitivity of eigenvalues to system parameters can indicate "the cause" of oscillations; secondly, a state variable reduction method can indicate their source.

The variation of the eigenvalues of the $[A]$ matrix with system parameters is indicative of the effect that changes in the system will have on stability. Each time a system parameter or operating point changes, the $[A]$ matrix and corresponding eigenvalue change.

The basic method for calculating eigenvalue sensitivities was taken from Van Ness et al.[50]:

$$S_i = \frac{\partial \lambda_i}{\partial \alpha} = \frac{\left(\frac{\partial [A]}{\partial \alpha} X_i, V_i\right)}{(X_i, V_i)} \qquad (2.76)$$

where: X_i are the eigenvectors of $[A]$,

V_i are the eigenvectors of $[A]^t$ ($[A]$ transposed).

In the program written here, any parameter variation was assumed to be a linear function of a variable, α.

Using equation (2.65) for the formulation of the $[A]$ matrix, it is clear that all the main parameters of the a.v.r. and speed governor are located in matrices $[K_1]$, $[K_2]$ and $[K_3]$ only. If equation (2.76) is applied to equation (2.65), hence:

$$\frac{\partial [A]}{\partial \alpha} = -[K_1]^{-1} \frac{\partial [K_1]}{\partial \alpha} [K_1]^{-1} \left\{ [K_3][K_5]^{-1}[K_4] - [K_2] \right\}$$

$$+ [K_1]^{-1} \left\{ \frac{\partial [K_3]}{\partial \alpha} [K_5]^{-1}[K_4] - [K_3][K_5]^{-1} \frac{\partial [K_5]}{\partial \alpha} [K_5]^{-1} [K_4] \right.$$

$$\left. + [K_3][K_5]^{-1} \frac{\partial [K_4]}{\partial \alpha} - \frac{\partial [K_2]}{\partial \alpha} \right\} \qquad (2.77)$$

For the particular case of the a.v.r. parameters, equation (2.77) can be simplified to:

$$\frac{\partial [A]}{\partial \alpha} = [K_1]^{-1} \left\{ \frac{\partial [K_3]}{\partial \alpha} [K_5]^{-1} [K_4] - \frac{\partial [K_2]}{\partial \alpha} \right\} \qquad (2.78)$$

In a similar way for the speed governor parameters, the simplified form is obtained as:

$$\frac{\partial [A]}{\partial \alpha} = -[K_1]^{-1} \frac{\partial [K_1]}{\partial \alpha} [K_1]^{-1} \left\{ [K_3][K_5]^{-1} [K_4] - [K_2] \right.$$

$$\left. - [K_1]^{-1} \frac{\partial [K_2]}{\partial \alpha} \right\} \qquad (2.79)$$

Once the eigenvectors of $[A]$ and $[A]^t$ and their eigenvalues are obtained, the eigenvalue sensitivities can be assessed by applying equations (2.76)-(2.79) as indicated above.

The flow diagram for this process is given in Figure 2.8.

Results are presented for this analysis in Table 2.12, showing that changes in a.v.r. (using a.v.r recommended by the IEEE Committee[16], Figure 2.9 and Table 2.11) parameters are related with the variations of the critical eigenvalues λ_3, λ_4, λ_7, λ_8, λ_9, λ_{10}, associated with the a.v.r. loops, and the mechanical oscillations.

The state variable reduction technique has been used by Alden and Nolan[28] to obtain reduced synchronous machine models on the basis of physical assumptions. A similar technique was used in this study to identify sources of oscillations. Once the characteristic matrix [A] is obtained, rows and columns can be eliminated systematically corresponding with each state variable no longer wanted. For example, applying this process to equation (2.80) and eliminating the last row and column, putting $\dot{y}_n = 0$ gives equation (2.81) and the reduced set is given by equation (2.82).

$$\begin{bmatrix} \dot{y}_1 \\ \dot{y}_2 \\ \vdots \\ \dot{y}_n \end{bmatrix} = \left[\begin{array}{ccc|c} a_{11} & a_{12} \cdots & & a_{1n} \\ a_{21} & a_{22} \cdots & & a_{2n} \\ \vdots & & & \vdots \\ \hline a_{n1} & a_{n2} & \cdots & a_{nn} \end{array}\right] \begin{bmatrix} y_1 \\ y_2 \\ \vdots \\ y_n \end{bmatrix} \qquad (2.80)$$

if $\dot{y}_n = 0$:

$$\begin{bmatrix} \dot{y}_{n-1} \\ \hline 0 \end{bmatrix} \left[\begin{array}{c|c} A_{11} & A_{12} \\ \hline A_{21} & A_{22} \end{array}\right] \begin{bmatrix} y_{n-1} \\ \hline y_n \end{bmatrix} \qquad (2.81)$$

$$[\dot{y}_{n-1}] = [A_{11} - A_{12}A_{22}^{-1} A_{21}][y_{n-1}] \qquad (2.82)$$

In this study the element by element elimination algorithm given by Kimbark[32] was used in order to avoid matrix inversions. This algorithm is indicated below, where the n^{th} element is to be eliminated:

$$a'_{jk} = a_{jk} - \frac{a_{jn}a_{nk}}{a_{nn}} \qquad (2.83)$$

where: a'_{jk} = new element of $[A]$,

a_{jk} = old element of $[A]$,

$j = 1,2,\ldots,n-1 \quad k = 1,2,\ldots,n-1$

The columns of Table 2.13 show the full matrix (column 2) eigenvalues, and in the following columns the remaining eigenvalues as rows and columns of the A matrix are removed. Identification is achieved by observing which eigenvalues disappear with which state variable. For instance, in the third column a state variable in the speed governor has been removed (h) and the eigenvalue -2.0 has been lost.

State variable elimination was carried out in the following order:

1. states related with the speed governor h, C and g;
2. state related with rotor speed n;
3. state related with the a.v.r. loop;
4. state related with damper winding in q axis;
5. state related with transient stator term in q axis;
6. state related with damper winding in d axis;
7. state related with transient stator term in d axis;
8. state related with field winding.

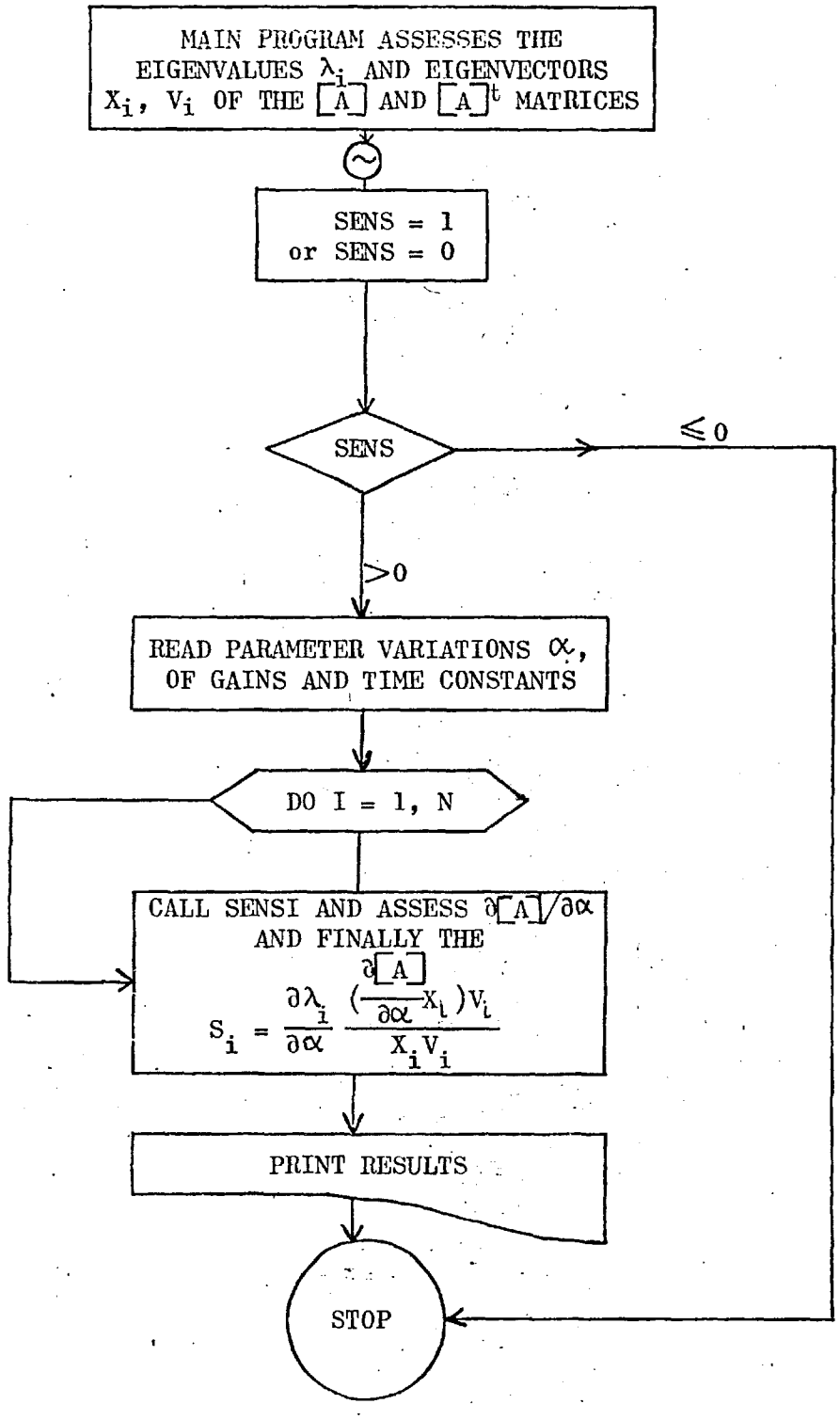

Figure 2.8: Flow diagram for sensitivity analysis of the eigenvalue λ_i using "SENSI" subroutine.

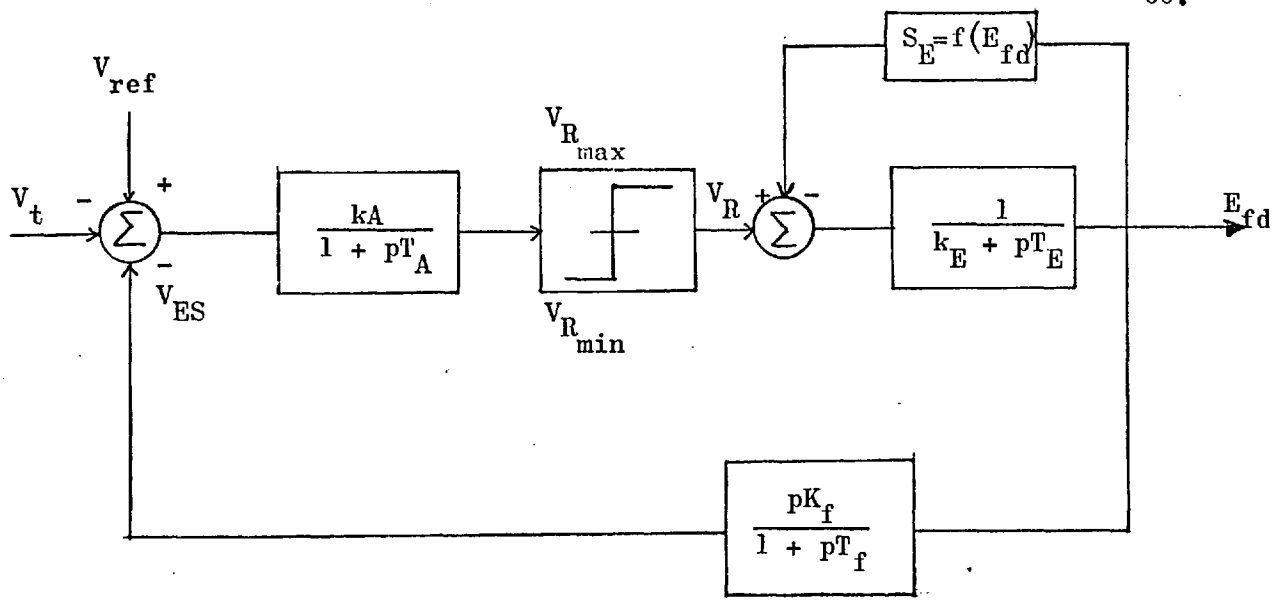

Figure 2.9: Type 1 excitation system representation IEEE Model.

K_A	=	50 amplifier gain
K_E	=	0.01 exciter gain
K_f	=	0.057 Regulator stabilizer feedback gain
T_A	=	0.02 sec. regulator time constant
T_E	=	0.146 sec. exciter time constant
T_f	=	0.45 Feedback time constant
$V_{R_{max}}$	=	1.0 p.u. Maximum value of regulator voltage
$V_{R_{min}}$	=	-1.0 p.u. Minimum value of regulator voltage

Table 2.11: Parameters of the excitation system IEEE Type 1 Model.

Eigenvalues without parameter variations	K_A	T_A	K_E	T_E	K_f	T_f
$\lambda_1\lambda_2$=-20.95±j745	-20.95±j745	-20.95±j745	-20.95±j745	-20.95±j745	-20.95±j745	-20.95±j745
$\lambda_3\lambda_4$=-25.66±39.35	-25.64±j46.24	-32.0±j42.34	-25.63±j39.32	-25.61±j46.22	-25.7±j43-38	-26.0±j46.55
λ_5 = -43.43	-43.43	-43.43	-43.43	-43.43	-43.43	-43.43
λ_6 = -31.37	-31.37	-31.37	-31.37	-31.37	-31.37	-31.37
$\lambda_{7,8}$=-0.534±j9.316	-0.533±j9.318	-0.534±j9.317	-0.533±j9.317	-0.532±j9.312	-0.54±j9.32	-0.541±j9.32
$\lambda_{9,10}$=-1.27±j1.341	-1.28±j1.341	-1.27±j1.345	-1.34±j1.32	-1.35±j1.315	-1.1 ± j1.2	-1.0 ± j1.5
λ_{11} = -0.596	-0.596	-0.596	-0.596	-0.596	-0.596	-0.596
λ_{12} = -0.0125	-0.0125	-0.0125	-0.0125	-0.0125	-0.0125	-0.0125
λ_{13} = -2.00	-2.00	-2.00	-2.00	-2.00	-2.00	-2.00

Table 2.12: Eigenvalue sensitivities of power system, with respect to the a.v.r. type no. 1^{16} parameters, (25% change).

Eigenvalues	Matrix Order										
	11	10	9	8	7	6	5	4	3	2	1
Stator Transient Terms	-20.9+j745 -20.9-j745	-20.9+j745 -20.9-j745	-20.9+j745 -20.9-j745	-20.9+j745 -20.9-j745	-29.60+j744 -29.60-j744	-30.8+j745 -30.8+j746	-17.1+j645 -17.1-j645	-20150.4	-18.5×10^3		
Damper Windings	-44.11 -31.38	-44.11 -31.27	-44.0 -30.7	-44.1 -32.33	-44.8 -38.0	-44.1 -36.9	-44.1	-43.0			
Mechanical Oscillations	-0.5+j9.31 -0.5-j9.31	-0.64+j9.9 -0.64-j9.9	-1.28+j12.5 -1.28-j12.5	-0.1+j1.57 -0.1-j1.57	-10.2	-10.3	-11.88	-11.7	-11.8	-11.9	-12.0
A.V.R. and Field Winding	-1.32+j2.58 -1.32-j2.58	-1.32+j2.58 -1.32-j2.58	-1.32+j2.57 -1.32-j2.57	-1.4+j2.6 -1.4-j2.6	-1.3+j2.5 -1.3-j2.5	-4.25	-4.30	-4.38	-4.37	-4.37	
Speed Governor	-0.596 -0.0125 -2.00	-0.596 -0.0125	-0.0129								

Table 2.13: Oscillating mode identification by state variable reduction technique.

The first two columns show the identification obtained in this way.

2.6 CONCLUSION

The effect of load characteristics has significant effect on the system stability and in some circumstances the effect is substantial. However, this effect depends on the magnitude of the load and the way in which each operating point is considered. Non-linear passive load may be either stabilizing or unstabilizing (δ_r = 70-98°, Figures 2.5-2.7), depending on the values of K_p and K_q. In the case of a big isolated load considered by an induction motor load representation, it was shown that the effect of inertia constant variation and the mechanical load representation do not affect the stability limit. A critical case was found when the induction motor load operated at near the pull out torque ($\widehat{T}_{max}$), which is rather unusual. A combined load seems to give a good approach for a better representation of the load. However, with this type of load the dynamic behaviour of the induction machines cannot be considered as it is essentially a static representation.

The two methods of oscillating mode identification by sensitivity analysis and state variable reduction technique, have been tried. The former method does not identify all the oscillating modes exactly and the state with which they are related. The latter is a simple process requiring comparatively little computer memory and is able to identify all the oscillating modes, by systematically isolating each state variable.

CHAPTER 3

DYNAMIC STABILITY IN MULTI-MACHINE SYSTEMS INCLUDING THE EFFECT OF LOAD CHARACTERISTICS

3.1 INTRODUCTION

Many works have been devoted to the analysis of the dynamic stability of multi-machine systems using the state space formulation and assessing the eigenvalues of the characteristic matrix of the system, in order to study the interaction between machines. A review of these investigations is given. All of this work has been directed towards the mathematical problems of system formulation, brought about by computer limitations and the difficulties of working with ill-conditioned matrices which are difficult to invert. No method has previously been devised to include the effect of the load characteristics.

In this chapter a small-signal dynamic model of an arbitrary number of interconnected power generating units including the effect of several load representations is developed in state space form. This form is convenient for the evaluation of system dynamic performance when conventional forms of control are utilized, and it also enables new forms of controllers to be developed using concepts of modern control theory. The analysis of large systems is limited by the memory capacity of the computer used. The use of sparsity techniques reduces the amount of memory required and has enabled the full machine representation including a.v.r. and speed governor equations for a system with a mixture of thermal and hydroelectric plants. With this model matrix inversion is not

necessary. However, the response of the system to a small disturbance can be checked by numerical integration. The computational arrangements of the method are described, where examples of its use are shown.

3.2 PAST WORK

The small perturbation analysis of interconnected systems using the eigenvalues method has received a great deal of attention during the past decade. An important aspect of these studies is the development of a suitable system dynamic model. For certain items of power system equipment in connection with the dynamic modelling of synchronous machines, this model may be exceedingly complex and a systematic method of handling the system equations using a digital computer becomes essential. A number of authors have acknowledged this by devoting entire papers to the problem[1,5,25,24,29,60]. However, none of them have included the effect of load characteristics in the system dynamic model. Reference 14 proposed a dynamic model including this effect but only for a single generator connected to an infinite bus-bar.

Laughton[1] proposed a method for dealing with the multi-machine case using matrix elimination to obtain the [A] matrix from the set of differential and algebraic equations, a submatrix of order n_e having to be inverted. Also the machine model used was very simple. Undrill[5] placed commendable emphasis on building the [A] matrix from submatrices representing system segments and this avoided large blocks of null elements. Nevertheless this procedure involves the inversion of an 11n x 11n matrix, where n is the number of units

included in the system. Alden and Zein[29] obtain the [A] matrix using the formulation based on the PQR Technique, i.e. the form of equation:

$$\begin{bmatrix} P \end{bmatrix} \begin{bmatrix} \dot{y} \\ z \end{bmatrix} = \begin{bmatrix} Q \end{bmatrix} \begin{bmatrix} y \end{bmatrix} + \begin{bmatrix} R \end{bmatrix} \begin{bmatrix} u \end{bmatrix}$$

which gives the efficiency of submatrix build up. This method requires the inversion of an n_v order matrix, where n_v is the number of algebraic variables. Anderson et al.[60] used the PQR method, but the state equations and output equations for each unit are formed separately and are subsequently interconnected to the network. This procedure requires the inversion of 15^{th} order matrices n times, where n is the number of machines included in the system. In all of these works nonsynchronous loads were represented by constant admittances incorporated in the admittance network matrix.

Other methods have been used to model single generators connected to an infinite bus bar. Anderson[25] considered a single machine system, both linear and non-linear models being considered using the PQR method. Mauricio and Semlyen[14] presented a new formulation of the dynamic model of a single generator connected to an infinite bus bar, as explained in Chapter 2. With this method a submatrix, $[K_5]$, of order n_a has to be inverted where n_a is the number of algebraic equations. For big systems this submatrix can become very ill-conditioned. Mauricio and Semlyen[14] indicated that the same problem occurs for a system of two generators and an induction motor load.

3.3 DERIVATION OF THE STATE SPACE FORMULATION FOR MULTI-MACHINE SYSTEMS

The method described in this section is an adaptation of that proposed by Mauricio and Semlyen[14], described in Chapter 2. The system model may be open or closed-loop. In the latter case, set points such as desired terminal voltages or speed changer settings are explicitly available. This form enables novel schemes of control to be derived directly using various methods of multi-variable control system design. The procedure presented here avoids the need to directly invert any submatrix in obtaining the [A] characteristic matrix. A matrix inversion-multiplication is obtained instead, which copes with the ill-condition and sparsity of a submatrix. Neither of these advantages were directly available using the procedure recommended by Mauricio and Semlyen[14].

The method requires that the state of the system be described in terms of a set of first order differential equations in terms of the perturbed values in the form:

$$\dot{y}(t) = [A]\ y(t) + [B]\ u(t) \qquad (3.1)$$

The [A] matrix may then be examined for stability using eigenvalue analysis.

3.3.1 System Representation

Any power system has the configuration shown in Figure 3.1, in which three types of components are identified, namely synchronous machines, linear passive networks and non-synchronous loads. Each

synchronous machine is described by the set of Park's equations[13,14] as given in Appendix B.1. The network is described by the power load flow equations of Newton-Raphson polar form given in Chapter 2 for a simple power system and developed for a multi-machine system in Appendix B.1. In order to investigate how the load characteristics affect the system stability several types of load have been considered. These are:

1. Non-linear passive loads, which are a function of voltage[38], the function being variable.

2. Shackshaft's load model[39], having a constant impedance passive load in parallel with induction motors. Power consumption is related to voltage and phase variations.

These two types of load are incorporated in the network equations, as shown in Appendix B.1.

The excitation systems are assumed to have a single time constant[14]. Each primemover is controlled by an appropriate speed governor. A typical hydrospeed governor similar to that used in Reference 55 was used for the hydraulic plants and for the thermal plants the arrangement was based on the Kingsnorth and Didcot installations[63]. Block diagrams and equations for both types are given in Appendix B.2.

3.3.2 Derivation of the State Equations

The complete system of differential and algebraic equations has, after linearization, the general form:

$$[K]\begin{bmatrix}\dot{y}(t)\\ y(t)\\ z\end{bmatrix} = [B_o]\,u(t) \qquad (3.2)$$

which can be rewritten in a developed form as:

$$[K_1]\,\dot{y}(t) + [K_2]\,y(t) + [K_3]\,z = [B_o]\,u(t) \qquad (3.3)$$

$$[K_4]\,y(t) + [K_5]\,z = [0] \qquad (3.4)$$

These equations give the state space equation (3.5), which may be used to assess the dynamic stability of the system:

$$\dot{y}(t) = [A]\,y(t) + [B]\,u(t) \qquad (3.5)$$

where:
$$[A] = [K_1]^{-1}\left\{[K_3][K_5]^{-1}[K_4] - [K_2]\right\} \qquad (3.6)$$

$$[B] = [K_1]^{-1}[B_o] \qquad (3.7)$$

Numerical difficulties were to be expected in the inversion of the submatrix $[K_5]$ for multi-machine systems as this matrix was found to be very ill-conditioned even for small systems[14]. In order to avoid this difficulty, the new formulation described in this section reduced some of the algebraic equations in equation (3.4), minimizing the order of $[K_5]$, thus reducing computer storage and processing time. Also, instead of inverting $[K_5]$ in equation (3.6) by a direct method, it was solved as a set of real linear equations

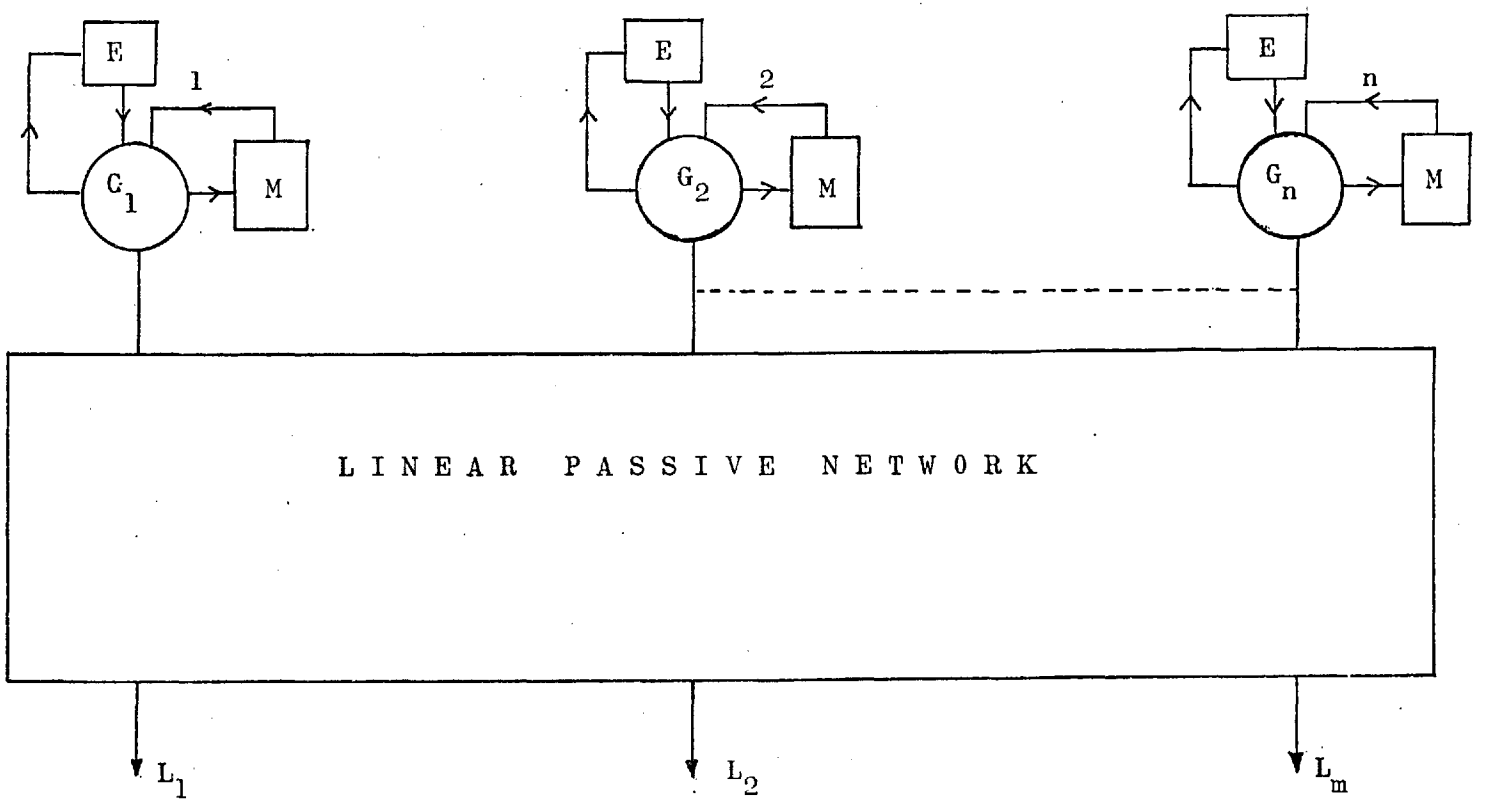

Figure 3.1: Configuration of typical power system for dynamic stability studies. E-excitation system, M-primemover system, G-synchronous machines.

with multiple right-hand sides, $[K_5][X_{SOL}] = [K_4]$, by Crout's method[31], which gives directly the product $[K_5]^{-1}[K_4]$ required in equation (3.6).

As the $[K]$ matrix in equation (3.2) is extremely sparse, sparse matrix techniques are applied for the storage of the submatrices in equations (3.3) and (3.4). This technique is applied mainly when the $[K_1]^{-1}$ elements were obtained directly without the inversion of that matrix, and stored as the submatrices $[K_2]$, $[K_3]$ and $[B_o]$ in equations (3.6) and (3.7). This gives a simpler form of $[A]$ matrix which is easier to use.

The state variables for the description of n machines is selected as:

$$y(t)^t = [\ \Delta\psi_{fd_1}\ \Delta\psi_{d_1}\ \Delta\psi_{kd_1}\ \Delta\psi_{q_1}\ \Delta\psi_{kq_1}\ \Delta E_{fd_i}\ \Delta\delta r_1\ \Delta n_1$$
$$\Delta\omega h_1\ \Delta\omega h_2\ \Delta\omega i_2\ \ldots\ \Delta\psi_{fd_n}\ \Delta\psi_{d_n}\ \Delta\psi_{kd_n}\ \Delta\psi_{q_n}$$
$$\Delta\psi_{kq_n}\ \Delta E_{fd_n}\ \Delta\delta r_n\ \Delta n_n\ \Delta gf_n\ \Delta g_n\ \Delta h_n] \qquad (3.8)$$

The algebraic variables for an n machine and m node system are selected and ordered as follows:

$$z^t = [\Delta\delta_1\ \Delta V_1\ \ldots\ \Delta\delta_m\ \Delta V_m\ \Delta P_1\ \Delta Q_1\ \ldots\ \Delta P_m\ \Delta Q_m\ \Delta V_{d1}\ \ldots$$
$$\Delta V_{dn}\ \Delta V_q\ \ldots\ \Delta V_{qn}\ \Delta i_{fd_1}\ \Delta i_{d_1}\ \Delta i_{kd_1}\ \Delta i_{q_1}\ \Delta i_{kq_1}\ \ldots$$
$$\Delta i_{fd_n}\ \Delta i_{d_n}\ \Delta i_{kd_n}\ \Delta i_{q_n}\ \Delta i_{kq_n}] \qquad (3.9)$$

Non-linear passive loads with only voltage dependence have been taken into the analysis. The linearized form can be expressed

as in Chapter 2 by:

$$\Delta P_{Li} = K_{pi} \frac{P_{Li}}{V_i} - \Delta V_i \tag{3.10}$$

$$\Delta Q_{Li} = K_{qi} \frac{Q_{Li}}{V_i} - \Delta V_i \tag{3.11}$$

$i = 1, 2, \ldots, n^o$ of load.

A combined load was also taken into the analysis; the linearized form of the equations is obtained in Chapter 2 and they are repeated in this section as follows:

$$\Delta P_{Li} = \left[2V_i(G_{mi}+G_{si}) - V_{mi}Y_{mi}\cos(\theta_{mi}+\delta_i)\right]\Delta V_i + \left[V_i V_{mi} Y_{mi} \sin(\theta_{mi}+\delta_i)\right]\Delta\delta_i \tag{3.12}$$

$$\Delta Q_{Li} = \left[2V_i(G_{mi}+G_{si}) - V_{mi}Y_{mi}\sin(\theta_{mi}+\delta_i)\right]\Delta V_i - \left[V_i V_{mi} Y_{mi} \cos(\theta_{mi}+\delta_i)\right]\Delta\delta_i \tag{3.13}$$

$i = 1, 2, \ldots,$ no. of load.

The detailed linearized system equations for a two-machine system and three nodes are given in Appendix B.1. These equations are arranged in order to obtain the equations (3.3) and (3.4). This sample system is given as an example, but the method and the program are general for n machines and m nodes, only being limited by the computer storage capacity. The program was written in Fortran IV for CDC 6400 and Cyber 174 computers, available at the Imperial College, and is able to hold a system of nine machines with full representation (7 states), a.v.r. (1 state) and speed governor (3 states), and thirteen nodes with a variety of load characteristics.

3.3.3 Selection of the Angular Reference

An important point in the stability studies of multi-machine systems is the selection of the angular reference. For the present analysis the method presented by Undrill[5] was used. He considered that the network frequency is identical to that of one arbitrarily chosen machine so that the network reference rotates in synchronism with the axes (d_j, q_j) of that machine. This implies that the rotor angle deviation $\Delta\delta_r$ of the j^{th} machine is always zero and that rotor angle changes may conveniently be expressed relative to the rotor angle of this machine in the system model, so that in general:

$$\Delta\delta r_{ij} = \Delta\delta r_i - \Delta\delta r_j \qquad (3.14)$$

This expresses the rotor displacement of the i^{th} machine relative to the j^{th}, as defined in Figure 3.2. It follows directly from equation (3.14) by differentiation, that:

$$p\Delta\delta r_{ij} = \omega_o(\Delta n_i - \Delta n_j) \qquad (3.15)$$

The procedure to implement these changes in equation (3.5) when the j^{th} machine is the selected reference is:

(i) delete the $\Delta\delta r_j$ and $p\Delta\delta r_j$ from the vectors $\dot{y}(t)$ and $y(t)$;

(ii) delete the row corresponding to $p\Delta\delta r_j$ and the column corresponding to $\Delta\delta r_j$ in the $[K]$ matrix of equation (3.2) before the $[A]$ matrix is built up;

(iii) delete the row corresponding to $p\Delta\delta r_j$ in matrix $[B_o]$ of equation (3.2);

(iv) subtract ω_o from the elements of $[K]$ matrix whose column corresponds to Δn_j and whose row corresponds to $p\Delta\delta r_j$.

This change leaves (3.5) of order 11n-1 with all rotor angles referred to the j^{th} machine. It should be remembered that the j^{th} or reference machine does not represent an infinite bus bar. If it is desired to simulate an infinite bus bar as the reference, all that is required is to delete its speed variable from $\dot{y}(t)$ and $y(t)$ and to delete the corresponding row and column from the $[K]$ matrix, equation (3.2)

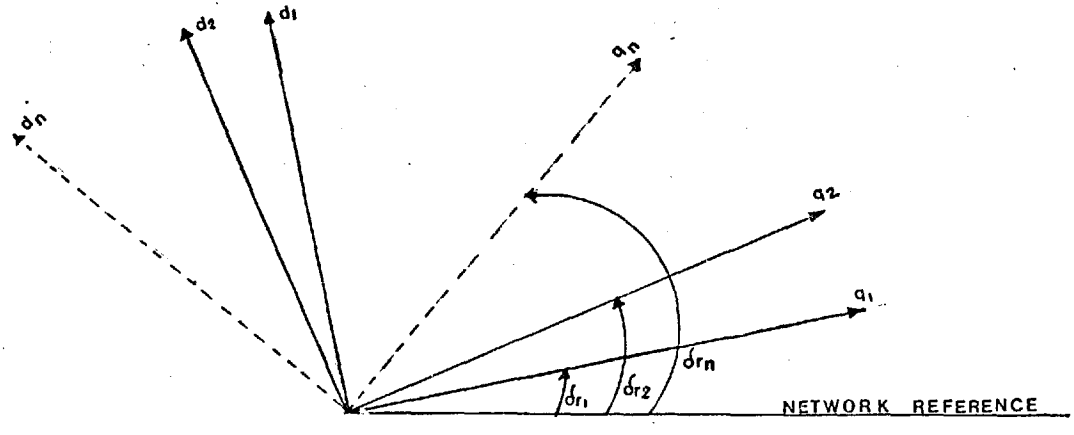

Figure 3.2: Angular relationships between network reference frame and synchronous machine reference axes.

3.4 DIGITAL COMPUTER PROGRAM

A computer program based on the above formulation has been written which makes a dynamic stability analysis of a multi-machine power system in which the effect of load characteristics is considered. The main features of the program are described below.

For this sort of analysis a very large number of matrices is required. The dimensions of these matrices are in general different and if each matrix is represented and stored in a separate two-dimensional array, the storage capacity required becomes excessive even for a very small power system. In this program only four matrices in two-dimensional array have been used for storing and assessing all the matrices required by the method. This was based on the logic of the computing approach; once the information in an array has been used, the array may easily be used for storing the information of other matrices with different dimensions. Furthermore, because of the structure of the matrices explained in Section 3.3.2, sparsity techniques have been used, and substantial computer memory saving has been made.

A general block diagram of the program is given in Figure 3.3, and the basic steps given below. In any dynamic stability analysis, load flow calculations are required to determine the operating point of the system. These calculations are not included in the main program but the variables at each operating point are calculated from the magnitude and phase angle of the voltages and the active and reactive powers at each node, already provided in a magnetic tape by a separate load flow program. After that the

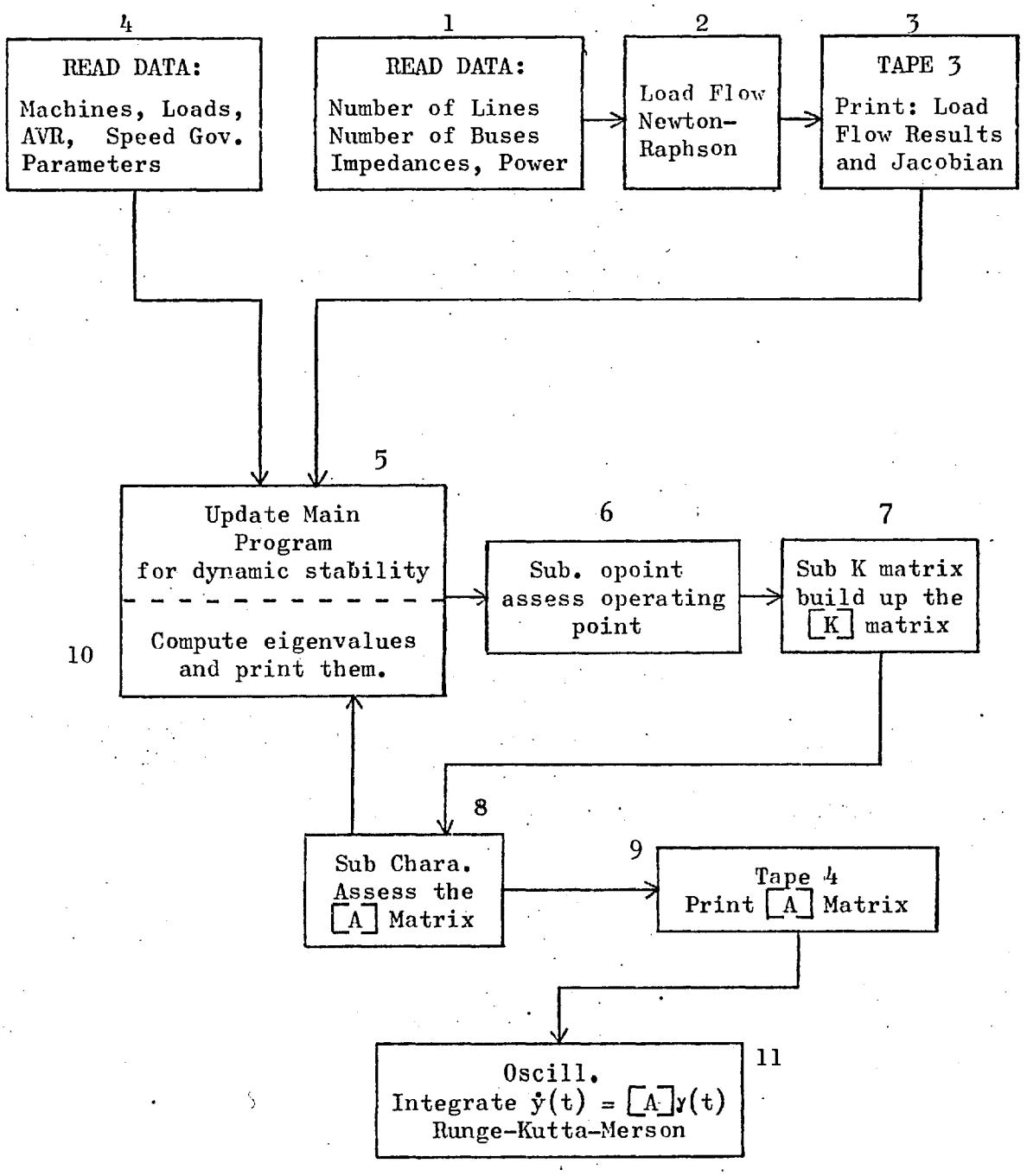

Figure 3.3: Block diagram of the multi-machine dynamic stability computer program.

submatrices of the [K] matrix are built up systematically in order to assess the [A] characteristic matrix of the system. Once this matrix is obtained a standard subroutine[31] is used to compute the eigenvalues of [A] . The eigenvalues of a linear dynamical system correspond to its natural modes of oscillation, with each real part giving the reciprocal decay time constant or damping coefficient of a mode and each pair of imaginary parts giving a natural angular frequency. The necessary and sufficient condition for dynamic stability is that all the eigenvalues have negative real parts, while the forcing frequencies which could lead to hunting problems may be determined by examination of the imaginary parts of the eigenvalues. Thus the program provides a direct check on dynamic stability simply by checking the eigenvalues for positive real parts. This program can also determine the eigenvectors of the system if it is required. Furthermore, the program can use another magnetic tape in order to save the [A] matrix, which may be used to check the results by integrating a system of linear equations $\dot{y}(t) = [A]\, y(t)$, giving the the free response of the system for a small disturbance, using an integration Kutta-Merson subroutine[31]. This method uses five intermediate stages in an interval to get the Last-Value. The Kutta-Merson process uses the equations:

$$y_1 = y_o + \frac{1}{3} hf\ (x_o, y_o)$$

$$y_2 = y_o + \frac{1}{6} hf\ (x_o, y_o) + \frac{1}{6} hf\ (x_o + \frac{1}{3}h, y_1)$$

$$y_3 = y_o + \frac{1}{8} hf\ (x_o, y_o) + \frac{3}{8} hf\ (x_o + \frac{1}{3}h, y_2)$$

$$y_4 = y_o + \frac{1}{2} hf\ (x_o, y_o) + \frac{3}{2} hf\ (x_o + \frac{1}{3}h, y_2) + 2hf(x_o + \frac{1}{2}h, y_3)$$

$$y_5 = y_o + \frac{1}{6} hf\ (x_o, y_o) + \frac{2}{3} hf\ (x_o + \frac{1}{2}h, y_3) + \frac{1}{6} hf\ (x_o + h, y_4)$$

The value of y accepted at the end of the step h is:

$$y = \frac{1}{5}(y_4 - y_5)$$

The results of the integration are plotted by Library subroutine and kept in microfilm.

3.5 APPLICATIONS AND RESULTS

In this section results of dynamic stability studies for two multi-machine systems, one of two machines and three bus-bars, and the other of four machines and five bus-bars, are presented. The systems are shown in Figures 3.4 and 3.5. A variety of load representations was tried in both systems. Finally, a system of nine machines and thirteen bus-bars shown in Figure 3.10 was tested.

In all the cases analysed in this section, the parameters of the units were those given by Davison et al[59]. All the machines were assumed to be of the same capacity, i.e. 1.0 p.u. Data are given in Table 3.1. The values of power, voltage and phase angle obtained by a standard load flow analysis are indicated on each system diagram. These systems were specified quite arbitrarily, but they are intended to be representative of typical real systems. In all cases the action of the speed governors is represented by the models given in Appendix B.2 and the a.v.r. are considered in a classic single time constant representation[14].

In this analysis it was found that the eigenvalues associated with the machine transient stator terms have very high

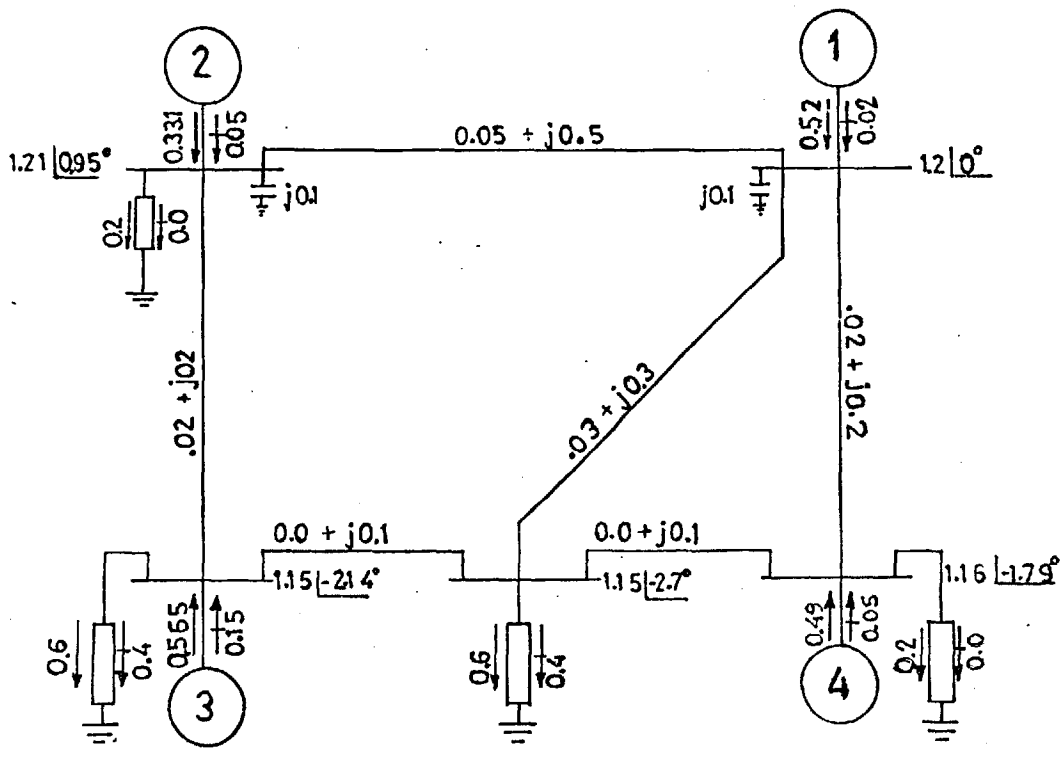

Figure 3.4: Four-machine system, all values are in p.u. referred to a common base.
1,2 Thermoelectric machines.
3,4 Hydroelectric machines.

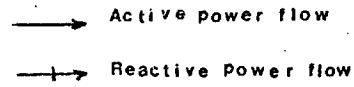

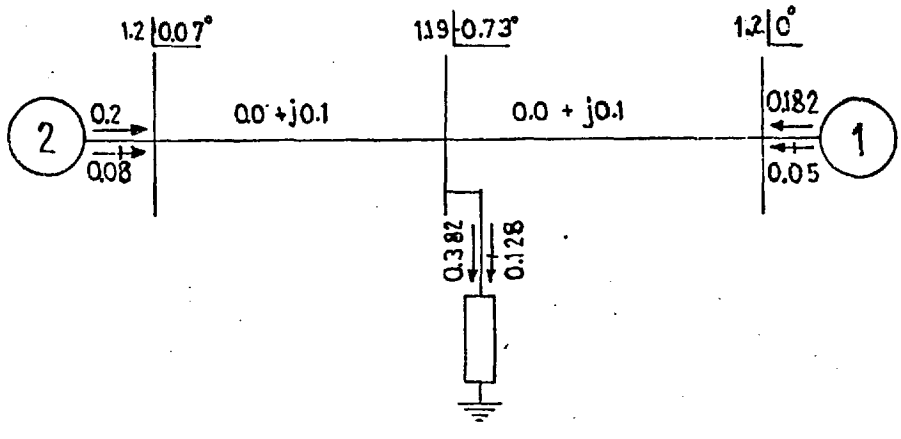

Figure 3.5: Two-machine system, all values are in p.u. referred to a common base.
1, Thermoelectric machine.
2, Hydroelectric machine.

X_{ffd}	= 2.018	X''_q	= 0.175
X_{afd}	= 1.89	r_{fd}	= 0.00124
X_d	= 2.04	r_{kd}	= 0.013
X_{fkd}	= 1.89	r_{kq}	= 0.0261
X_{akd}	= 1.89	r_s	= 0.00125
X_{kkd}	= 1.908	T''_{do}	= 0.031
X_q	= 2.04	T'_{do}	= 4.3
X_{akq}	= 1.89	T''_{qo}	= 0.0167
X_{la}	= 0.15	H	= 6.75
X'_d	= 0.27	K_r	= -20
X''_d	= 0.175	T_E	= 0.5

Table 3.1: Representative parameters of a 500 MW thermal machine, and a.v.r. constants. Machine parameters are in p.u. at rated power base.

Note: The only change made in the constants of the hydraulic machine (apart from the speed governor representation) is in the constant X_q which was assumed equal to X_q = 1.29 p.u. following Davison et al[59].

damping and a very high natural frequency when a steady state network representation is used, and loads are represented as constant impedances, i.e. $K_p = K_q = 2$ for the non-linear passive form.

When loads are non-linear and passive with coefficients K_{pi}, K_{qi} approaching constant current or constant power or when a combined load is considered and the induction motor load is dominant, this eigenvalue can become highly undamped, indicating an oscillatory system. Table 3.2 shows the eigenvalues for the two-machine system of Figure 3.5 with non-linear passive loads, $K_p = K_q = 2$, $K_p = K_q = 1$, and $K_p = K_q = 0$. A variety of load configurations in both systems Figure 3.4 and Figure 3.5 were considered at each bus-bar. Tables 3.3 and 3.4 indicate when this eigenvalue is negative or positive.

It appears that when an infinite bus bar is considered as the reference machine, this mode of oscillation is absent. A test was performed with a four-machine system, Figure 3.4, but considering all the units as hydroelectric plants with similar data to those used for the system in Chapter 2. Results are shown in Table 3.5.

Figures 3.6-3.9 show the results when the integration subroutine is applied in order to check the eigenvalue results without an infinite bus bar being present and load is constant impedance. A small disturbance in the field flux of 0.05 p.u. was applied to machine no. 1 of the two-machine system in Figure 3.5. The machine is well damped, confirming the eigenvalues of Table 3.2, column 1. The multi-machine system shown in Figure 3.10 was used in order to check the computer program capacity. A typical output of the program for this system is shown in Tables 3.6 and 3.7. The $[A]$ matrix was of the order 98 and the c.p. time was 101.8 seconds.

$K_p = 2$ $K_q = 2$	$K_p = 1$ $K_q = 1$	$K_p = 0$ $K_q = 0$
$-1.52\times10^{5} + j5.70\times10^{3}$	-5.980×10^{8}	$+1.59 \times 10^{4}$
$-1.52\times10^{5} - j5.70\times10^{3}$	-1.72×10^{4}	-1.61×10^{5}
$-1.76\times10^{1} + j6.02\times10^{2}$	$-1.76\times10^{1} + j6.02\times10^{2}$	$-1.76\times10^{1} + j6.02\times10^{1}$
$-1.76\times10^{1} - j6.02\times10^{2}$	$-1.76\times10^{1} - j6.02\times10^{2}$	$-1.76\times10^{1} - j6.02\times10^{1}$
-5.13×10^{1}	-5.13×10^{1}	-5.13×10^{1}
-3.90×10^{1}	-3.88×10^{1}	-3.86×10^{1}
-3.63×10^{1}	-3.62×10^{1}	-3.62×10^{1}
$-0.34\times10^{1} + j0.77\times10^{1}$	$-0.34\times10^{1} + j0.77\times10^{1}$	$-0.33\times10^{1} + j0.77\times10^{1}$
$-0.34\times10^{1} - j0.77\times10^{1}$	$-0.34\times10^{1} - j0.77\times10^{1}$	$-0.33\times10^{1} - j0.77\times10^{1}$
-1.0×10^{1}	-1.0×10^{1}	-1.0×10^{1}
-0.697×10^{1}	-0.715×10^{1}	-0.733×10^{1}
-0.333×10^{1}	-0.430×10^{1}	-0.430×10^{1}
$-0.101\times10^{1}+j0.283\times10^{1}$	$-0.101\times10^{1}+j0.280\times10^{1}$	$-0.100\times10^{1}+j0.277\times10^{1}$
$-0.101\times10^{1}-j0.283\times10^{1}$	$-0.101\times10^{1}-j0.280\times10^{1}$	$-0.100\times10^{1}-j0.277\times10^{1}$
$-0.153\times10^{1}+j0.135\times10^{1}$	$-0.153\times10^{1}+j0.135\times10^{1}$	$-0.153\times10^{1}+j0.135\times10^{1}$
$-0.153\times10^{1}-j0.135\times10^{1}$	$-0.153\times10^{1}-j0.135\times10^{1}$	$-0.153\times10^{1}-j0.135\times10^{1}$
$-0.116 + j0.914$	$-0.114 + j0.917$	$-0.112 + j0.92$
-0.182	-0.182	-0.182
-0.999	-0.999	-0.999
-1.0×10^{2}	-1.0×10^{2}	-1.0×10^{2}

Table 3.2: Typical output showing the eigenvalues of a two-machine system. Load represented as non-linear passive load.

Case	Load Coefficient		$\lambda < 0$ $\lambda > 0$
	K_p	K_q	
1	1	1	-
2	1.5	1.5	-
3	2.0	0	-
4	3	0	-
5	3	2	-
6	0	0	+
7	1	0	+
8	0	1	+
9	0	6	+
10	0	2	+
11	Combined load including 60% induction motor load.		+

Table 3.3: Sign of an eigenvalue for different load configurations of a two-machine and three-node system.

Case	Bus No 2		Bus No 3		Bus No 4		Bus No 5		$\lambda<0$ $\lambda>0$
	K_p	K_q	K_p	K_q	K_p	K_q	K_p	K_q	
1	0	0	2	2	0	0	2	2	-
2	0	0	0	0	2	2	2	2	-
3	1	1	1	1	1	1	2	2	-
4	0	0	2	2	2	2	0	0	-
5	1	1	1	1	2	2	2	2	-
6	2	2	2	2	1	1	1	1	-
7	2	2	2	2	2	2	2	2	-
8	0	2	0	2	2	2	2	2	-
9	0.5	2	2	0	0.1	1.5	2	0	-
10	1.1	1.5	0.1	1.5	2	2	2	2	-
11	2	0	2	0	2	0	2	0	-
12	1	1	1	1	1	1	1	1	+
13	0	0	0	0	0	0	0	0	+
14	1	1	2	2	0	0	0	0	+
15	0.5	2	0.5	2	0.5	2	0.5	2	+
16	0	2	0	2	0	2	0	2	+
17	0	0	0	0	0	0	2	2	+
18	2	2	Combined Load: 6% Induction Motor Load		2	2	Combined Load: 6% Induction Motor Load		-
19	2	2	Combined Load: 47% Induction Motor Load		2	2	Combined Load% 47% Induction Motor Load		+

Table 3.4: Sign of an eigenvalue for different load configurations of a four-machine system and five nodes.

Non-linear passive load $K_p=K_q=0$ Machine no. 1 as a reference.	Non-linear passive load $K_p=K_q=0$ Infinite bus-bar as reference.
Matrix of order 42	Matrix of order 33
-1.98×10^{3}	
$+1.74 \times 10^{3}$	
$-0.30\times10^{2} \pm j0.573\times10^{3}$	$-0.32\times10^{2} \pm j0.706\times10^{3}$
$-0.24\times10^{2} \pm j0.478\times10^{3}$	$-0.27\times10^{2} \pm j0.511\times10^{3}$
$-0.19\times10^{2} \pm j0.44\times10^{3}$	$-0.19\times10^{2} \pm j0.45\times10^{3}$
-0.46×10^{2}	-0.46×10^{2}
-0.45×10^{2}	-0.45×10^{2}
-0.45×10^{2}	-0.44×10^{2}
-0.40×10^{2}	-0.37×10^{2}
-0.38×10^{2}	-0.35×10^{2}
-0.36×10^{2}	-0.32×10^{2}
-0.34×10^{2}	
-0.22×10^{2}	
$-0.138\times10^{1} \pm j0.131\times10^{2}$	$-0.129\times10^{1} \pm j0.126\times10^{2}$
$-0.109\times10^{1} \pm j0.115\times10^{2}$	$-0.80\times10^{1} \pm j0.10\times10^{2}$
$-0.125\times10^{1} \pm j0.113\times10^{2}$	$-0.126\times10^{1} \pm j0.114\times10^{2}$
$-0.121\times10^{-1} \pm j0.282$	
-0.185×10^{1}	-0.113×10^{1}
-0.180×10^{1}	-0.151×10^{1}
-0.171×10^{1}	-0.122×10^{1}
-0.628×10^{1}	-0.17×10^{1}
-0.114×10^{1}	-0.18×10^{1}
-0.121×10^{1}	-0.13×10^{1}
-0.130×10^{1}	
-0.134×10^{1}	
-0.326	-0.42
-0.42	-0.42
-0.42	-0.42
-0.42	
-0.89×10^{-2}	-0.88×10^{-2}
-0.89×10^{-2}	-0.88×10^{-2}
-0.89×10^{-2}	-0.88×10^{-2}
-2.00	
-2.00	-2.00
-2.00	-2.00
-2.00	-2.00

Table 3.5: Four-machine system dynamic stability results when non-linear passive load representation and different reference machine representation are considered.

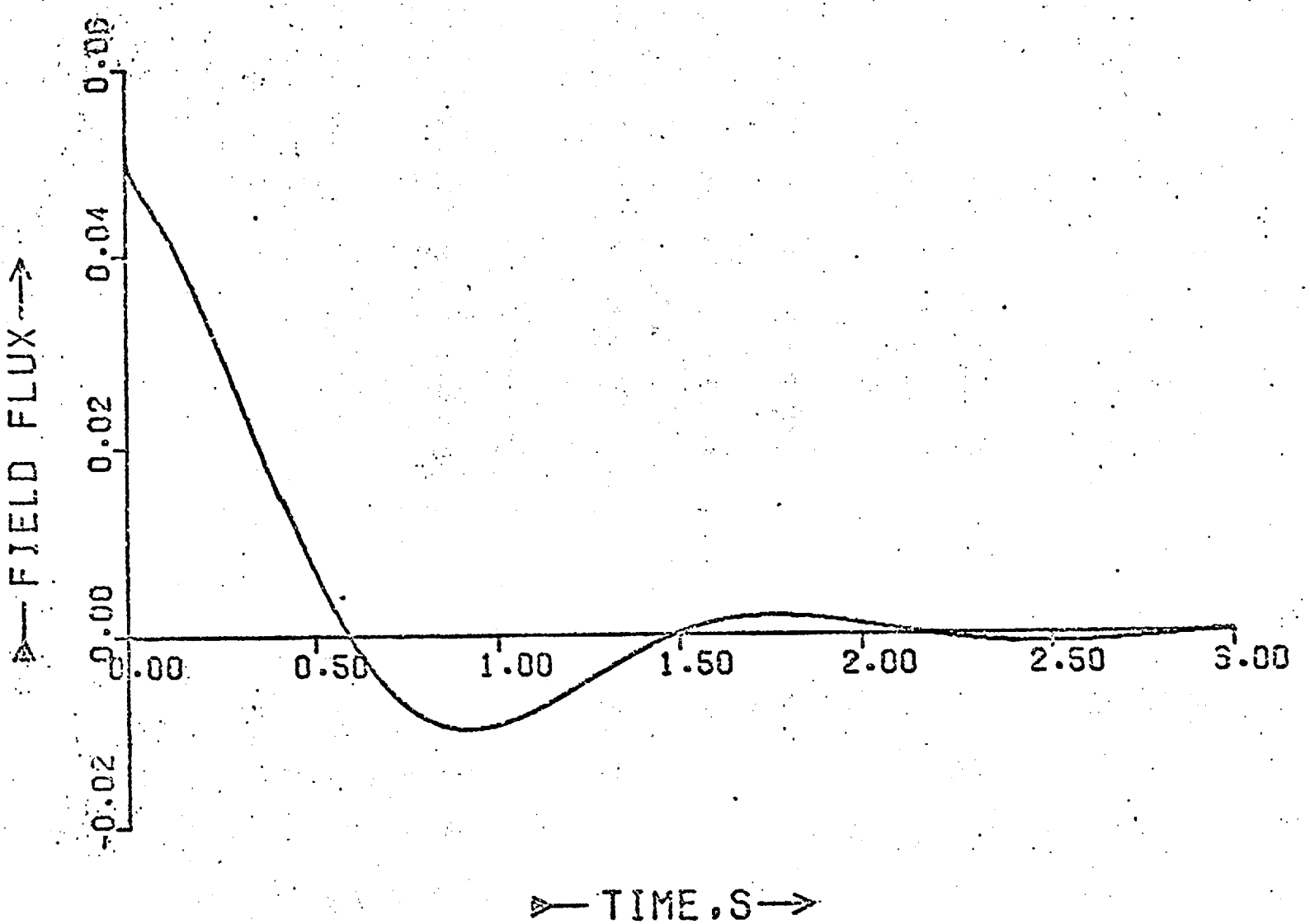

Figure 3.6: Response in the field flux after a disturbance of $\Delta\psi_{fd_1}$ = 0.05p.u.

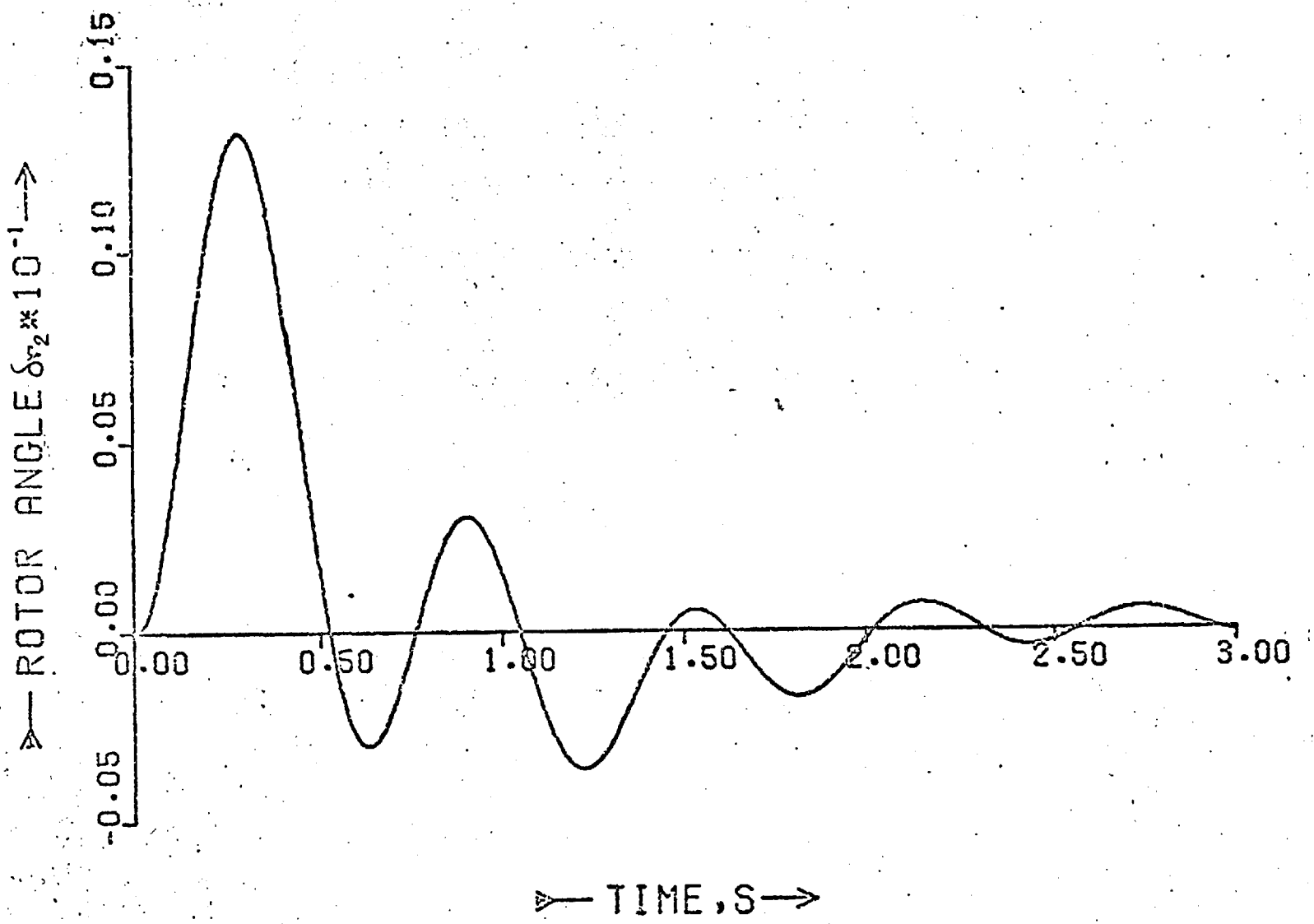

Figure 3.7: Rotor oscillation δ_{r2} after a disturbance of $\Delta\psi_{fd1} = 0.05$ p.u.

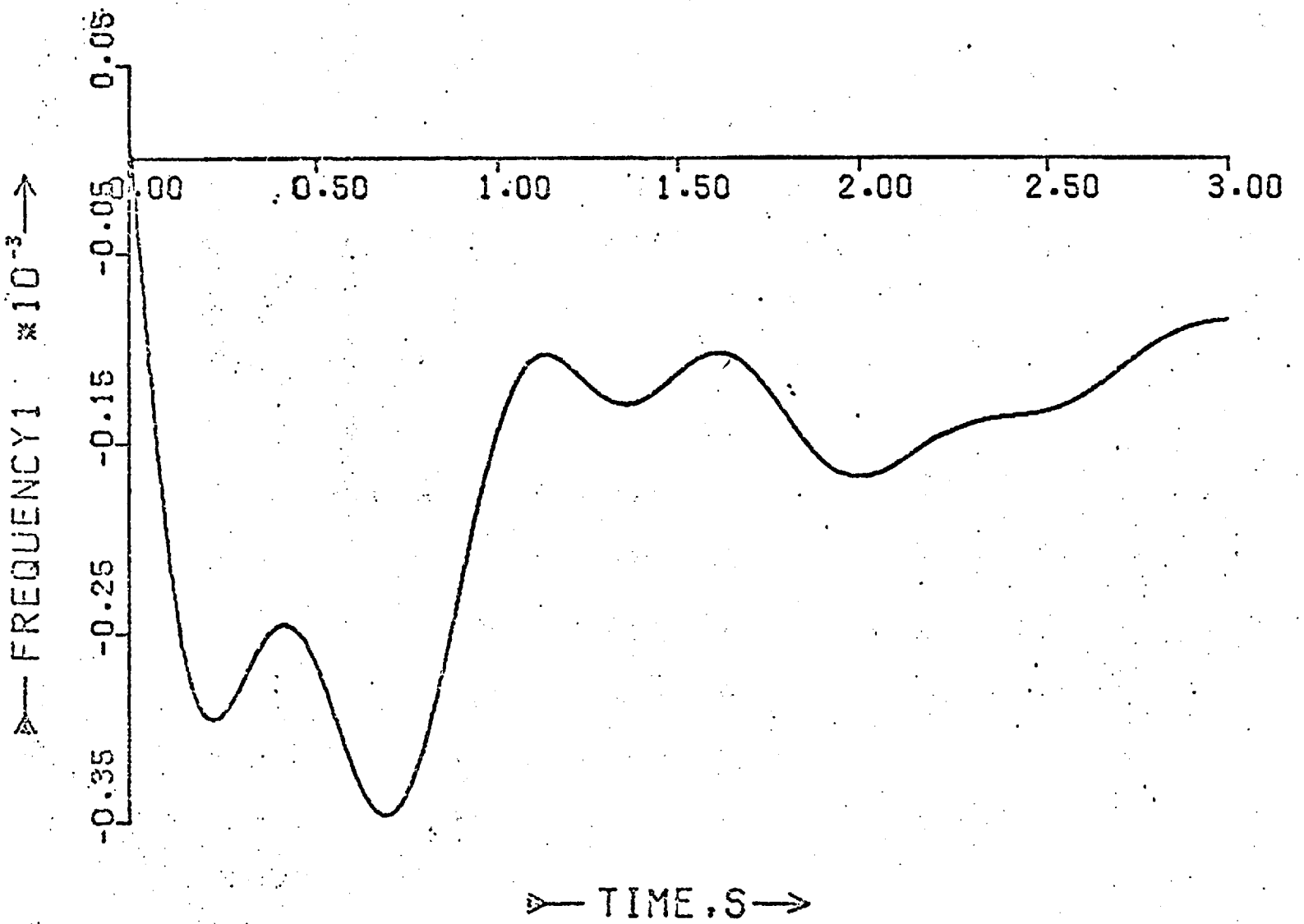

Figure 3.8: Machine No. 1 frequency oscillation (n_1) after a disturbance of $\Delta\psi_{fd_1}$ = 0.05 p.u.

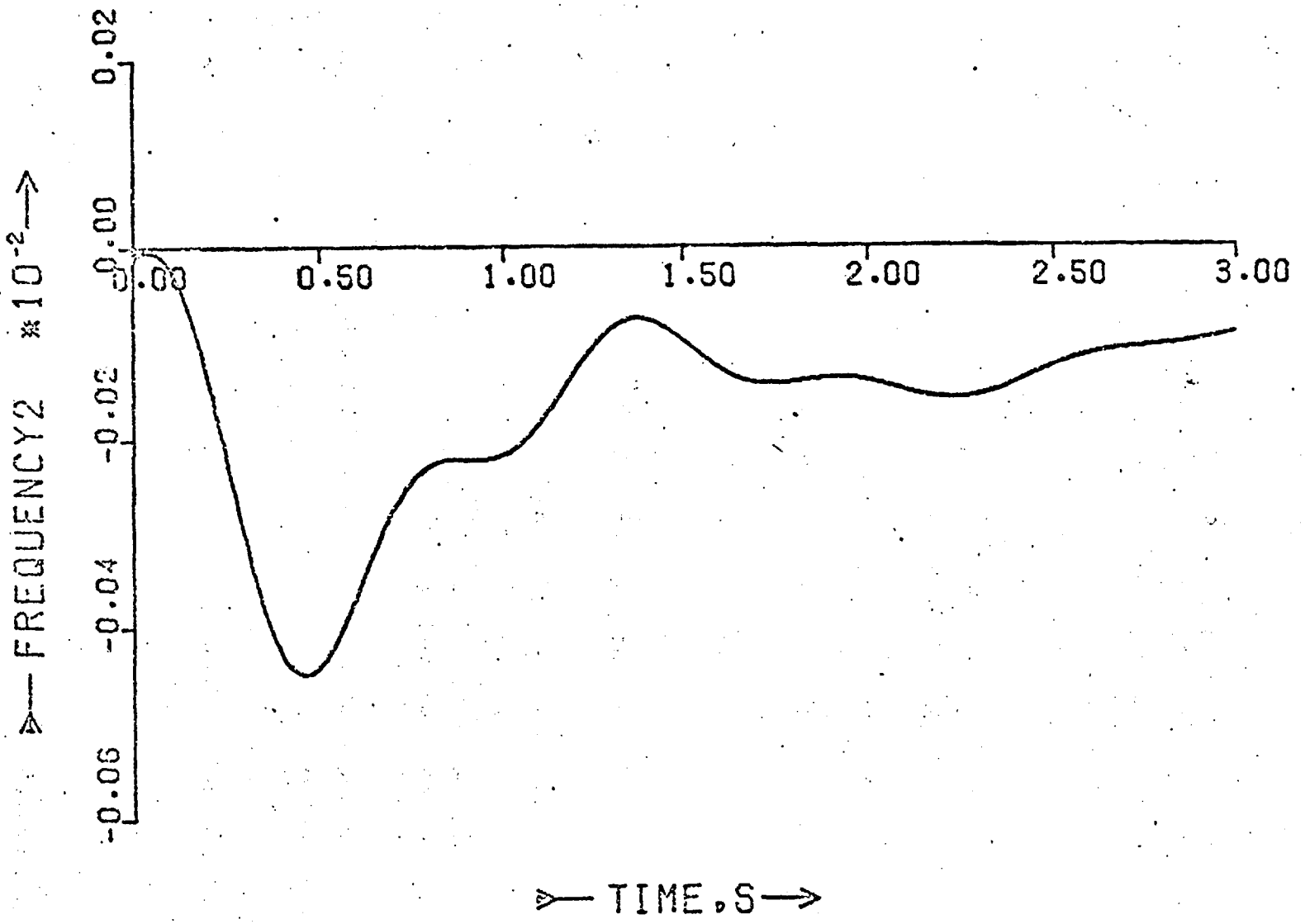

Figure 3.9: Machine No. 2 frequency oscillation (n_2) after a disturbance of $\Delta\psi_{fd_1}$ = 0.05 p.u.

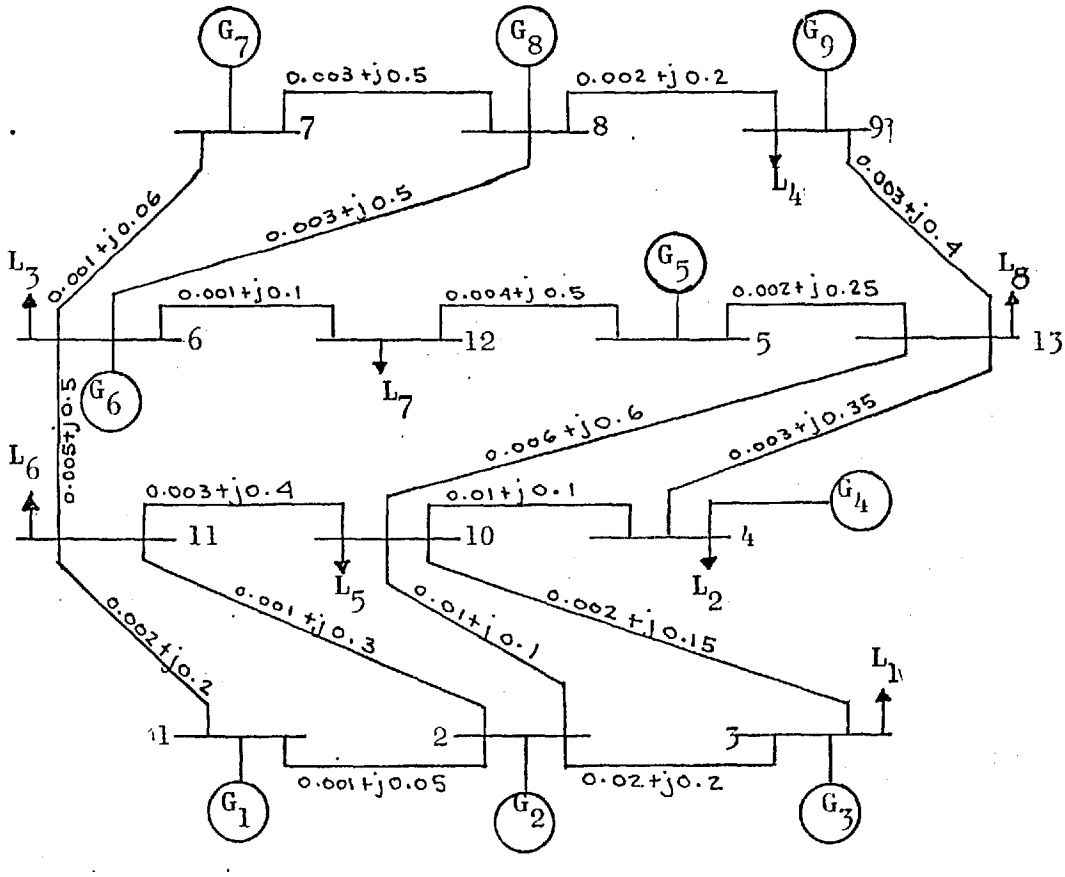

Figure 3.10: Nine-machine and thirteen-node system. Values are in p.u. referred to a common base.

Bus Number	Voltage V Magnitude	Delta (degrees)	P_G	Q_G	P_L	Q_L
1	1.150	0	0.105	0.068		
2	1.151	-0.169	0.400	0.200		
3	1.155	-1.367	0.300	0.300	-0.400	-0.100
4	1.150	-0.753	0.200	0.100	-0.200	
5	1.227	8.184	0.600	0.300		
6	1.263	10.599	0.700	0.400	-0.200	
7	1.280	11.827	0.500	0.300		
8	1.300	13.260	0.600	0.200		
9	1.293	10.788	0.700	0.500	-0.500	-0.100
10	1.135	-1.580			-0.800	-0.500
11	1.133	-0.240			-0.500	-0.400
12	1.229	8.056			-0.700	-0.400
13	1.170	2.285			-0.800	-0.400

Table 3.6: Operating point for a nine-machine and thirteen-node system.

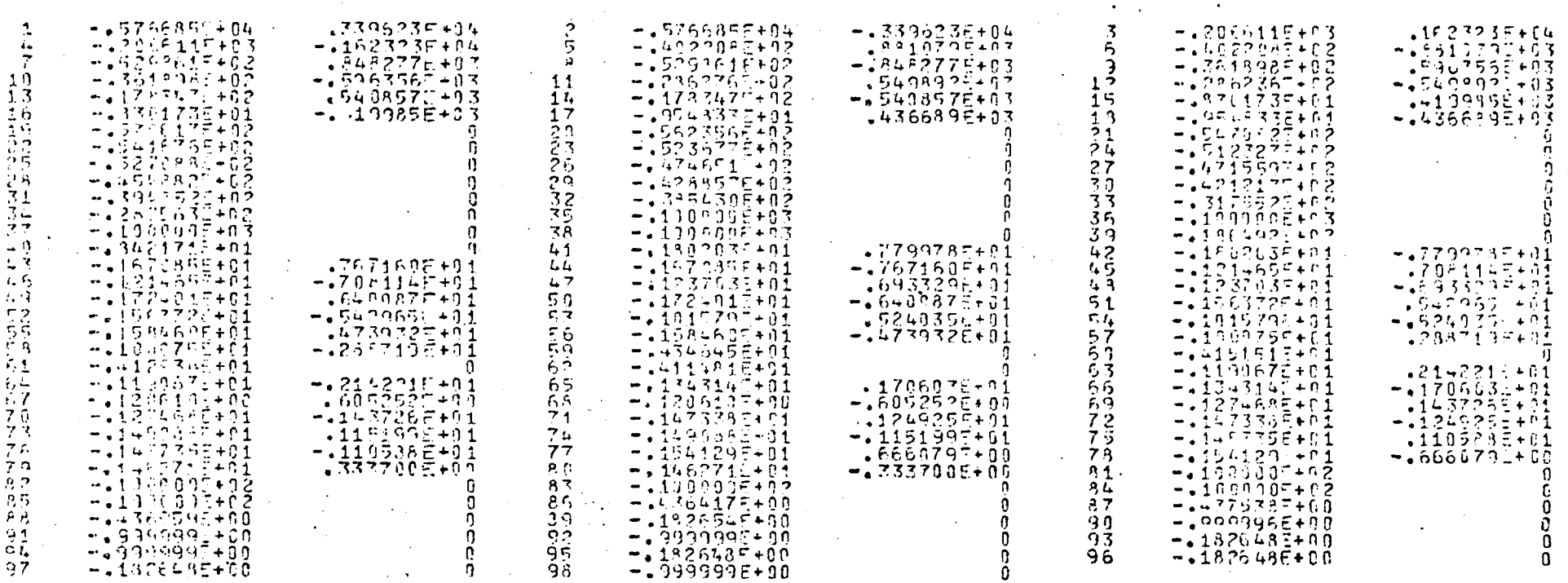

Table 3.7: Eigenvalues for a nine-machine and thirteen-node system.

3.6 CONCLUSION

The signal dynamic model of an arbitrary number of interconnected power generating units including the effect of load characteristics has been developed and implemented in a digital simulation in normal state space form. The results have been checked by integrating the system equations for a small disturbance. In particular:

(i) Different load representations have been included in a multi-machine dynamic stability program, machines being represented in full with a.v.r. and speed governor control equations. The program is able to represent loads as non-linear static loads which are functions of voltage and also as combined loads composed of constant impedance and an equivalent induction motor load. The problem of getting ill-conditioned matrices during the construction of the [A] matrix has been sorted out by making a small rearrangement in the way the algebraic equations are built up, and avoiding matrix inversion. An additional feature of the present model is that an open or closed loop model may be obtained and the system inputs appear explicitly in the state space form.

(ii) It was found that transient stator terms produced very highly damped modes of oscillation when loads were represented as constant impedance, but when the load was represented as non-linear and passive, with coefficients K_{p_i}, K_{q_i} approaching constant power, this mode of oscillation had negative damping. When the reference machine was considered as an infinite bus bar, this undamped oscillation was not present even for a constant power load characteristic.

CHAPTER 4

THE EFFECT OF LOAD CHARACTERISTICS ON THE DESIGN OF FEEDBACK CONTROLLERS OF GENERATORS

4.1 INTRODUCTION

The steady-state stability of power systems becomes doubtful when transmission distances are large and special precautions may become necessary. In recent years the optimal linear regulator theory of linear time-invariant systems with quadratic performance indices has been applied to design controllers for power systems for obtaining improved dynamic behaviour of these systems[52,53,55].

Anderson[52] and Yu et al[55] have suggested multiple feedback controllers, considering a power system consisting of a hydro-generator with exciter, AVR and governor connected to an infinite bus bar through a transmission line. The non-linear mathematical model describing this system was linearized around an operating point to obtain a linear time-invariant state model of the system, valid for small disturbances. Closed form solutions to the minimum integral control problem can be readily obtained if the system is represented in the standard notation by the equation:

$$\dot{y}(t) = [A]\, y(t) + [B]\, u(t) \qquad (4.1)$$

where $[A]$ and $[B]$ are, respectively, nxn and nxp matrices, $y(t)$ is an nxl vector and $u(t)$ is a pxl vector.

Defining a quadratic performance index:

$$J = \int_0^\infty (y'Qy + u'Ru)dt \qquad (4.2)$$

where Q and R are constant positive-definite symmetric matrices and, as usual, the primes denote transposition; Yu et al[55] derived a feedback law in the form:

$$u(t) = -R^{-1}B'Ky(t) \tag{4.3}$$

where K is the constant nxn positive-definite symmetric gain matrix which is the solution of the algebraic equation:

$$KBR^{-1}B'K - Q - A'K - KA = 0 \tag{4.4}$$

The resulting closed loop system defined by the equation:

$$\dot{y}(t) = Gy(t) \tag{4.5}$$

where:

$$G = A - BR^{-1}B'K$$

is asymptotically stable, that is, the eigenvalues of the matrix G all have negative real parts, with better dynamic response than the uncontrolled system given by equation (4.1). In this method the weighting matrices Q and R, specified in the performance index, are arbitrary and a systematic search is necessary to obtain values which give a suitable response.

In this chapter an alternative approach using modal control theory[57,58] is used which directly yields the feedback law while shifting the closed loop eigenvalues to the desired locations. It is well known that any eigenvalues are obtainable for a closed-loop system if the open loop system is controllable. However, in many practical situations only the critical eigenvalues require re-location, and so long as the part of the system with which they are principally associated is controllable, they may be moved

by the addition of feedback loops. This method is used in this chapter to stabilise the performance of the pumped storage station at Ludington (U.S.A.) which was found to be unstable when pumping in extreme conditions[54]. Feedback controllers are designed for several operating conditions, including the effect of local load on the station h.v. bus bar. It is shown that the nature of the load can change the design of the controller.

4.2 METHOD OF ANALYSIS

For this study the power system equations are expressed in the state space form, equation (4.1), by linearizing the differential and algebraic equations around the operating point using the methods explained in Chapters 2 and 3 and that given by Baker et al[47] shown in Appendix C.1.

In order to improve the transient response of the system for small perturbations, the eigenvalues of the $[A]$ matrix are assessed. The impulse response of the system without additional control was also obtained. If the response is unsatisfactory, the system behaviour can be improved by shifting the 'r' critical eigenvalues $\lambda_1, \lambda_2, \ldots, \lambda_r$ using modal control technique[57], to the corresponding new locations $\varrho_1, \varrho_2, \ldots, \varrho_r$, leaving the other eigenvalues undisturbed in the closed loop system.

4.2.1 Theoretical Approach

Modal control theory, given by Porter and Crossley[57], is merely that of generating the input vector of a system by linear feedback of the state vector in such a way that prescribed eigenvalues are associated with the dynamical modes of the resulting closed-loop system. The critical eigenvalues are shifted to the left-hand side of the complex plane such that in the closed-loop system all the eigenvalues are situated within a prescribed region which ensures adequate stability.

4.2.2 Single Input Modal Control Systems

In the case of a state-controllable linear system whose state can be influenced by only one input (or control) variable, $u(t)$, equation (4.1) has the form:

$$\dot{y}(t) = [A]\, y(t) + bu(t) \tag{4.6}$$

where b is an nxl vector and $u(t)$ is a scalar.

The proportional-controller gains necessary to alter 'r' system eigenvalues from $\lambda_1, \lambda_2, \ldots, \lambda_r$, to any desired new positions $e_1, e_2, \ldots, e_r$ are given by:

$$K_j = \frac{\prod_{i=1}^{r} (e_i - \lambda_j)}{p_j \prod_{\substack{i=1 \\ i \neq j}}^{r} (\lambda_i - \lambda_j)} \tag{4.7}$$

which indicates that K_j is calculable if:

$$p_j \neq 0 \qquad (j = 1, 2, \ldots, r),$$

that is, the 'r' modes of the system are controllable and defined by the equation:

$$p_j = V_j^t b \tag{4.8}$$

where V_j is the eigenvector corresponding to the j^{th} eigenvalue of the transposed matrix $[A]$ of the uncontrolled system. The feedback gain vector g is given by:

$$g = \sum_{j=1}^{r} K_j V_j, \tag{4.9}$$

yielding an input variable u(t) given below. If all the elements of the state vector y(t) can be measured by appropriate transducers or estimated by means of an observer:

$$u(t) = F\, y(t) \tag{4.10}$$

where: $F = g^t$.

The control law obtained by substituting from equations (4.7) and (4.9) into equation (4.10) has the form:

$$u(t) = \left[\sum_{j=1}^{r} \frac{\prod_{i=1}^{r} (\varrho_i - \lambda_j) V_j^t}{p_j \prod_{\substack{i=1 \\ i \neq j}}^{r} (\lambda_i - \lambda_j)} \right] y(t) \tag{4.11}$$

This control law will alter the eigenvalues $\lambda_1, \lambda_2, \ldots, \lambda_r$ of the uncontrolled system to prescribed new values $\varrho_1, \varrho_2, \ldots, \varrho_r$, leaving the remaining (n-r) eigenvalues unaltered. It follows by substituting the expression for u(t) given in equation (4.11) into

equation (4.6) that the governing equation of the resulting closed-loop system is:

$$\dot{y}(t) = [A]\, y(t) + b\, F\, y(t) \qquad (4.12)$$

which may be compressed to:

$$\dot{y}(t) = G\, y(t) \qquad (4.13)$$

The eigenvalues and eigenvectors depend upon the feedback loops.

4.2.3 Illustrative Example

The theory of single-input modal control presented in the preceding section can be illustrated by designing a feedback controller for a sample third order system for which the state equation (4.6) has the form:

$$\dot{y}(t) = \begin{bmatrix} -2 & -1 & 1 \\ 1 & 0 & 1 \\ -1 & 0 & 1 \end{bmatrix} y(t) + \begin{bmatrix} 1 \\ 1 \\ 1 \end{bmatrix} u(t) \qquad (4.14)$$

The eigenstructure of this system is given by the following matrices:

$$\Lambda = \begin{bmatrix} 1 & 0 & 0 \\ 0 & -1+j & 0 \\ 0 & 0 & -1-j \end{bmatrix} \qquad (4.15a)$$

$$U = \begin{bmatrix} 0 & 5 & 5 \\ 1 & -3-j4 & -3+j4 \\ 1 & 2+j & 2-j \end{bmatrix} \tag{4.15b}$$

$$V = \frac{1}{10}\begin{bmatrix} -2 & 1+j & 1-j \\ 2 & j & -j \\ 8 & -j & j \end{bmatrix} \tag{4.15c}$$

Λ = nxn eigenvalue matrix of $[A]$ and $[A]^1$.

$U = [u_1\ u_2\ \ldots\ u_n]$ nxn modal matrix of $[A]$.

u_i $(i = 1, 2, \ldots, n)$ eigenvectors of $[A]$.

$V = [v_1\ v_2\ \ldots\ v_n]$ nxn modal matrix of $[A]^1$.

v_j $(j = 1, 2, \ldots, n)$ eigenvectors of $[A]^1$.

n = 3 for this particular example.

The corresponding mode-controllability matrix is:

$$P = V' b = \frac{1}{10}\begin{bmatrix} 8 \\ 1+j \\ 1-j \end{bmatrix} \tag{4.16}$$

In the absence of control (open loop) the system (4.14) has the eigenvalues $\lambda_1 = 1$, $\lambda_2 = -1+j$, $\lambda_3 = -1-j$. It is unstable because of λ_1, but controllable by the input u(t) since $p_1 \neq 0$. The second and the third modes are asymptotically stable and are also both controllable by u(t) since $p_2 \neq 0$ and $p_3 \neq 0$.

The eigenvalues can be changed to $\varrho_1 = -1$, $\varrho_2 = -2+j2$, and $\varrho_3 = -2-j2$ by the proportional controller gains (K_5) associated with the appropriate vectors $v_1^!$, $v_2^!$ and $v_3^!$.

$$K_1 = \frac{(\varrho_1 - \lambda_1)(\varrho_2 - \lambda_1)(\varrho_3 - \lambda_1)}{p_1(\lambda_2 - \lambda_1)(\lambda_3 - \lambda_1)} = -6.5 \qquad (4.17a)$$

$$K_2 = \frac{(\varrho_1 - \lambda_2)(\varrho_2 - \lambda_2)(\varrho_3 - \lambda_2)}{p_2(\lambda_1 - \lambda_2)(\lambda_3 - \lambda_2)} = 7+j \qquad (4.17b)$$

$$K_3 = \frac{(\varrho_1 - \lambda_3)(\varrho_2 - \lambda_3)(\varrho_3 - \lambda_3)}{p_3(\lambda_1 - \lambda_3)(\lambda_2 - \lambda_3)} = 7-j \qquad (4.17c)$$

Equations (4.7) and (4.11) indicate that the required feedback control law is given by the expression:

$$u(t) = K_1 v_1^! y(t) + K_2 v_2^! y(t) + K_3 v_3^! y(t) \qquad (4.18)$$

which, in this case, assumes the form:

$$u(t) = 2.5\, y_1(t) - 1.5\, y_2(t) - 5\, y_3(t) \qquad (4.19)$$

The G matrix of the closed loop system defined by equations (4.14) and (4.19) is:

$$G = \begin{bmatrix} 0.5 & -2.5 & -4 \\ 3.5 & -1.5 & -4 \\ 1.5 & -1.5 & -4 \end{bmatrix}$$

and the eigenvalues of this matrix are:

$$\varrho_1 = -1, \quad \varrho_2 = -2+j2 \quad \text{and} \quad \varrho_3 = -2-j2$$

as required.

4.3 MULTI-INPUT MODAL CONTROL SYSTEMS

The theory for single input systems presented in Section 4.2.2 can be used sequentially to design feedback loops for multi-input systems governed by state equations of the form (4.1). Thus, if the input matrix $[B]$ has the partitioned form:

$$[B] = [b_1 \; b_2 \; \cdots \; b_p] \tag{4.19}$$

then equation (4.1) can be expressed as:

$$\dot{y}(t) = [A]\, y(t) + \sum_{i=1}^{p} b_i \, u_i(t) \tag{4.20}$$

Hence Porter's[57] modal control method applicable to single input systems can be applied sequentially to the system described by equation (4.1) using a multi-stage design procedure, by dividing the 'r' dominant eigenvalues into 'p' groups and shifting in 'p' stages. Only one input defined by Pai et al[61] as the dominant input is used at each stage. Each $u_i(t)$ in equation (4.20) will therefore have the form:

$$u_i(t) = \sum_{j=1}^{r} K_j^{(i)} \, v_j(i)' \, y(t) = g_i' \, y(t) \qquad (i = 1,2,\ldots,p) \tag{4.21}$$

where $K_j^{(i)}$ are the proportional controller gains associated with the i^{th} stage of the design procedure. The resulting closed-loop system has the form shown in Figure 4.1. If 'r_1' eigenvalues are shifted in the first stage by using the input $u_1(t)$, the modal controller gains associated with the first groups are determined by:

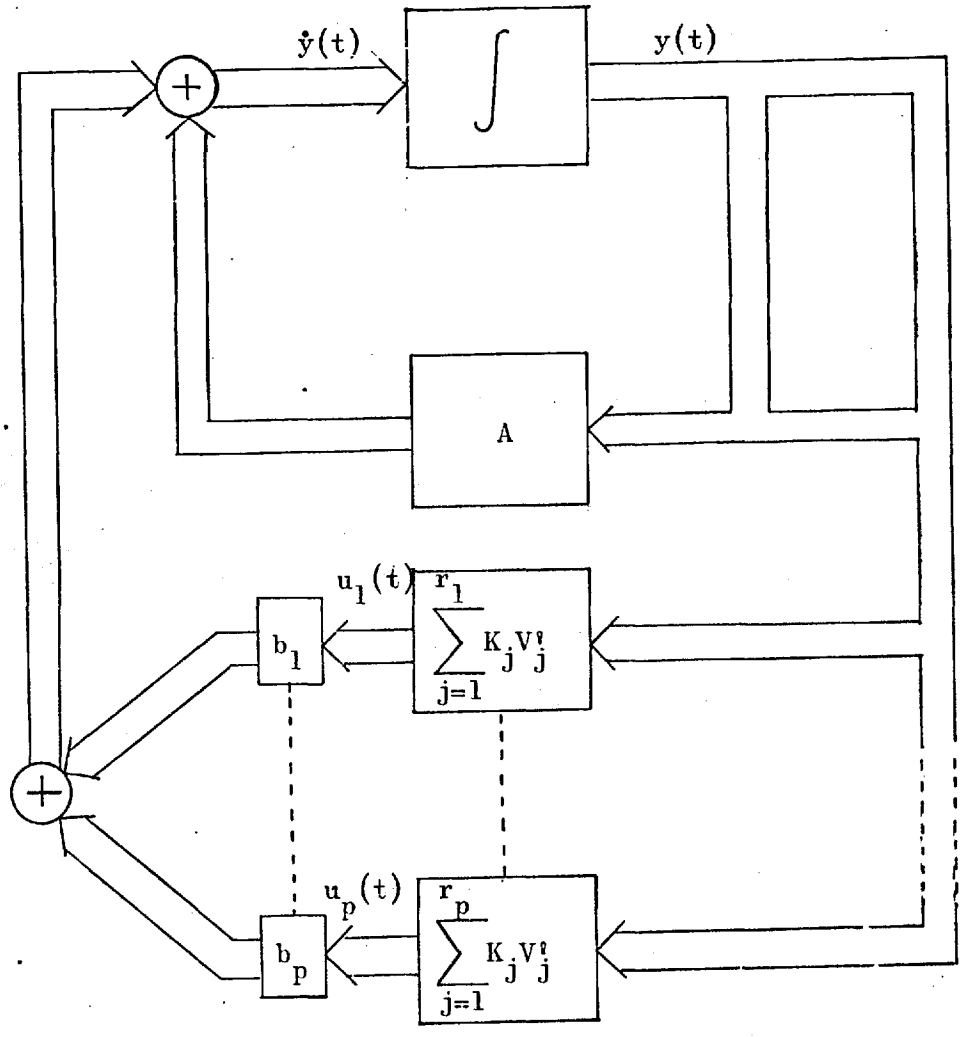

Figure 4.1: Controller design structure.

$$K_j = \frac{\prod_{i=1}^{r_1} (\varrho_i - \lambda_j)}{p_j \prod_{\substack{i=1 \\ j \neq i}}^{r_1} (\lambda_i - \lambda_j)} \qquad (j = 1,2,\ldots, r_1) \tag{4.22}$$

where: $p_j = v_j^t b_1$ (4.23)

Then the feedback gain vector g_1 is given by:

$$g_1 = \sum_{j=1}^{r_1} k_j v_j \tag{4.24}$$

After shifting the first group of eigenvalues, the system matrix for the controlled system becomes:

$$[A]_1 = [A] + b_1 g_1^t \tag{4.25}$$

The matrix $[A]_1$ is used for shifting the second group of eigenvalues and the method is applied sequentially for all the groups, only the dominant input being used for each group.

$$[A]_p = [A] + b_1 g_1^t + b_2 g_2^t + \ldots + b_p g_p^t \tag{4.26}$$

Hence the feedback law is expressed as:

$$u(t) = F\, y(t) \tag{4.27}$$

where the p^{th} row of the modal controller matrix is given by:

$$F_p = g_p^t \tag{4.28}$$

4.3.1 Criterion for the Selection of the Dominant Input

If additional inputs are used for feedback control, these provide means of optimizing the feedback structure. The criterion used here is that of dividing the total number of eigenvalues to be shifted into groups, each group controlled by one particular input called by Pai et al[61] the dominant input for that group. In applying the multi-stage design procedure, the modes to be controlled at the i^{th} stage are chosen on the basis of the magnitudes of the elements of the appropriate mode-controllability matrix:

$$P_i = V_i^{!} B_i \qquad (i = 1,2,\ldots,p) \qquad (4.29)$$

It is evident from equation (4.22) that the gain K_j will be minimum when the P_j element of the controllability matrix is maximum. Hence the optimal modal controller feedback matrix F is obtained if the control input $u_p(t)$ for shifting the j^{th} eigenvalue is so chosen that the absolute value of p_j is maximum. Such an input is known as the dominant input. All eigenvalues for which $u_p(t)$ is the dominant input form the p^{th} group.

4.3.2 Sector Criterion

To preassign the new locations for the critical eigenvalues of the uncontrolled system so as to improve its dynamic behaviour, a sector criterion given by Pai et al[58] is used, which is based on the fundamental concept of damping ratio ζ and undamped natural frequency ω_n, as explained in Figure 4.2.

The new locations for the first critical pair of complex conjugate eigenvalues of the uncontrolled system $(\alpha \pm j\beta)$ are

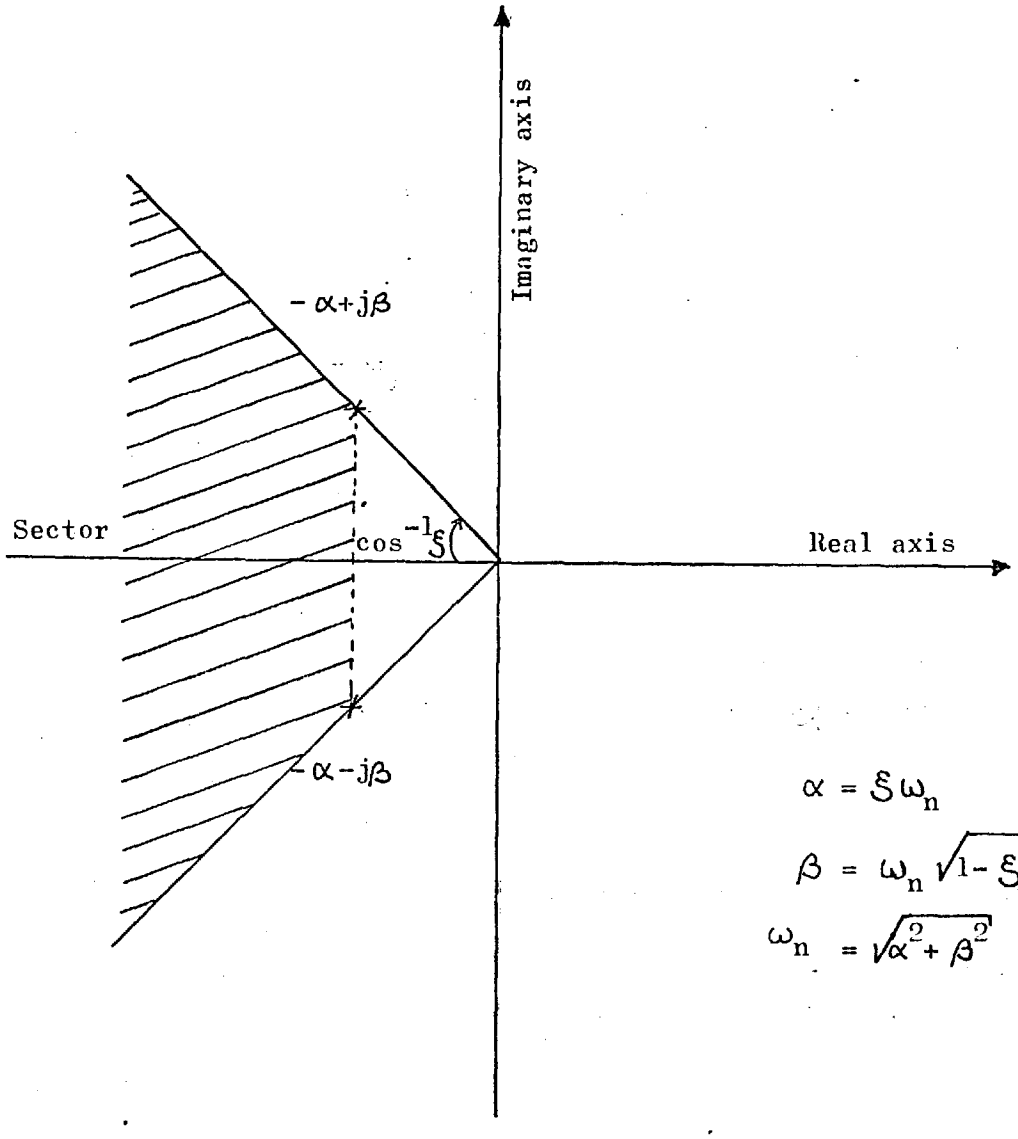

Figure 4.2: Sector definition.

assigned with a desired degree of damping ratio and undamped natural frequency. The remaining critical complex eigenvalues ζ and ω_n are specified to lie within the sector shown in Figure 4.2 to the left of the first pair. The new location for the critical real eigenvalues is arbitrarily chosen such that its value is sufficiently large and negative. However, this choice of new locations for the critical eigenvalues has to be modified when the control law results in high feedback gains which are not practicable. The gains of the feedback matrices obtained for various cases are compared by using a performance index (P.I.) defined by Pai et al[61]:

$$P.I. = \sum_{i=1}^{p} \sum_{j=1}^{n} F_{ij}^{2} \qquad (4.30)$$

4.4 APPLICATION AND RESULTS

A schematic diagram of the power station studied in this section is given by Figure 4.3. Using the published data[54] shown in Table 4.1, the system at Ludington was represented as a single-machine infinite bus-bar system. The electrical machines are studied at full load in both pumping and generating modes. The power station contains six units of 325 MVA each. The machine terminal power was taken as 1.04 p.u. during pumping and 1.0 p.u. during generation. These figures are referred to a base of 1950 MVA.

The AVRs keep the machine terminal voltage constant at about 1.02 p.u. and the infinite bus bar voltage was taken to be 1.00 p.u. During pumping, the gate controls being fixed in one position, transient response was improved by using modal control

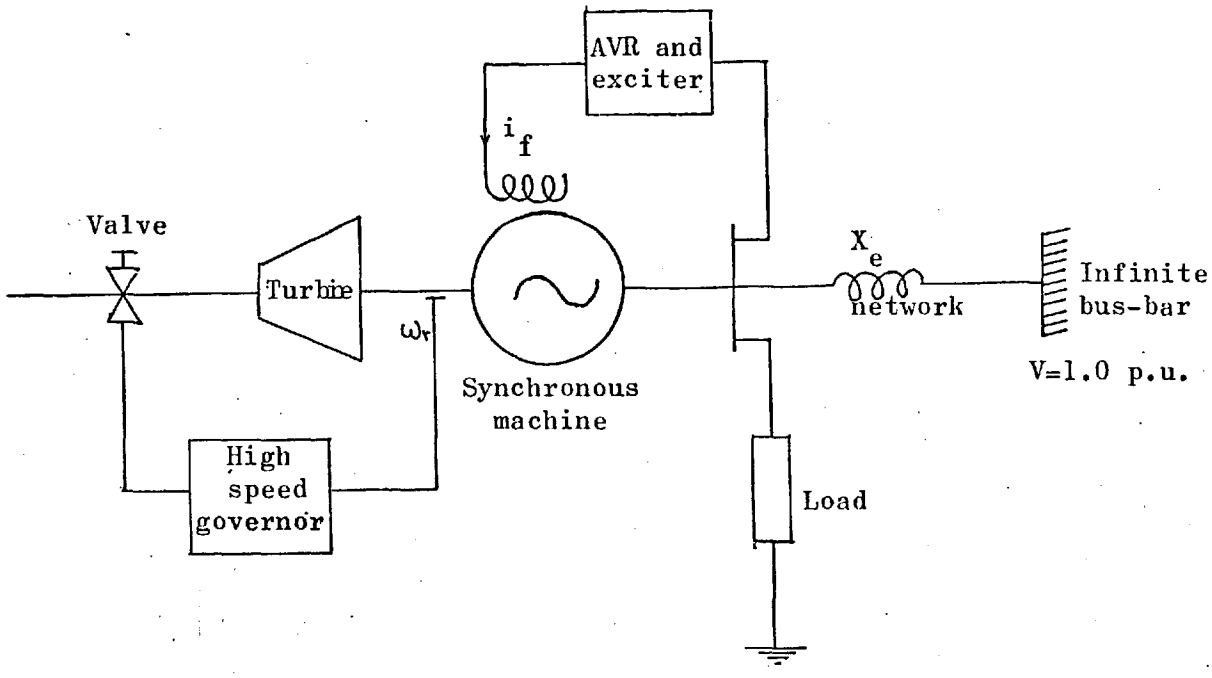

Figure 4.3: The power system at Ludington.

Symbol	Description	Value in p.u.
X_d	d-axis armature reactance	0.85
X_q	q-axis armature reactance	0.48
X_{md}	d-axis magnetizing reactance	0.73
X_{mq}	q-axis magnetizing reactance	0.36
X_{fd}	field reactance	0.935
X_{kd}	d-axis damper reactance	0.89
X_{kq}	q-axis damper reactance	0.46
r_s	armature resistance	0.0016
r_{kd}	d-axis damper resistance	0.014
r_{kq}	q-axis damper resistance	0.014
r_{fd}	field resistance	0.00041
H	inertia constant	7.5 sec
X_e	transmission line + transformer reactance	0.49
r_e	transmission line + transformer resistance	0.00

Table 4.1: Power system parameters.

at the excitation reference voltage, and the effect of different network representation was analysed. During generation, similar control was applied to the excitation reference and the speed reference point, and the effect of various types of load coupled at the machine terminals was considered.

The synchronous machine in both cases was represented by Park's equation of 7^{th} order in p.u. explained in Chapter 2. The excitation system was the IEEE Type No. 1 model (3^{rd} order), similar to that given in Section 2.5, and in generating mode the speed governor was represented by a 3^{rd} order model similar to that used in Chapter 3, Figure B.2.3. Data for both systems are given in Tables 4.2 and 4.3, respectively. In Appendix C.1 the non-linear and linear dynamic system equations are given in detail.

4.4.1 Pumping Mode Operation

The following cases were studied during pumping with the speed governor out of service throughout:

Case 1: The AVR was connected to the system (conventional control).

Case 2: No control loops were considered in the system, i.e. the AVR was out of service (manual control).

Case 3: The AVR was in service, together with modal control.

The non-linear system equations were linearized about the operating point shown in Table 4.4. The linear equations in this part of the analysis were considered in the manner of Baker and

Symbol	Description	Value
K_A	Regulator gain	38.6
T_A	Regulator amplifier time constant	0.1 sec
K_E	Exciter gain	0.182
T_E	Exciter time constant	0.133 sec
K_F	Regulator stabilizing loop gain	0.015
T_F	Regulator stabilizing time constant	0.5 sec
$S_{E_{x,max}}$	Exciter saturation function	0.247
$S_{75}E_{x\ max}$		0.038
$V_{R,max}$(p.u.)	Maximum value of V_R	1.64
$V_{R,min}$(p.u.)	Minimum value of V_R	-1.08

Table 4.2: AVR and Excitation System Parameters.

Symbol	Description	Value
δp	Permanent droop	0.045
Tg	Gate time constant	0.1 secs.
Ta	Governor actuator time constant	0.01 sec.
μ_a	Governor actuator gain	1.0
TW	Water column time constant	1.6 secs.

Table 4.3: Speed Governor Parameters.

Symbol	Description	Value in p.u.
δr	rotor angle respect to infinite bus	-52.8 (deg)
P.F.	power factor (over-excited)	0.96
V_2	terminal voltage	1.02
V_b	infinite bus bar voltage	1.00
P	active power	-1.04
i_d	d-axis current	-0.668
i_q	q-axis current	-0.825
v_d	d-axis voltage	0.397
v_q	q-axis voltage	0.940
E_{fd}	excitation voltage	1.506
i_{fd}	field current	2.063

Table 4.4: Operating point for pumping mode.

Krause[47] using the sign convention explained in Chapter 2. In this representation the transient network terms are included directly. Later in this chapter an alternative network representation is discussed. The state variables for the synchronous machine when pumping mode are:

$$y(t) = [\Delta i_q \; \Delta i_d \; \Delta i_{kq} \; \Delta i_{kd} \; \Delta i_{fd} \; \Delta n \; \Delta \delta r \; \Delta E_{fd}, \; \Delta V_R, \; \Delta V_{ES}]^T \tag{4.31}$$

Table 4.5 shows the eigenvalues of the system for Case 1 and Case 2. From these eigenvalue locations it can be seen that the system can be stabilized, but the transient response is highly unsatisfactory. The plot of the eigenvalues for Case 1, given in Figure 4.4, shows that all but the conjugate pair associated with the natural mechanical oscillation appear in the stable left-hand half-plane. Figure 4.5 shows that the transient response of the system with conventional control (AVR loop only) is quite oscillatory and unstable. When manual control of the terminal voltage is applied the response is as in Figure 4.6. The system is stable but is poorly damped.

The single input modal control method explained in Section 4.2.2 was used to obtain the gain of feedback loops to move the critical eigenvalues firstly to the positions shown in column 2 of Table 4.6, and then to those in columns 3 and 4. The basic control structure is illustrated in Figure 4.7. The transient response, Figures 4.8 to 4.10, is very much better. The resulting feedback gains needed to bring about this relocation are shown in Table 4.7.

Three network representations were then used in order to show how transient network terms affect the dynamics of the system

Location of oscillation	AVR Control only	No Control Loops
Stator winding	-1.039 + j 377 -1.039 - j 377	-1.039 + j 377 -1.039 - j 377
d-axis damping winding q-axis damping winding	-17.83 -15.99	-17.82 -15.93
Excitation system stabilizer	-5.42 + j 7.32 -5.42 - j 7.32	
AVR and field winding	-2.15 + j2.238 -2.15 - j2.238	-18.5
Mechanical	+0.273 + j4.74 +0.273 - j4.74	-0.223 + j4.94 -0.223 - j4.94

Table 4.5: Eigenvalues of the equivalent machine infinite bus-bar Ludington system.

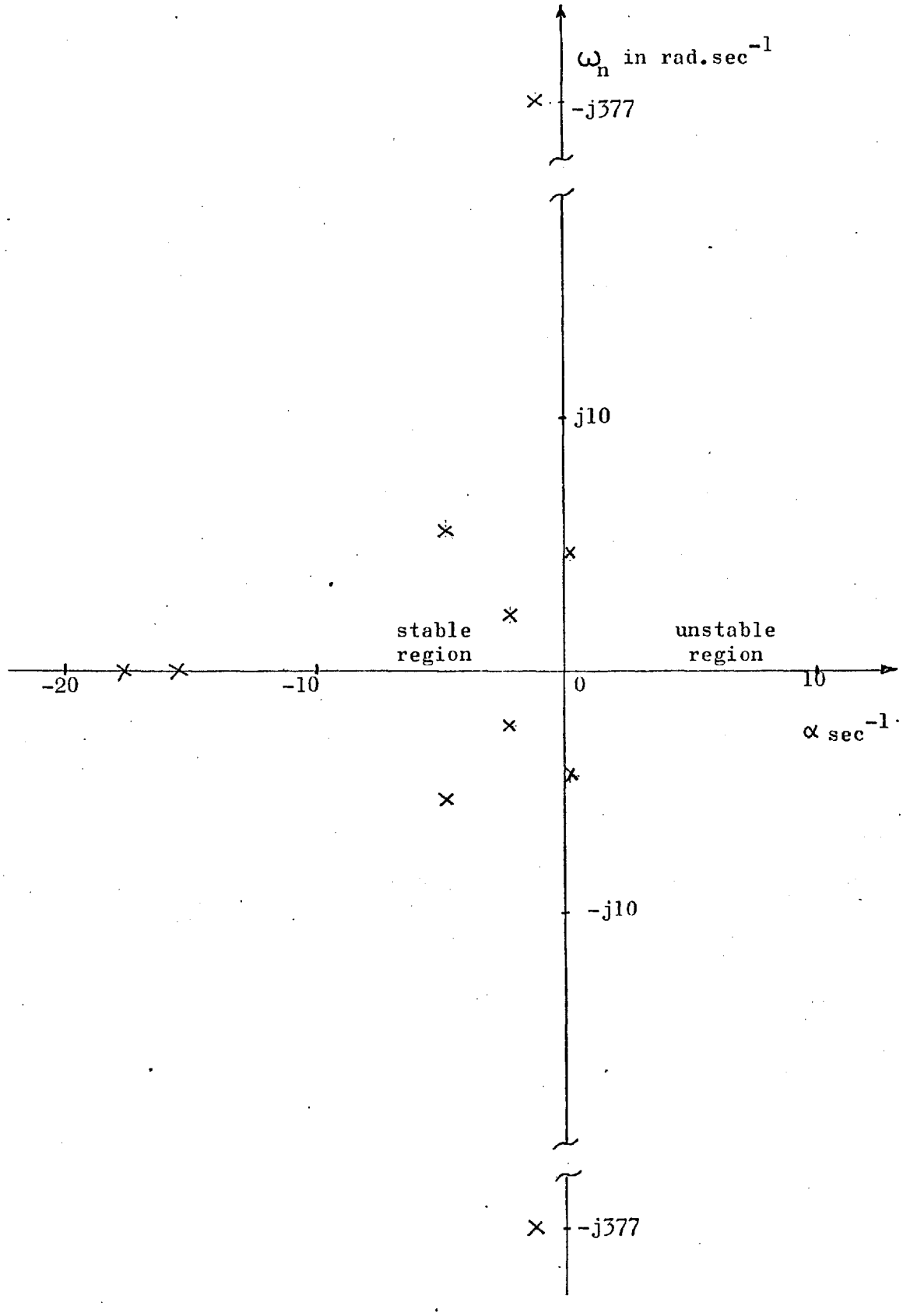

Figure 4.4: Eigenvalues for the one-machine infinite bus bar equivalent of Ludington when conventional control is used during pumping mode.

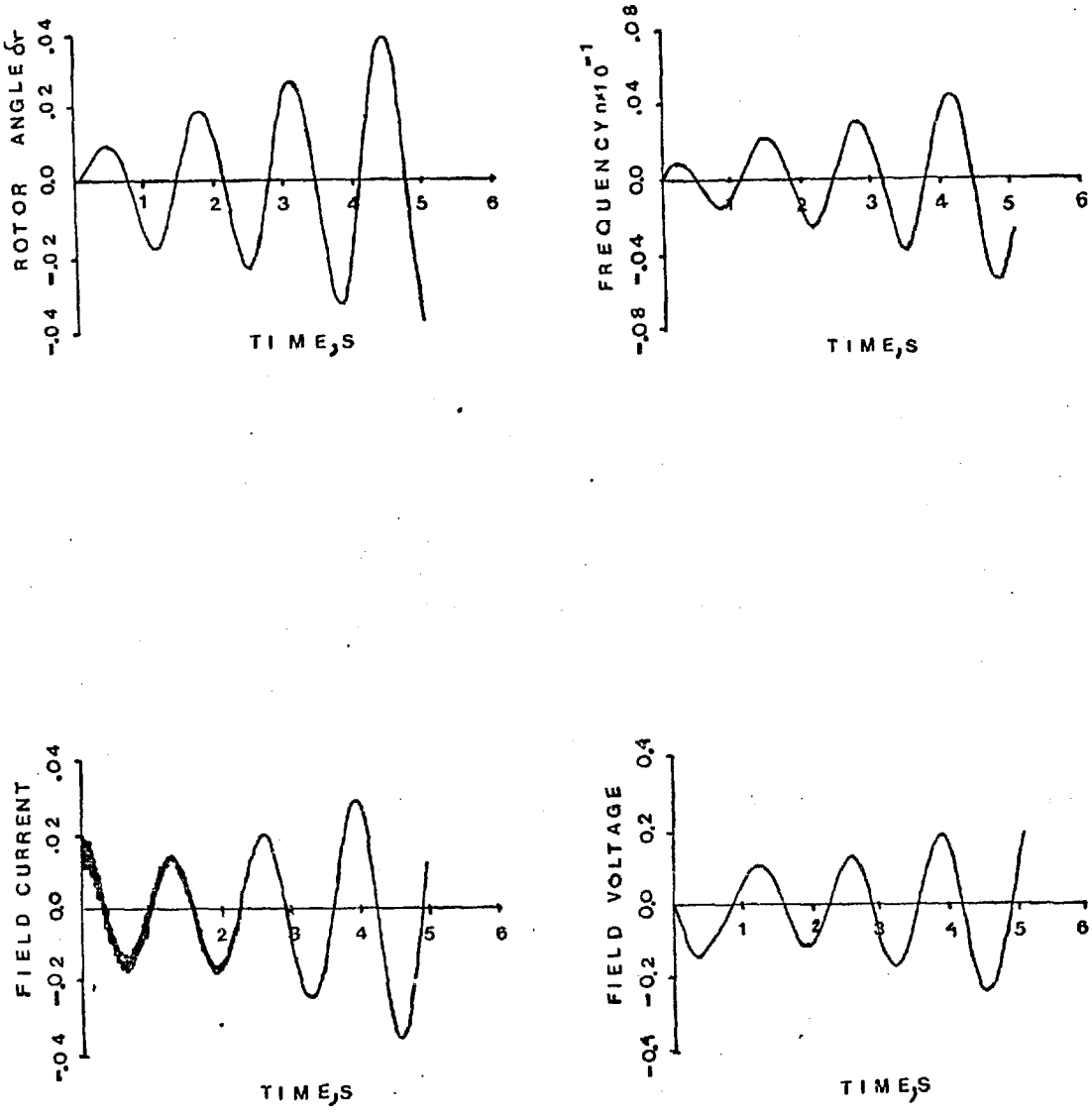

Figure 4.5: Various system variable responses following a change of $\Delta i_{fd} = 0.01$ p.u. with conventional control.

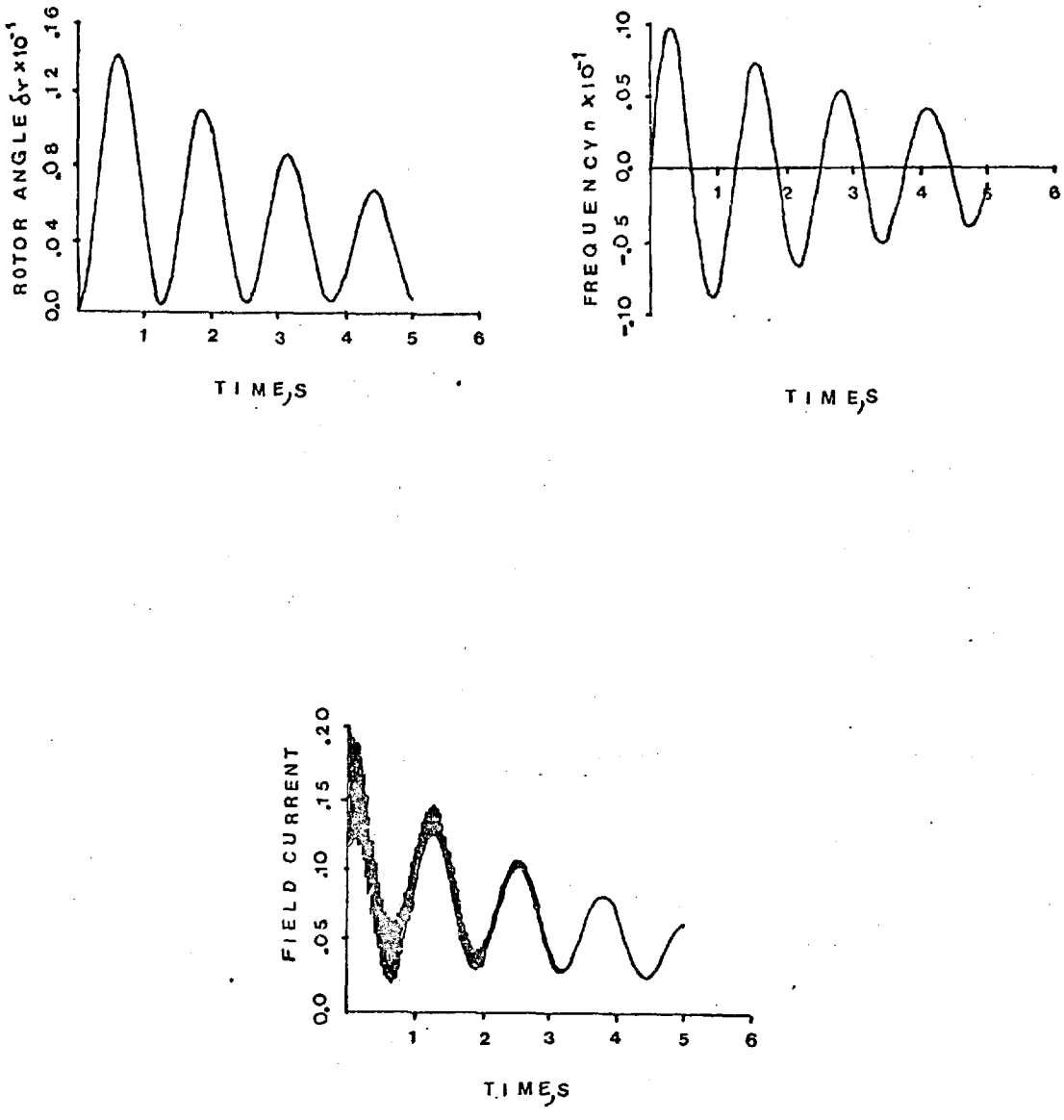

Figure 4.6: Various system variable responses following a change of $\Delta i_{fd} = 0.01$ p.u. when manual control is applied.

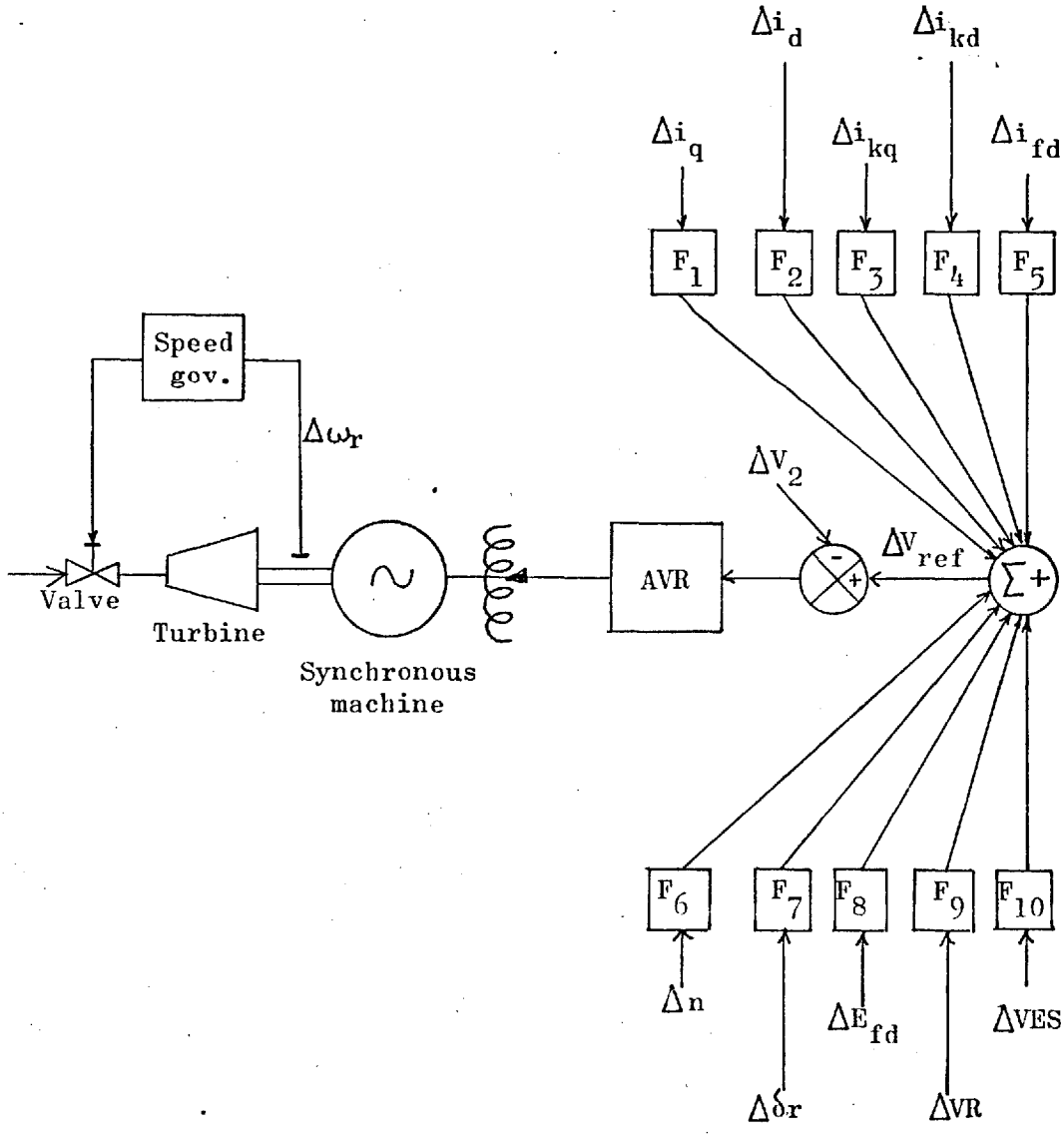

Figure 4.7: Control structure.

AVR Control only	Modal Control 1 P.I. = 2176	Modal Control 2 P.I. = 68	Modal Control 3 P.I. = 93
$-5.4 \pm j7.3$	$-6.0 \pm j8.0$	$-6.0 \pm j8.0$	$-6.0 \pm j8.0$
$+0.27 \pm j\ 4.7$	$-2.0 \pm j5.0$	$-0.8 \pm j5.0$	$-0.95 \pm j\ 5.0$
$-2.15 \pm j\ 2.2$	$-4.0 \pm j3.0$	$-3.0 \pm j.30$	$-3.0 \pm j3.0$

Table 4.6: Critical eigenvalues during pumping.

Gain	P.I. = 2176	P.I. = 68	P.I. = 93
F_1	-0.087	-0.025	-0.029
F_2	-1.854	-0.900	-0.945
F_3	-0.117	-0.037	-0.041
F_4	-1.861	-0.896	-0.941
F_5	-2.365	-1.152	-1.208
F_6	-46.460	-7.920	-9.371
F_7	0.933	0.372	0.430
F_8	0.009	0.016	0.0139
F_9	-0.024	-0.012	-0.013
F_{10}	-1.857	-1.324	-1.294

Table 4.7: Optimal gains of the controller when pumping.

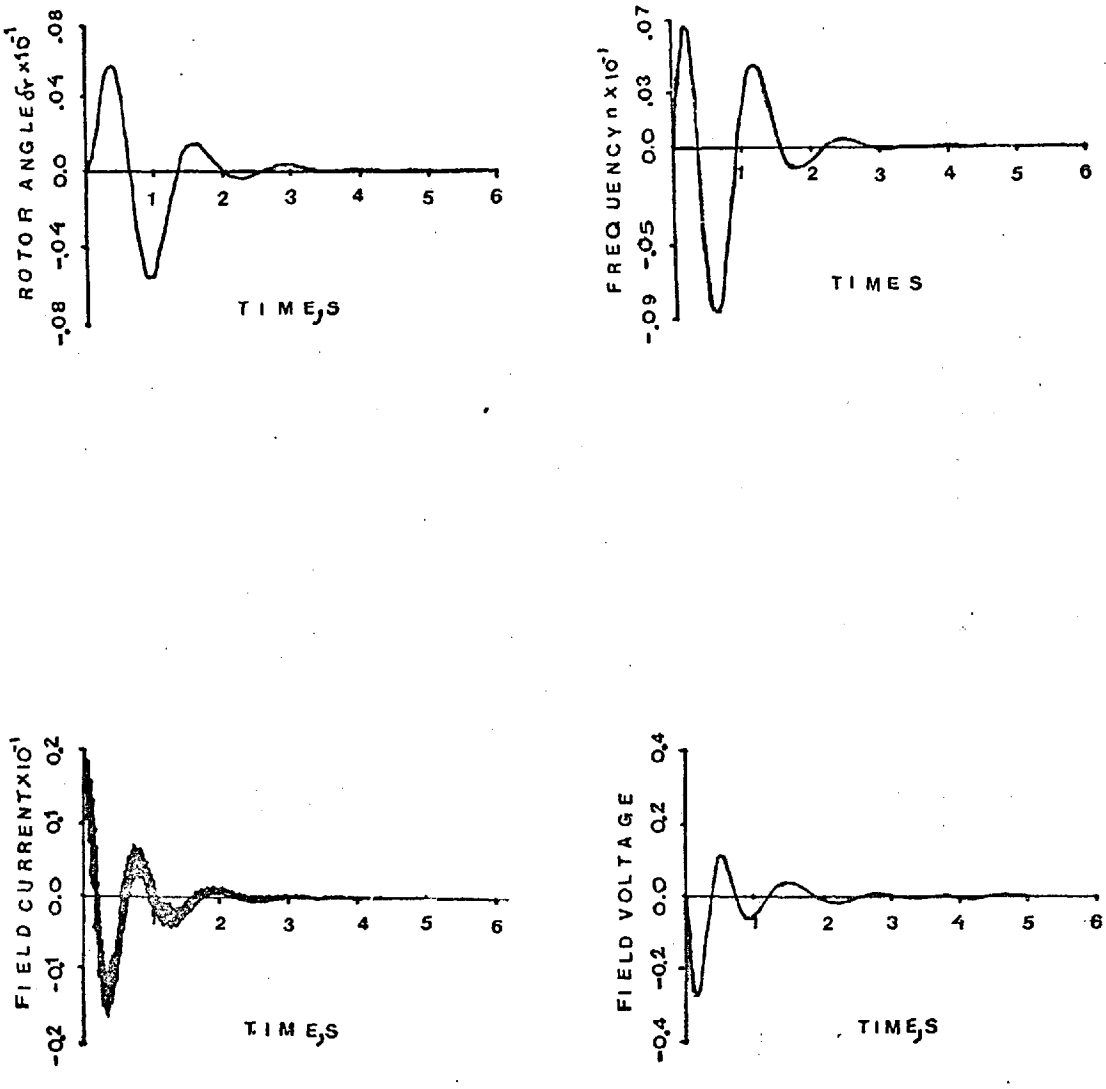

Figure 4.8: System variable responses following a change of $\Delta i_{fd} = 0.01$ p.u with further control loops to give the eigenvalues in position 1 (Table 4.5).

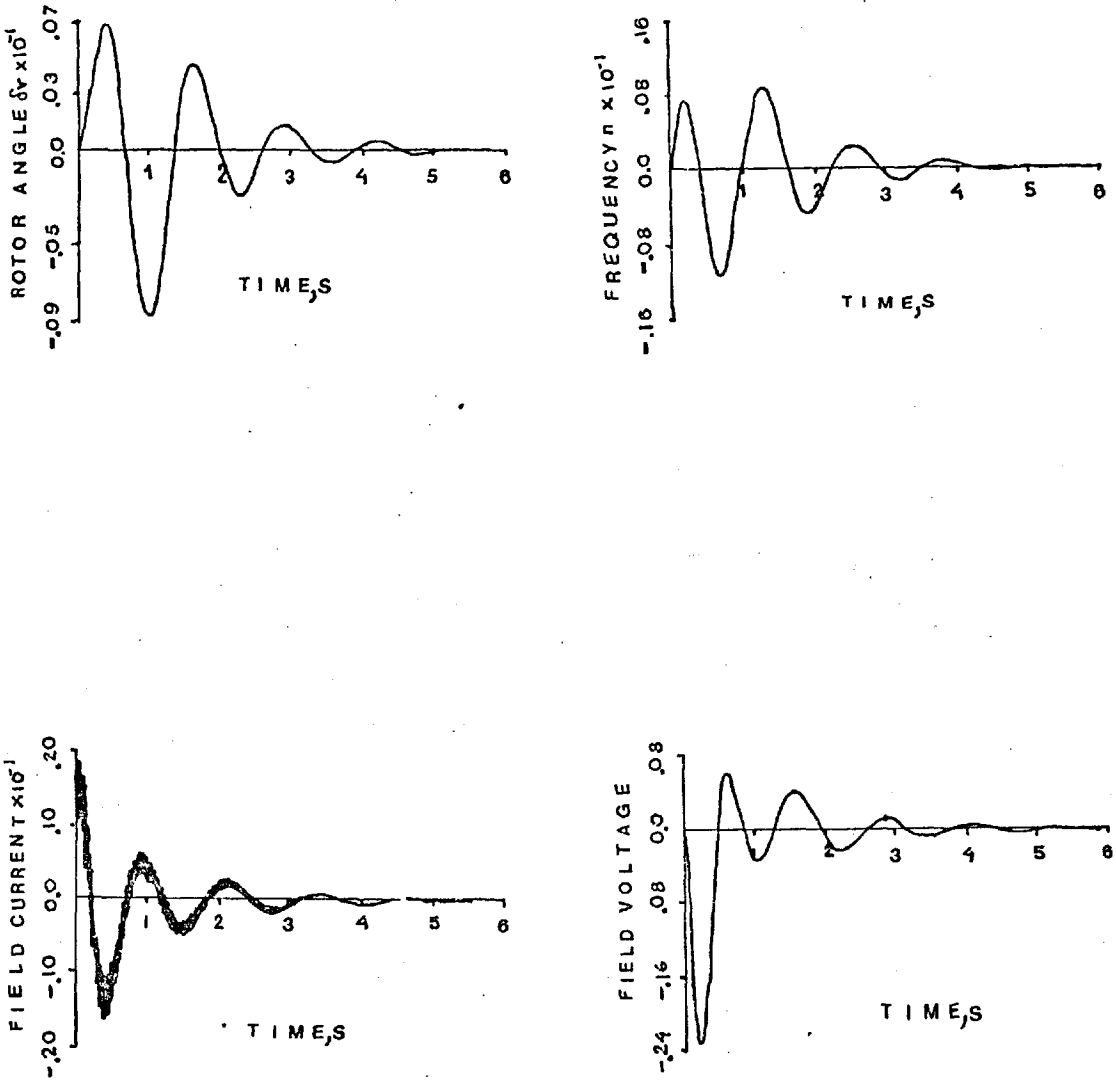

Figure 4.9: System variable responses following a change of $\Delta i_{fd} = 0.01$ as in Figure 4.8, with eigenvalues in poaition 2.

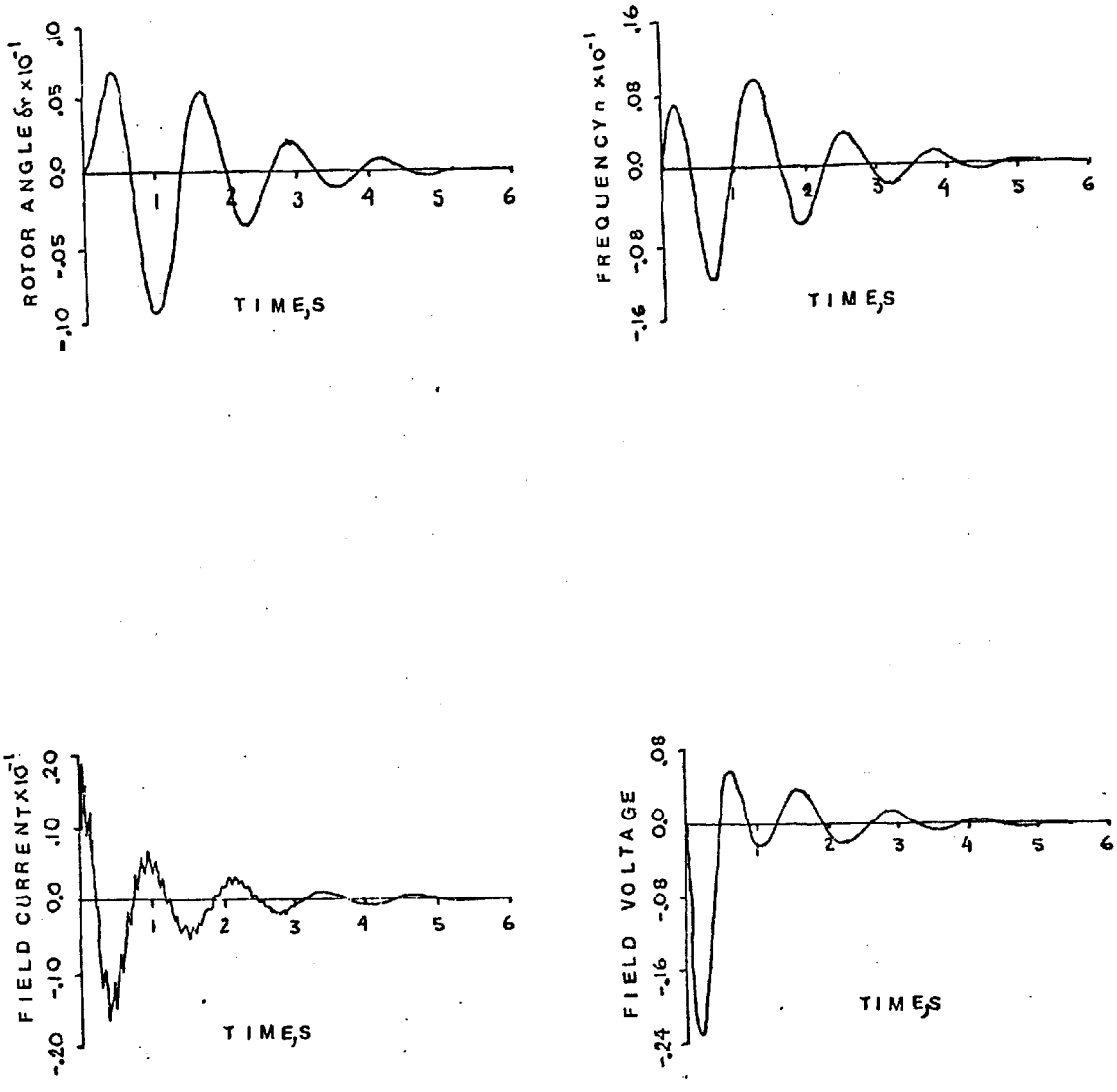

Figure 4.10: System variable responses following a change of $\Delta i_{fd} = 0.01$ as in Figure 4.9 with eigenvalues in position 3.

and change the optimal design of the feedback controllers:

(i) Line and transformer reactances coupled with the machine reactance in the classical way following Baker and Krause[47] which includes the stator transients.

(ii) Steady-state algebraic node equations of the form $I = YV$ following Alden and Zein El-Din[29].

(iii) Steady-state algebraic representation by Newton-Raphson power equations, explained and used in Chapters 2 and 3 of this thesis.

Table 4.8 shows the eigenvalues of the power system for these three network representations. Table 4.9 shows the values of the gains required to move the six critical eigenvalues to position 3, Table 4.6, column 4. In Appendix C.1 the equations and the methods by which the state space representation was built up for the three different network representations are shown in detail. Figures 4.11 and 4.12 show the field current response following an impulsive change of $\Delta i_{fd} = 0.01$ p.u. when transient network terms are included and excluded respectively.

The mode of oscillation which was troublesome at Ludington (the mechanical one) is clearly revealed whether or not the network transient terms are included in the calculation. When the network transient terms are omitted, the natural frequency of the modes associated with the stator windings is very high and is highly damped, but the unstable oscillating mode damping appears more damped. If network transient network terms are included, the natural

Location of Oscillation	Classical network representation including transient network terms	Classical network representation excluding transient network terms	Algebraic node equation of the form I = YV	Algebraic Newton-Raphson power equations
Stator windings	$-1.04 \pm j\ 377$	$-11.76 \pm j\ 1304$	$-11.78 \pm j1304$	$-11.78 \pm j\ 1304$
d-axis damping winding	-17.83	-17.81	-17.83	-17.83
q-axis damping winding	-15.90	-16.00	-16.00	-16.00
Excitation system stabilizer	$-5.42 \pm j7.32$	$-5.43 \pm j\ 7.30$	$-5.40 \pm j\ 7.36$	$-5.40 \pm j7.36$
AVR and field winding	$-2.15 \pm j\ 2.2$	$-2.14 \pm j2.2$	$-2.14 \pm j2.2$	$-2.14 \pm j\ 2.2$
Mechanical	$+0.273 \pm j\ 4.74$	$+0.258 \pm j2.75$	$+0.262 \pm j2.75$	$+0.262 \pm j\ 4.75$

Table 4.8: Eigenvalues of the power system during pumping mode with different network representations.

Gains	Classical network representation with transient network terms	Classical network representation without transient network terms	Algebraic mode equations I = YV	Algebraic Newton-Raphson power equations
F_1	-0.029	-0.033	-1.29	-1.29
F_2	-0.945	-0.942	0.0048	0.0048
F_3	-0.041	-0.04	0.0094	0.0093
F_4	-0.941	-0.93	0.0084	0.0089
F_5	-1.200	-1.20	-0.098	-0.098
F_6	-9.370	-9.05	-0.013	-0.013
F_7	0.43	-0.42	0.013	0.013
F_8	0.013	0.014	-1.28	-1.28
F_9	0.013	-0.013	0.43	0.43
F_{10}	-1.290	-1.30	-9.26	-9.27

Table 4.9: Optimal gains of the controller during pumping mode, for different network representations.

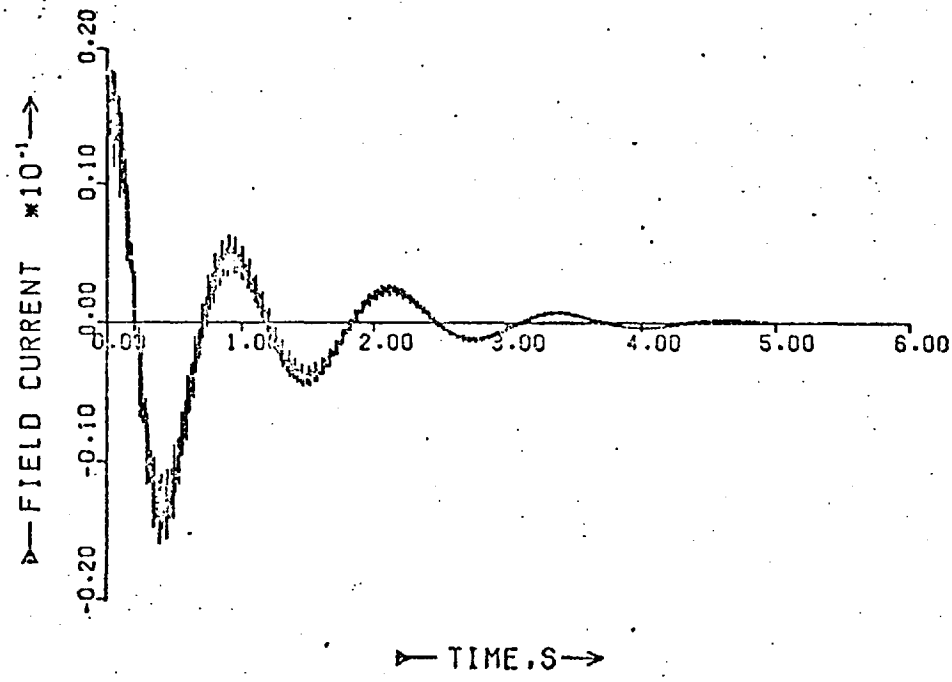

Figure 4.11: Field current response after a Δi_{fd} = 0.01 p.u. impulse, considering classical network representation with transient network terms.

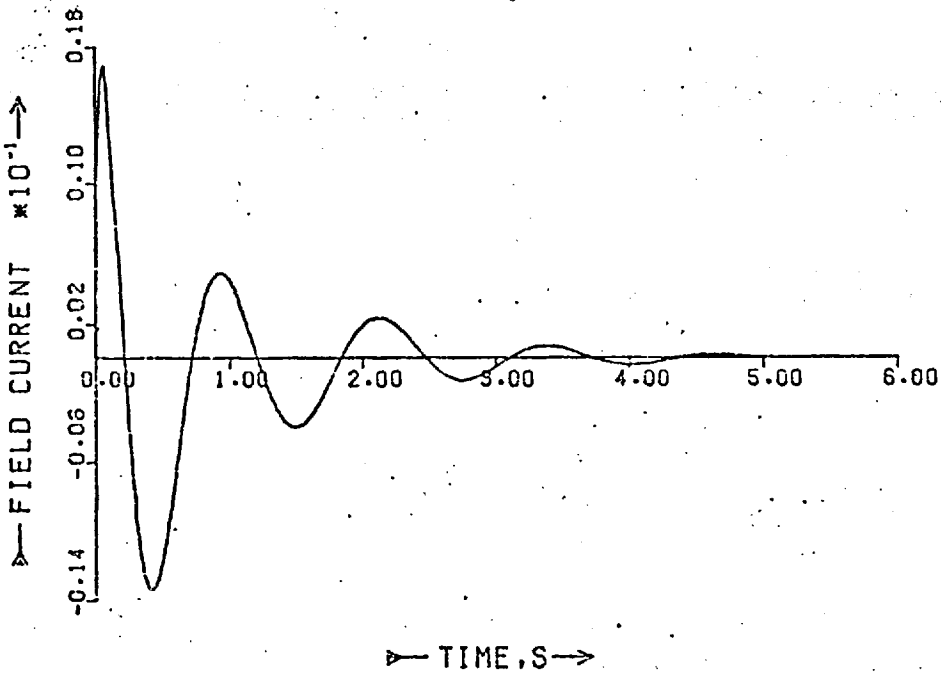

Figure 4.12: Field current response after a Δi_{fd} = 0.01 p.u. impulse, considering classical network representation without transient network terms.

frequency of the modes associated with the stator windings becomes that of the supply and the damping of these modes and the unstable one is decreased. Thus the use of more approximate models can give rise also to error in the design of the feedback controller.

4.4.2 Generating mode operation

In the second part of the analysis, the generator mode of operation was studied for the same power station with the a.v.r. and governor acting, giving a system of order 13. In addition two levels of load were added at the machine bus-bar. Load was taken in non-linear passive form as described by equations (2.49) and (2.50) for which several values of K_p and K_q were considered. Secondly, the combined load proposed by Shackshaft et al[39], also described in Chapter 2 by equations (2.55) and (2.56), was used. System equations are similar to those given in Appendix C.1, when steady-state Newton-Raphson power equations for the network representation were used with the addition of speed governor equations. Multi-input modal control technique given in Section 4.3 was used to obtain the feedback loops to the reference levels of the voltage regulator and the speed governor from all the system states. As for the pumping mode, it was assumed that all the state variables were available to be fed-back either being measurable or available from an observer. The state variables for the synchronous machine when generating were:

$$y(t) = [\Delta\psi_{fd}, \Delta\psi_{d}, \Delta\psi_{rd}, \Delta\psi_{q}, \Delta\psi_{rq}, \Delta V_R, \Delta E_{fd}, \Delta V_{ES}, \Delta\delta r, \Delta n, \Delta g, \Delta gf, \Delta h]^T \qquad (4.32)$$

Operating conditions are given in Table 4.10 when machines were considered to be at full load. Tables 4.11 and 4.12 give the natural positions of the critical eigenvalues and their new positions obtained by modal control designed feedback loops, for both conditions of load. Tables 4.13 and 4.14 give the gains for the state variables of equation (4.32) required to bring about this re-location, and it will be seen that the magnitudes vary noticeably with the magnitude and type of load. The combined load appears to contribute appreciable damping during heavy load conditions (compared to local generation) and therefore the optimal feedback gains required are lower than with the other load characteristics considered. The contrary occurs when light local load was considered. Also, it will be noted that the optimal control gains are more sensitive to changes in K_p than to changes in K_q.

4.5 CONCLUSION

Modal control methods may be used to determine feedback gains necessary to reposition critical eigenvalues and improve the stability of power systems. The optimal feedback gains required for particular positions of the eigenvalues depend upon the magnitude and characteristics of the load. Also, the network representation seems to be important in the controller design, approximate models can give rise to error in the design of these controllers. In view of the variation of load characteristics with the time of day, it seems unlikely that any single controller can be continuously optimal. A process in which feedback gains are adapted as conditions change might be useful.

Symbol	Description	Light load p.u. values	Heavy load p.u. values
δr	rotor angle respect to infinite bus	44 (deg.)	10 (deg.)
P.F.	power factor under-excited	0.95	0.95
V_2	terminal voltage	1.03	1.0
V_b	infinite bus-bar voltage	1.0	1.0
P	active power	1.0	1.0
P_L	load active power	0.19	1.5
Q_L	load reactive power	0.06	0.4
i_d	d-axis current	-0.62	-0.78
i_q	q-axis current	0.79	0.84
v_d	d-axis voltage	-0.37	-0.40
v_q	q-axis voltage	0.96	0.81
ψ_d	d-axis flux	0.96	0.81
ψ_q	q-axis flux	0.38	0.40

Table 4.10: Operating point for generating mode.

$K_p = 2$	1	0	2	0	1	0	3	0	Combined Load	Relocation
$K_q = 2$	1	0	0	2	0	1	0	3	25% Induction Motor	
$-5.30 \pm j7.3$	$-5.30 \pm j7.3$	$-5.30 \pm j7.3$	$-5.3 \pm j7.3$	$-5.40 \pm j7.3$	$-5.30 \pm j7.3$	$-5.30 \pm j7.3$	$-5.30 \pm j7.29$	$-5.40 \pm j7.36$	$-4.1 \pm j6.22$	$-7.5 \pm j9.4$
$+0.17 \pm j4.8$	$+0.15 \pm j4.8$	$+0.12 \pm j4.9$	$+0.2 \pm j4.8$	$+0.11 \pm j4.9$	$+0.16 \pm j4.8$	$+0.12 \pm j4.9$	$+0.22 \pm j4.78$	$+0.10 \pm j4.91$	$+0.45 \pm j3.8$	$-1.0 \pm j5.0$
$-2.10 \pm j2.2$	$-2.00 \pm j2.2$	$-2.00 \pm j2.2$	$-2.1 \pm j2.2$	$-2.00 \pm j2.2$	$-2.10 \pm j2.2$	$-2.00 \pm j2.2$	$-2.20 \pm j2.24$	$-1.90 \pm j2.23$	$-3.8 \pm j1.92$	$-4.5 \pm j3.0$
-1.4	-1.4	-1.4	-1.4	-1.4	-1.4	-1.4	-1.4	-1.4	-1.5	-2.5
-.42	-.42	-.42	-.42	-.42	-.42	-.42	-.42	-.42	-.40	-1.5

Table 4.11: Critical eigenvalues with conventional control when generating and as relocated. Light local load conditions.

$K_p = 2$ $K_q = 2$	1 1	0 0	2 0	0 2	1 0	0 1	3 0	0 3	Combined Load 25% Induction Motor	Relocation
$-5.6\pm j7.3$	$-5.4\pm j6.9$	$-4.9\pm j6.2$	$-5.3\pm j6.8$	$-5.4\pm j6.9$	$-5.2\pm j6.6$	$-5.2\pm j6.7$	$-5.5\pm j7.0$	$-5.6\pm j7.2$	$-5.3\pm j6.8$	$-7.5\pm j9.4$
$-.29\pm j4.9$	$-.25\pm j4.9$	$-.19\pm j4.9$	$-.33\pm j4.9$	$-.18\pm j4.9$	$-.27\pm j4.9$	$-.19\pm j4.9$	$-.34\pm j5.0$	$-.18\pm j4.9$	$-.18\pm j5.3$	$-1.0\pm j5.0$
$-1.4\pm j2.1$	$-1.7\pm j2.4$	$-2.3\pm j2.7$	$-1.7\pm j2.4$	$-1.7\pm j2.3$	$-1.9\pm j2.3$	$-1.9\pm j2.5$	$-1.5\pm j2.3$	$-1.5\pm j2.2$	$-1.7\pm j2.4$	$-4.5\pm j3.0$
-1.4	-1.4	-1.4	-1.4	-1.4	-1.4	-1.4	-1.4	-1.4	-1.4	-2.5
-.42	-.42	-.42	-.42	-.42	-.42	-.42	-.42	-.42	-.42	-1.5

Table 4.12: Critical eigenvalues with conventional control when generating and as relocated. Heavy load condition.

Note: Induction motor load parameters are equal to those of the largest motor given in Table 2.7 , Chapter 2.

Gains	$K_p = 2$ $K_q = 2$	1 1	0 0	2 0	0 2	1 0	0 1	3 0	0 3	Combined Load
F_{V_1}	-3.47	-3.44	-3.40	-3.46	-3.42	-3.43	-3.41	-3.48	-3.42	-4.47
F_{V_2}	-0.01	-0.01	-0.01	-0.01	-0.01	-0.01	-0.01	-0.01	-0.01	-0.02
F_{V_3}	-0.03	-0.03	-0.02	-0.03	-0.02	-0.03	-0.02	-0.03	-0.02	-0.19
F_{V_4}	-0.02	0.02	-0.02	-0.02	-0.02	-0.02	-0.02	-0.02	-0.02	-0.02
F_{V_5}	0.21	-0.22	0.23	0.21	0.23	0.22	0.23	0.20	0.23	0.17
F_{V_6}	-0.03	-0.03	-0.03	-0.03	-0.03	-0.03	-0.03	-0.03	-0.03	-0.03
F_{V_7}	0.06	0.06	0.06	0.06	0.06	0.06	0.06	0.06	0.06	0.13
F_{V_8}	-4.11	-4.05	-3.99	-4.10	-4.01	-4.04	-4.00	-4.15	-4.02	-6.60
F_{V_9}	-0.78	-0.25	-0.92	-0.77	-0.93	-0.84	-0.93	-0.71	-0.93	0.41
$F_{V_{10}}$	34.17	33.44	32.52	34.19	32.49	33.45	32.51	34.79	34.47	112.39
$F_{V_{11}}$	1.57	1.63	1.70	1.55	1.72	1.62	1.71	1.48	1.73	-0.37
$F_{V_{12}}$	0.31	0.32	0.33	0.31	0.33	0.32	0.33	0.30	0.33	0.29
$F_{V_{13}}$	2.35	2.41	2.50	2.33	2.51	2.41	2.50	2.26	2.52	1.36
F_{G_1}	0.01	0.01	0.01	0.01	0.01	0.01	0.01	0.01	0.01	0.05
F_{G_2}	-0.00	-0.00	-0.00	-0.00	-0.00	-0.00	-0.00	-0.00	-0.00	-0.00
F_{G_3}	-0.006	-0.006	-0.005	-0.006	-0.005	-0.006	-0.005	-0.007	-0.005	-0.009
F_{G_4}	-0.00	-0.00	-0.00	-0.00	-0.00	-0.00	-0.00	-0.00	-0.00	-0.00
F_{G_5}	0.011	0.011	0.011	0.011	-0.011	0.011	0.011	0.011	0.011	0.007
F_{G_6}	-0.00	-0.00	-0.00	-0.00	-0.00	-0.00	-0.00	-0.00	-0.00	-0.00
F_{G_7}	-0.004	-0.004	-0.004	-0.004	-0.004	-0.004	-0.004	-0.005	-0.003	-0.008
F_{G_8}	0.14	0.13	0.12	0.14	0.12	0.13	0.12	0.15	0.12	0.27
F_{G_9}	0.57	0.57	0.57	0.57	0.57	0.57	0.57	0.57	0.57	0.56
$F_{G_{10}}$	3.56	3.54	3.51	3.56	3.51	3.54	3.51	3.59	3.51	5.07
$F_{G_{11}}$	23.32	23.33	23.34	23.32	23.34	23.33	23.34	23.31	23.34	21.96
$F_{G_{12}}$	-2.17	-2.17	-2.17	-2.17	-2.17	-2.17	-2.17	-2.17	-2.17	-2.08
$F_{G_{13}}$	0.82	0.82	0.82	0.82	0.82	0.82	0.82	0.82	0.82	0.59

Table 4.13: Optimal gains from state variables (1-13 defined in equation (4.32)) to the voltage regulator F_V, and governor F_G reference settings. Light local load condition.

Gains	$K_p = 2$ $K_q = 2$	1 1	0 0	2 0	0 2	1 0	0 1	3 0	0 3	Combined Load
F_{V_1}	-3.55	-3.47	-3.32	-3.42	-3.51	-3.38	-3.43	-3.45	-3.58	-2.98
F_{V_2}	-0.01	-0.01	-0.02	-0.01	-0.02	-0.01	-0.02	-0.01	-0.02	-0.00
F_{V_3}	-0.04	-0.04	-0.04	-0.03	-0.04	-0.03	-0.04	-0.03	-0.05	-0.04
F_{V_4}	0.02	0.02	0.02	0.02	0.02	0.02	0.02	0.02	0.02	0.02
F_{V_5}	0.14	0.18	0.35	0.13	0.35	0.18	0.35	0.11	0.35	0.09
F_{V_6}	-0.03	-0.03	-0.03	-0.03	-0.03	-0.03	-0.03	-0.03	-0.03	-0.03
F_{V_7}	0.06	0.06	0.05	0.06	0.06	0.05	0.05	0.06	0.06	0.04
F_{V_8}	-4.22	-4.07	-3.85	-4.04	-4.11	-3.96	-4.00	-4.10	-4.20	-3.34
F_{V_9}	-0.36	-0.51	-1.14	-0.32	-1.14	-0.48	-1.14	-0.25	-1.13	-0.52
$F_{V_{10}}$	27.58	37.02	70.07	24.43	71.24	34.98	70.81	19.38	71.50	3.55
$F_{V_{11}}$	0.14	0.32	1.06	0.13	1.01	0.31	1.03	0.04	0.99	0.41
$F_{V_{12}}$	0.11	0.14	0.30	0.09	0.31	0.13	0.31	0.07	0.32	0.09
$F_{V_{13}}$	0.65	0.91	2.09	0.54	2.10	0.84	2.10	0.41	2.11	0.69
F_{G_1}	0.03	0.02	0.01	0.03	0.01	0.02	0.01	0.03	0.01	0.01
F_{G_2}	-0.00	-0.00	-0.00	-0.00	-0.00	-0.00	-0.00	-0.00	-0.00	-0.00
F_{G_3}	-0.01	-0.00	-0.00	-0.01	-0.00	-0.00	-0.00	-0.01	-0.00	-0.00
F_{G_4}	-0.00	-0.00	-0.00	-0.00	-0.00	-0.00	-0.00	-0.00	-0.00	-0.00
F_{G_5}	0.01	0.01	0.01	0.01	0.01	0.01	0.01	0.01	0.01	0.01
F_{G_6}	-0.00	-0.00	-0.00	-0.00	-0.00	-0.00	-0.00	-0.00	-0.00	-0.00
F_{G_7}	-0.01	-0.00	-0.00	-0.01	-0.00	-0.00	-0.00	-0.01	-0.00	-0.00
F_{G_8}	0.23	0.16	0.08	0.24	0.08	0.17	0.08	0.31	0.08	0.18
F_{G_9}	0.57	0.57	0.57	0.57	0.57	0.57	0.57	0.57	0.57	0.57
$F_{G_{10}}$	3.60	3.60	3.70	3.60	3.70	3.60	3.70	3.50	3.70	3.20
$F_{G_{11}}$	23.13	23.10	23.04	23.13	23.04	23.10	23.04	23.18	23.05	23.43
$F_{G_{12}}$	-2.16	-2.15	-2.15	-2.16	-2.15	-2.15	-2.15	-2.16	-2.15	12.18
$F_{G_{13}}$	0.80	0.80	0.80	0.81	0.80	0.80	0.80	0.81	0.80	0.25

Table 4.14: Optimal gains from state variables (1-13 defined in equation (4.52)) to the voltage regulator F_V, and governor F_G, reference settings. Heavy local load condition.

CHAPTER 5

MODAL CONTROL OF MULTI-MACHINE POWER SYSTEMS INCLUDING THE EFFECT OF LOAD CHARACTERISTICS

5.1 INTRODUCTION

A number of modern control techniques have been developed in order to control the generators in a multi-machine system, using multistate feedback signals to the avr and speed governor setting reference points[59,61,62]. However, all of them have considered the loads as constant impedances, which are included in the matrix network equation (Davison et al[59] and Pai et al[61]).

In this chapter the effect of load characteristics on the design of feedback modal controllers of a multi-machine system has been investigated. Non-linear passive load with characteristics of the type proposed by the IEEE Working Group[38] and also a combined load proposed by the CEGB Group[39] which have been discussed in previous chapters, were applied in the system. The results indicate that a global modal controller that requires feedback from all the state variables in the multi-machine system will act in a manner far from optimal if the nature of the load is not taken into account.

Since it is not practicable to feedback all the state variables in a multi-machine system, a local modal controller was designed, where feedback to each machine comes from its individual state variables. This is of importance because of the costs and other problems involved in telemetering of feedback signals between

various machines in the system which could be spread over a wide geographical area. The method of designing this controller was similar to that proposed by Pai et al,[61] in which local control is derived from the global controller, disconnecting the feedback paths from the state variables that do not belong to a particular machine. This technique was applied to a three-machine system.

5.2 METHOD OF ANALYSIS

The modal control theory of Chapter 4 applied there to a single-machine infinite bus bar system is applied here to the design of global and local controllers for a multi-machine power system.

5.2.1 Global Modal Control

The multi-machine system, including terminal relations, is expressed in the state space form by using the method described in Section 3.3.2:

$$\dot{y}(t) = [A]y(t) + [B]u(t) \qquad (5.1)$$

The eigenvalues of the [A] matrix are determined and also the impulse response of the open loop system is obtained.

The addition of feedback loops, as explained earlier in Section 4.2.4, gives:

$$\dot{y}(t) = ([A] + [B][F])\, y(t) \qquad (5.2)$$

or

$$\dot{y}(t) = G\, y(t) \qquad (5.3)$$

the eigenvalues of which can be controlled by the choice of F, using the dominant input and sector criterion defined in Sections 4.3.1 and 4.3.2, respectively, for the relocation of the eigenvalues.

In a global design for a large multi-variable system using the criterion of Section 4.3.1 some inputs might not be used. This would make the global control scheme unsuitable for adaptation to local control, for some of the inputs would be absent.

Here, each input has assigned to it for control at least one eigenvalue (or complex pair). The eigenvalues given for control to a particular input are found by examining the magnitudes of the elements in the column of the controllability matrix, P, corresponding with the input, and selecting the largest absolute value. The row number corresponds with the eigenvalue. In choosing to exert control through the largest input-eigenvalue links, the gains K_j required in the proportional feedback loops are minimised.

$$K_j = \frac{\prod_{i=1}^{r} (\varrho_i - \lambda_j)}{p_j \prod_{\substack{i=1 \\ j \neq i}}^{r} (\lambda_i - \lambda_j)} \qquad (5.4)$$

In order to compare the gains of the feedback matrices obtained for various load characteristics in the system, a performance index (P.I.) defined in Chapter and repeated here, is defined as follows:

$$P.I. = \sum_{i=1}^{p} \sum_{j=1}^{n} F_{ij}^2 \qquad (5.5)$$

5.2.2 Local Modal Control

Since it is not practicable to feedback all the state variables in a multi-machine system, a local modal controller was designed. This was achieved by first obtaining the global controller feedback matrix using complete state feedback from all machines and then making the elements of this feedback matrix corresponding to state variables from other machines equal to zero as was proposed by Pai et al[61]. However, it was found that using this method the dynamic stability of the system deteriorated. Much better results were obtained when one signal (defined as the dominant signal) from each of the other machines was fed to each of those that otherwise lacked stability. This method avoided the use of feedback between machines that were closely tied electrically, or the need to obtain a suboptimal controller as Pai et al[61] required. The signal chosen for feedback was that with the highest feedback gain in the global controller. The structure of the global and local control feedback matrices is indicated in Figure 5.1.

5.3 THE COMPUTER PROGRAM

The method of multi-input modal control applied to a single-machine infinite bus-bar system described in previous sections was implemented in a digital computer program. This program is able to handle up to four interconnected synchronous machines represented by 11^{th} order equations, including the a.v.r. and speed governor control systems. The global and local control of a power system consisting of three interconnected synchronous machines was designed with this computer program.

$$\begin{bmatrix} u_1(t) \\ u_2(t) \\ u_3(t) \end{bmatrix} = \begin{bmatrix} F_{11} & F_{12} & F_{13} \\ F_{21} & F_{22} & F_{23} \\ F_{31} & F_{32} & F_{33} \end{bmatrix} \begin{bmatrix} y_1(t) \\ y_2(t) \\ y_3(t) \end{bmatrix}$$

(a) Global control.

$$\begin{bmatrix} u_1(t) \\ u_2(t) \\ u_3(t) \end{bmatrix} \begin{bmatrix} F_{11} & 0 & 0 \\ 0 & F_{22} & 0 \\ 0 & 0 & F_{33} \end{bmatrix} \begin{bmatrix} y_1(t) \\ y_2(t) \\ y_3(t) \end{bmatrix}$$

(b) Local control.

$$\begin{bmatrix} u_1(t) \\ u_2(t) \\ u_3(t) \end{bmatrix} \begin{bmatrix} F_{11} & 0 & 0 \\ 0 & F_{22} & 0 \\ 0 & * & F_{33} \end{bmatrix} \begin{bmatrix} y_1(t) \\ y_2(t) \\ y_3(t) \end{bmatrix}$$

(c) Local control with compensation (*) one dominant signal from machine 2 to machine 3.

Figure 5.1: Structure of feedback law for a three-machine system.

A general flow chart of the program is given in Figure 5.2. The state space formulation, the open loop eigenvalues and eigenvectors of the [A] and $[A]^{1}$ matrices are not included in the main program, but they are read from a magnetic tape, already provided by a separate dynamic stability program, described in Chapter 3, Section 3.4. After the design of the feedback controller is completed, the program can also use another magnetic tape to save the closed loop G matrix. Thus, equation (5.3) can be integrated numerically to give the response to a small disturbance.

5.4 THE SYSTEM, STUDIES AND RESULTS

The modal control method explained in previous sections is applied to a sample power system consisting of three interconnected synchronous machines shown in Figure 5.3. All three machines are assumed to have the same capacity, viz. 1.0 per unit with similar parameters to those given in Chapter 3, Table 3.1. Machine no. 3 is a hydraulic machine, while machines nos. 1 and 2 are thermal machines. The values of power, voltage and angle obtained by standard load flow analysis are indicated in Figure 5.3. The excitation and turbine-governor control systems were those used in Chapter 3. The constants of the system chosen and the formulation of the [A] and [B] matrices were also the same as those given and explained in Sections 3.3.1 and 3.3.2.

The machines were represented by 7^{th} order two-axis equations. The excitation systems were similar to those used in Chapter 3 with a single time constant (1^{st} order) and the speed

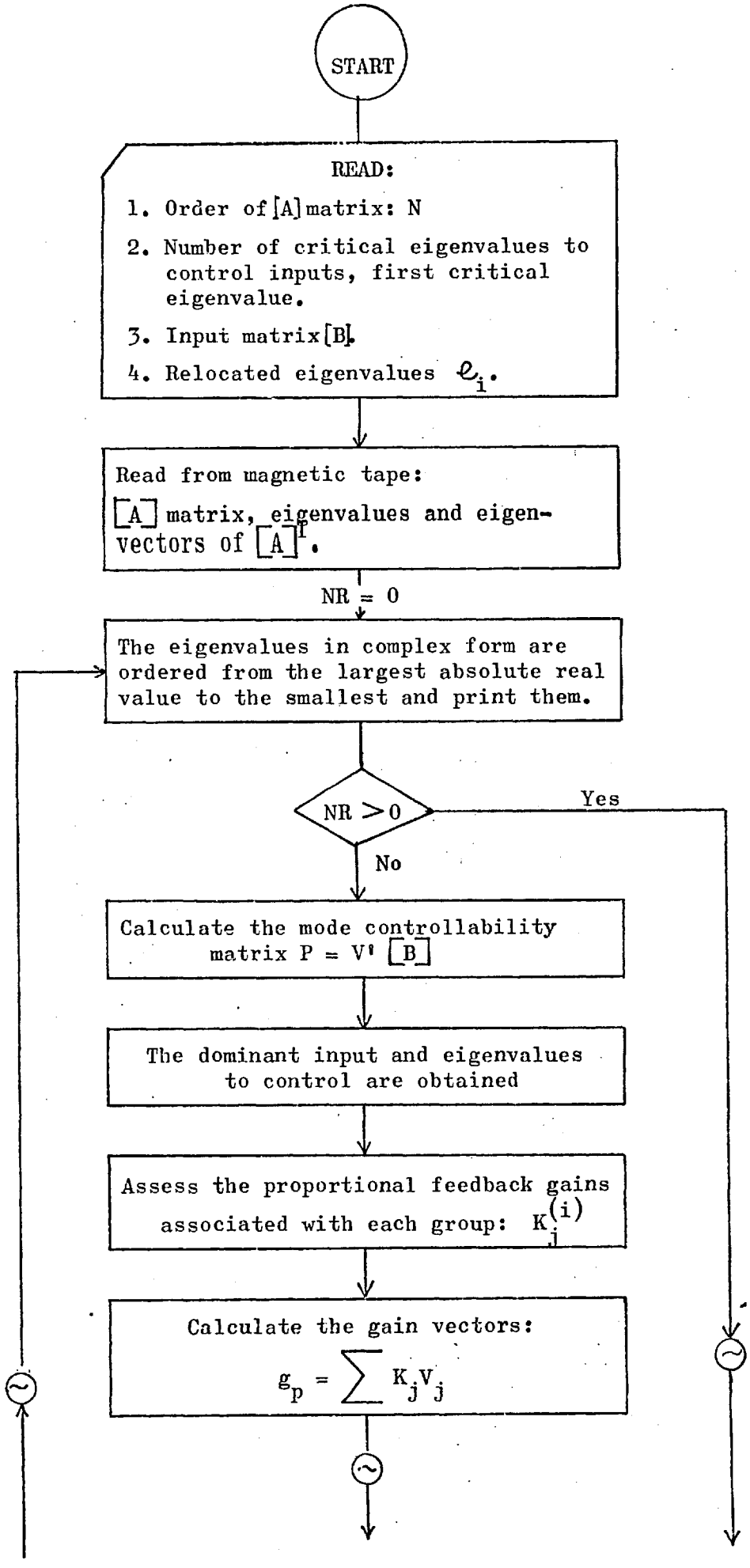
START
READ:
1. Order of [A] matrix: N
2. Number of critical eigenvalues to control inputs, first critical eigenvalue.
3. Input matrix [B].
4. Relocated eigenvalues e_i.
Read from magnetic tape:
[A] matrix, eigenvalues and eigenvectors of $[A]^T$.
NR = 0
The eigenvalues in complex form are ordered from the largest absolute real value to the smallest and print them.
NR > 0
Yes
No
Calculate the mode controllability matrix P = V' [B]
The dominant input and eigenvalues to control are obtained
Assess the proportional feedback gains associated with each group: $K_j^{(i)}$
Calculate the gain vectors:
$g_p = \sum K_j V_j$

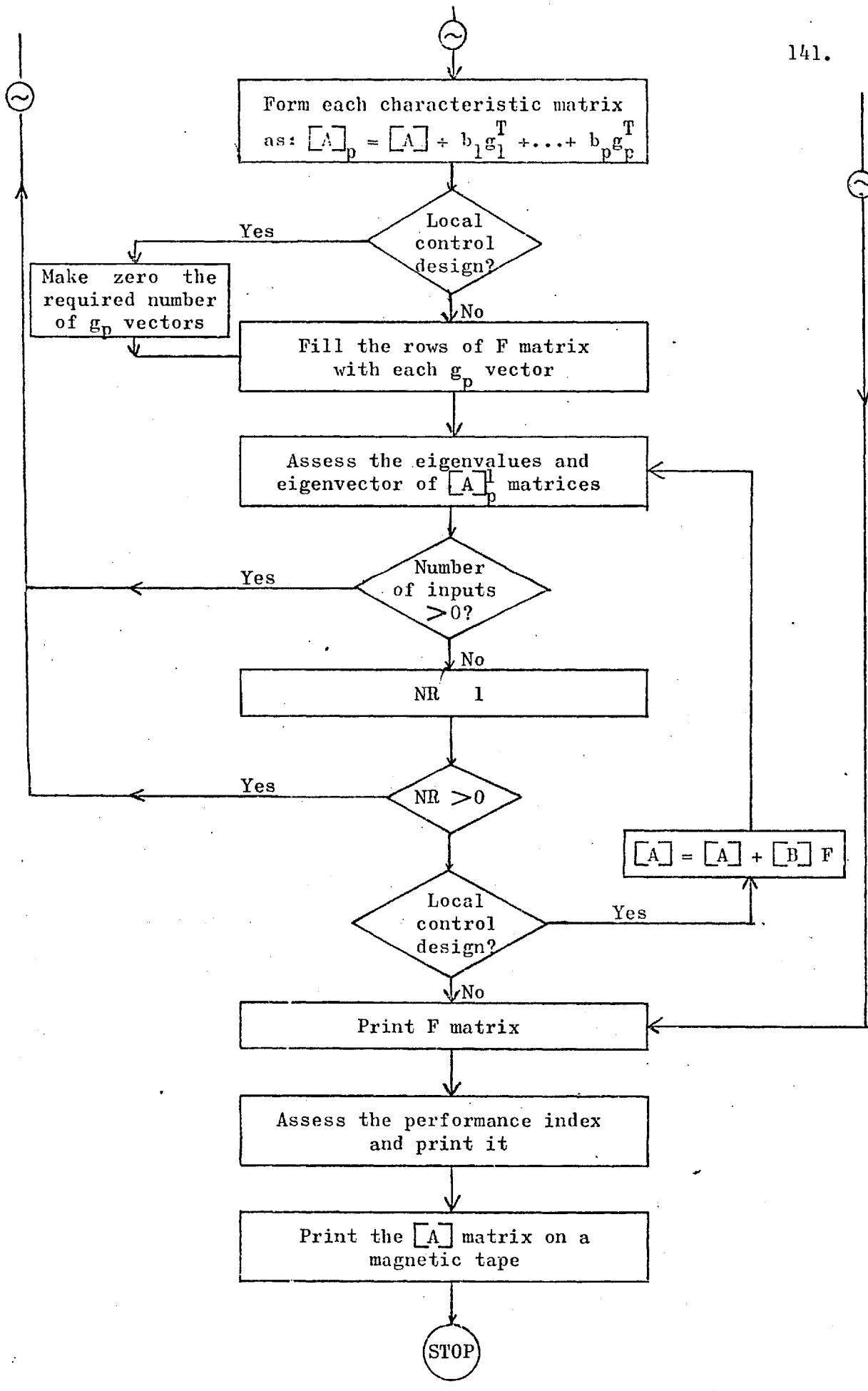

Figure 5.2: A general flow chart of the program for the design of a multi-input modal controller.

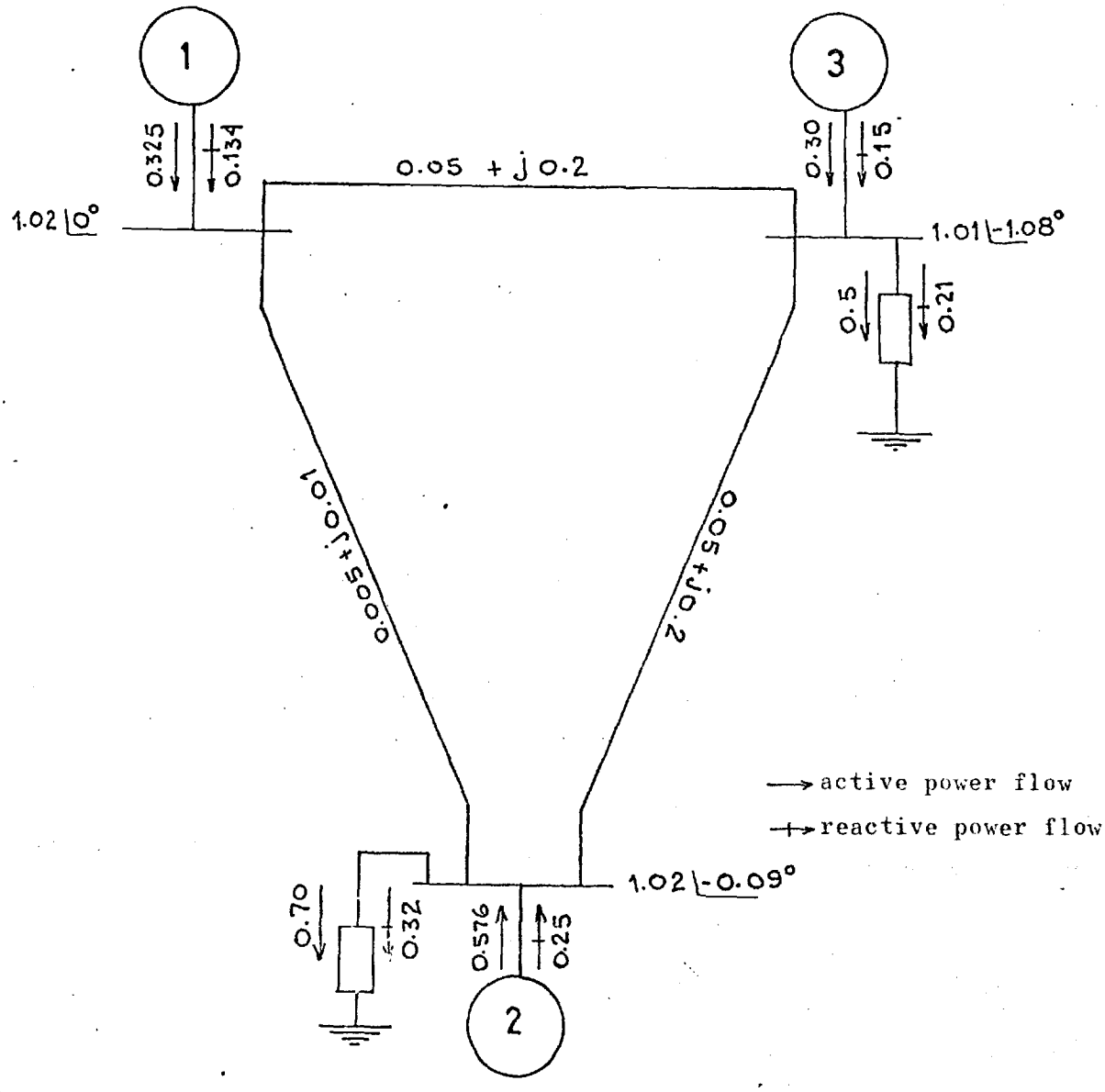

Figure 5.3: Multi-machine system.

governors were represented by a 3rd order model similar to those in Chapter 3, giving a total of eleven state variables per machine. It was assumed that all the state variables were available to be fed-back, etc. as before. The state variables for the system are in general:

$$y(t) = [\ \Delta\psi_{fd_1}\ \Delta\psi_{d_1}\ \Delta\psi_{kd_1}\ \Delta\psi_{q_1}\ \Delta\psi_{kq_1}\ \Delta E_{fd_1}\ \Delta\delta r_1\ \Delta n_1$$
$$\Delta\omega h_1\ \Delta\omega h_2\ \Delta\omega i_2 \cdots \Delta\psi_{fd_n}\ \Delta\psi_{d_n}\ \Delta\psi_{kd_n}\ \Delta\psi_{q_n}$$
$$\Delta\psi_{kq_n}\ \Delta E_{fd_n}\ \Delta\delta r_n\ \Delta n_n\ \Delta gf_n\ \Delta g_n\ \Delta h_n\ ]^T \qquad (5.6)$$

The control vector u(t) for each type of machine is:

Thermoelectric:

$$u(t) = [\ \Delta V_{ref}\ \ \Delta Y_o\ ]^T \qquad (5.7)$$

Hydroelectric:

$$u(t) = [\ \Delta V_{ref}\ \ \Delta u_{gov}\ ]^T \qquad (5.8)$$

For the multi-machine system consisting of three machines, the state and control vectors are:

$$y(t) = \begin{bmatrix} y_1(t) \\ y_2(t) \\ y_3(t) \end{bmatrix} \quad \text{and} \quad u(t) = \begin{bmatrix} u_1(t) \\ u_2(t) \\ u_3(t) \end{bmatrix}$$

where the subscripts 1, 2 and 3 refer to machines 1, 2 and 3, respectively. Machine no. 3 is picked as the reference machine and the rotor angles of the other machines are expressed relative to

that of the third machine. Hence $\Delta\delta r_3$ is eliminated from the state vector and the corresponding changes in the [A] matrix are made as given in Section 3.3.3. The order of the [A] matrix in this particular case is 32. All the considerations described in Section 3.5 with respect to the synchronous machines were also taken into account in this analysis.

In the network, the values of the line impedances are such that machine no. 3 can be considered to be remote from machines nos. 1 and 2, which are local machines to each other. Non-linear passive load with only voltage dependence was first considered, and secondly combined loads were used. Both are described in Section 2.2.4.

Global and local feedback controllers for the system shown in Figure 5.3 were obtained with different load characteristics. The conditions under which a local controller can function well are discussed.

The eigenvalues of the uncontrolled system with constant impedance loads ($K_p = K_q = 2$) are shown in Table 5.1. The response to an impulse of $\Delta\psi_{fd} = 0.1$ p.u. in machine no. 1 is shown in Figure 5.4. This indicates inadequate damping and the critical engenvalues which also include the complex conjugate pairs corresponding to mechanical oscillations were moved with a global controller to the positions shown in columns 2 and 3 of Table 5.1. Figure 5.5 gives the transient response for the improved system. The performance index (equation 4.30) is shown for both cases.

Table 5.2 shows the gains of the global controller 1 for constant impedance load. Table 5.3 shows the gains for a controller to produce similar eigenvalues when all the loads are combined loads

AVR and speed governor only	Global modal control 1	Global modal control 2
-4.17	-5.0	All are equal
-1.93	-7.0	as modal control 1
-1.61 + j6.9	-2.3 + j7.0	except the last
-1.61 - j6.9	-2.3 - j7.0	pair of conjugates
-1.41 + j0.97	-4.0 + j3.0	of critical
-1.41 - j0.97	-4.0 - j3.0	eigenvalues, in
-1.23 + j5.84	-2.1 + j6.0	which the damping
-1.23 - j5.84	-2.1 - j6.0	was increased as
-1.00	-3.0	it is indicated.
-0.99	-2.7	
-0.99 + j2.88	-2.6 + j5.0	
-0.99 - j2.88	-2.6 - j5.0	
-0.75	-2.0	
-0.182659	-1.8	
-0.182659	-1.5	
-0.16 + j.05	-1.0 + j2.0	-9.0 + j2.0
-0.16 - j.05	-1.0 - j2.0	-9.0 - j2.0
Performance Index P.I.	= 7098	= 71247

Table 5.1: Natural position of critical eigenvalues and as relocated.

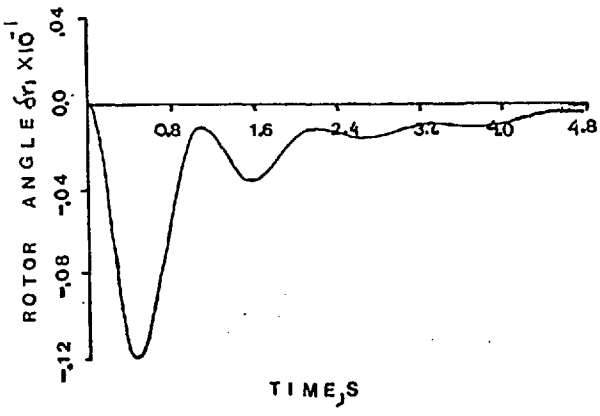

a) Rotor angle machine no. 1.

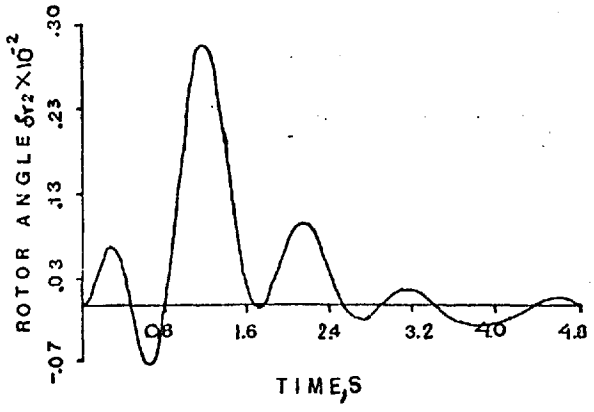

b) Rotor angle machine no. 2.

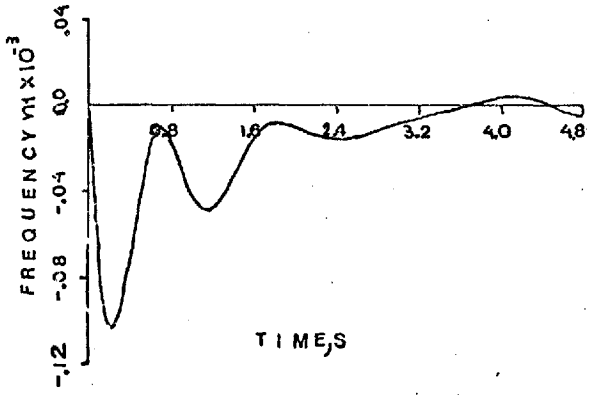

c) Frequency machine no. 1.

Figure 5.4: Rotor angles and frequency response to a small disturbance ($\Delta\psi_{fd_1}$ = 0.1 p.u.) open loop system.

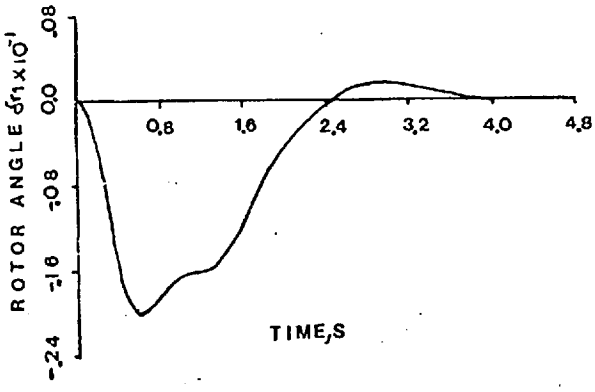

a) Rotor angle machine no. 1.

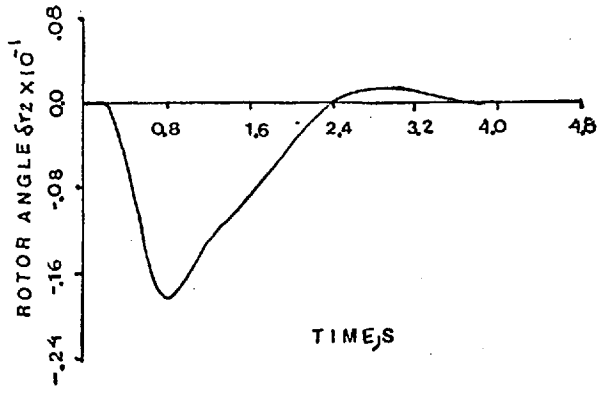

b) Rotor angle machine no. 2.

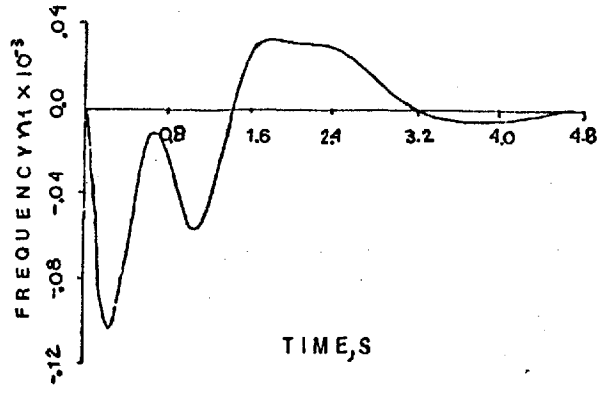

c) Frequency machine no. 1.

Figure 5.5: Rotor angles and frequency responses after a small disturbance ($\Delta\psi_{fd}$ = 0.1 p.u.) closed loop with global model colntrol 1.

Input		Elements of the feedback gain matrix, F									
$u_1(t)$ =	ΔV_{ref_1}	-0.034	-0.000	-0.001	0.000	0.004	-0.126	-0.003	0.626	-0.012	0.001	-0.019
		0.034	0.000	0.001	-0.000	-0.004	0.128	0.003	-0.613	0.012	-0.001	0.018
		-0.000	-0.000	-0.000	0.000	0.000	-0.000	-0.005	-0.000	0.000	-0.000	
	ΔY_{o_1}	-0.000	-0.000	-0.000	0.000	0.000	0.000	-0.000	0.000	-3.078	-0.331	-17.820
		-0.000	-0.000	-0.000	0.000	0.000	-0.000	0.000	0.000	4.980	0.330	17.820
		0.000	-0.000	-0.000	0.000	0.000	-0.000	0.000	0.000	-0.000	0.000	
$u_2(t)$ =	ΔV_{ref_2}	0.466	-0.000	0.040	-0.000	-0.110	0.027	0.092	-18.110	-0.025	-0.004	2.048
		-3.400	-0.004	-0.267	0.006	0.079	-0.111	-0.051	13.340	0.293	-0.011	-2.270
		-2.260	-0.002	-0.162	0.006	0.023	-0.038	0.951	-0.018	0.281	0.050	
	ΔY_{o_2}	-0.000	-0.000	-0.000	0.000	0.000	-0.000	-0.000	0.003	-0.000	-0.000	-0.003
		0.000	-0.000	0.000	-0.000	-0.000	-0.000	-0.000	0.002	-3.610	-0.455	-24.500
		-0.000	-0.000	-0.000	0.000	-0.000	-0.000	0.003	-0.000	0.000	0.000	
$u_3(t)$ =	ΔV_{ref_3}	-4.590	-0.007	-0.270	0.017	0.422	-0.196	-0.054	34.850	-0.160	-0.057	-6.910
		5.160	0.005	0.470	-0.001	-0.050	0.042	0.061	-44.590	-0.002	0.040	7.180
		-1.560	-0.003	0.007	0.017	0.165	-0.129	-0.580	0.081	-0.885	-0.036	
	Δu_{gov_1}	-0.281	0.000	-0.005	0.002	-0.112	-0.009	0.074	0.600	0.026	0.000	-0.167
		-0.400	-0.005	-0.152	-0.010	0.117	0.013	-0.111	40.120	0.083	0.067	-0.024
		-0.638	0.005	-0.012	0.004	-0.196	-0.023	-17.790	-0.056	0.615	0.025	

Table 5.2: Feedback matrix for global control, case 1, when loads are considered as non-linear passive load, $K_p = K_q = 2$.

Input	Elements of the feedback gain matrix, F										
$u_1(t) =$ ΔV_{ref_1}	-0.034	-0.000	-0.001	0.000	0.004	-0.126	-0.003	0.657	-0.013	0.001	-0.020
	0.034	0.000	0.001	-0.000	-0.004	0.127	0.003	-0.578	0.011	-0.001	0.017
	-0.000	0.000	-0.000	-0.000	-0.000	-0.000	-0.045	-0.000	0.003	-0.001	
ΔY_{o_1}	0.000	-0.000	0.000	0.000	0.000	0.000	-0.000	0.000	-3.010	-0.331	-17.820
	-0.000	-0.000	-0.000	0.000	0.000	-0.000	0.000	0.000	5.010	0.329	17.720
	-0.000	-0.000	-0.000	0.000	0.000	-0.000	0.000	0.000	-0.000	0.000	
$u_2(t) =$ ΔV_{ref_2}	0.580	0.000	0.044	-0.001	-0.026	0.022	0.008	-4.240	0.008	0.003	0.688
	-0.625	-0.000	-0.048	0.001	0.028	-0.031	-0.009	4.690	0.064	-0.003	-0.725
	0.034	0.000	0.052	-0.000	-0.000	0.006	-0.118	-0.003	0.032	-0.002	
ΔY_{o_2}	-0.000	-0.000	-0.000	0.000	0.000	-0.000	-0.000	0.001	-0.000	0.000	-0.000
	0.000	-0.000	0.000	0.000	0.000	-0.000	-0.000	0.001	-3.617	-0.456	-24.500
	-0.000	-0.000	-0.000	0.000	0.000	-0.000	0.003	-0.000	0.000	0.000	
$u_2(t) =$ ΔV_{ref_3}	-0.243	-0.001	-0.001	0.002	-0.016	-0.005	0.112	-7.690	-0.055	-0.008	0.862
	-1.920	-0.003	-0.130	0.004	0.065	-0.078	0.010	5.570	0.126	-0.031	-2.210
	-2.190	-0.001	-0.121	0.010	0.039	-0.085	-1.070	-0.020	0.546	0.125	
Δu_{gov_1}	3.390	0.000	0.361	0.007	0.022	0.120	-0.014	11.820	0.487	0.180	8.350
	-5.840	-0.019	-0.414	0.015	0.492	-0.522	0.662	92.530	0.274	0.048	-4.670
	0.543	-0.000	0.120	0.011	0.179	-0.008	38.080	-0.108	2.840	0.850	

Table 5.3: Feedback matrix for global control, Case 1, when load is considered as combined load.

described in Chapter 3 by equations (3.12) and (3.13). Table 5.4 shows a summary of the performance indices for several non-linear passive loads and combined loads. The index varies 1:1.6, depending on the character of the loads.

The local controller obtained by disconnecting feedback signals from other machines is shown in Figure 5.1b. The eigenvalues of the system when controlled in this way are shown in Table 5.5, column 1. Some of them are underdamped.

Reference[61] showed that if the global controller is chosen in such a way that all the closed loop eigenvalues are preassigned to a region further to the left of the line EF, Figure 5.6, in the complex plane, the local control derived from it gives satisfactory performance, but as a result of this a suboptimal control can be possible. Another method suggested by those authors[61] was to design a global controller for those machines which can be considered to be closely tied electrically, i.e. global control for machines nos. 1 and 2 together (feedback paths from machine no. 3 disconnected, and a local control for machine no. 3 separately (without any feedback from machines nos. 1 and 2). However, in the present analysis it was discovered that the coupling between machines was not only dependent on the system network structure but also on the way that the dominant inputs select the group of eigenvalues, as was mentioned earlier in Section 5.2.1.

Improvement was obtained in two ways:

Load Characteristics				Performance Index
Bus No. 2		Bus No. 3		
K_p	K_q	K_q	K_q	
2	2	2	2	7099
1	2	1	2	7103
2	1	2	1	7070
1.5	1.5	0.5	0.5	7034
2	1.8	0.8	1.3	7024
Combined Load 12% Induction Motor		Combined Load 8% Induction Motor		11730

Table 5.4: Performance index for different load characteristics. Global modal control 1.

Method 1:

Only those critical eigenvalues which deteriorated when the local control was derived from the global control structure by disconnecting the feedback paths from other machines, were moved far away from the line EF of Figure 5.6.

Method 2:

Once the structure of the global modal controller was known and how the groups of eigenvalues were relocated by the dominant inputs, the local controller was obtained by disconnecting the feedback paths from the other machines. If the system dynamic stability deteriorated, then it was possible to introduce a compensation of that undesirable oscillation by introducing some signals from other machines to those which require extra compensation. These extra signals have been selected as those which were associated with the largest feedback gains of the global control matrix. These signals were defined as dominant signals.

When the first method was applied, starting from the second global modal control design (relocation given in Table 5.1, column 3) the system was stable, as is shown by the eigenvalues given in Table 5.5, column 2 where only the last pair of conjugate eigenvalues were moved further away from the line EF of Figure 5.6 and not all of them as was proposed in Reference 61.

Finally, Method 2 was applied to the same power system, but it was found that only one dominant signal (speed n) was required to

Local Control eigenvalues	Local Control Method 1 eigenvalues	Local Control Method 2 eigenvalues
-5.5 + j1.19	-11.6 + j5.3	-6.2 + j0.4
-5.5 - j1.19	-11.6 - j5.3	-6.2 - j0.4
-3.4 + j5.36	-3.27 + j5.4	-3.3 + j5.4
-3.4 - j5.36	-3.27 - j5.4	-3.3 - j5.4
-3.0 + j5.31	-3.55 + j3.1	-3.1 + j2.4
-3.0 - j5.31	-3.55 - j3.1	-3.1 - j2.4
-1.86 + j5.07	-2.04 + j7.44	-1.82 + j6.25
-1.86 - j5.07	-2.04 - j7.44	-1.82 - j6.25
-2.99	-2.99	-2.99
-2.69	-2.69	-2.7
-1.79 + j6.77	-1.8 + j6.51	-2.9 + j6.73
-1.79 - j6.77	-1.8 - j6.51	-2.9 - j6.73
-1.09	-1.79	-0.94
-1.8	-1.8	-1.8
-1.5	-1.5	-1.5
-6.37	-6.36	-0.9 + j2.94
+0.578	-0.70	-0.9 - j2.94
Performance Index $P.I.$	= 31792	= 5054

Table 5.5: Closed loop eigenvalues of the local controller design.

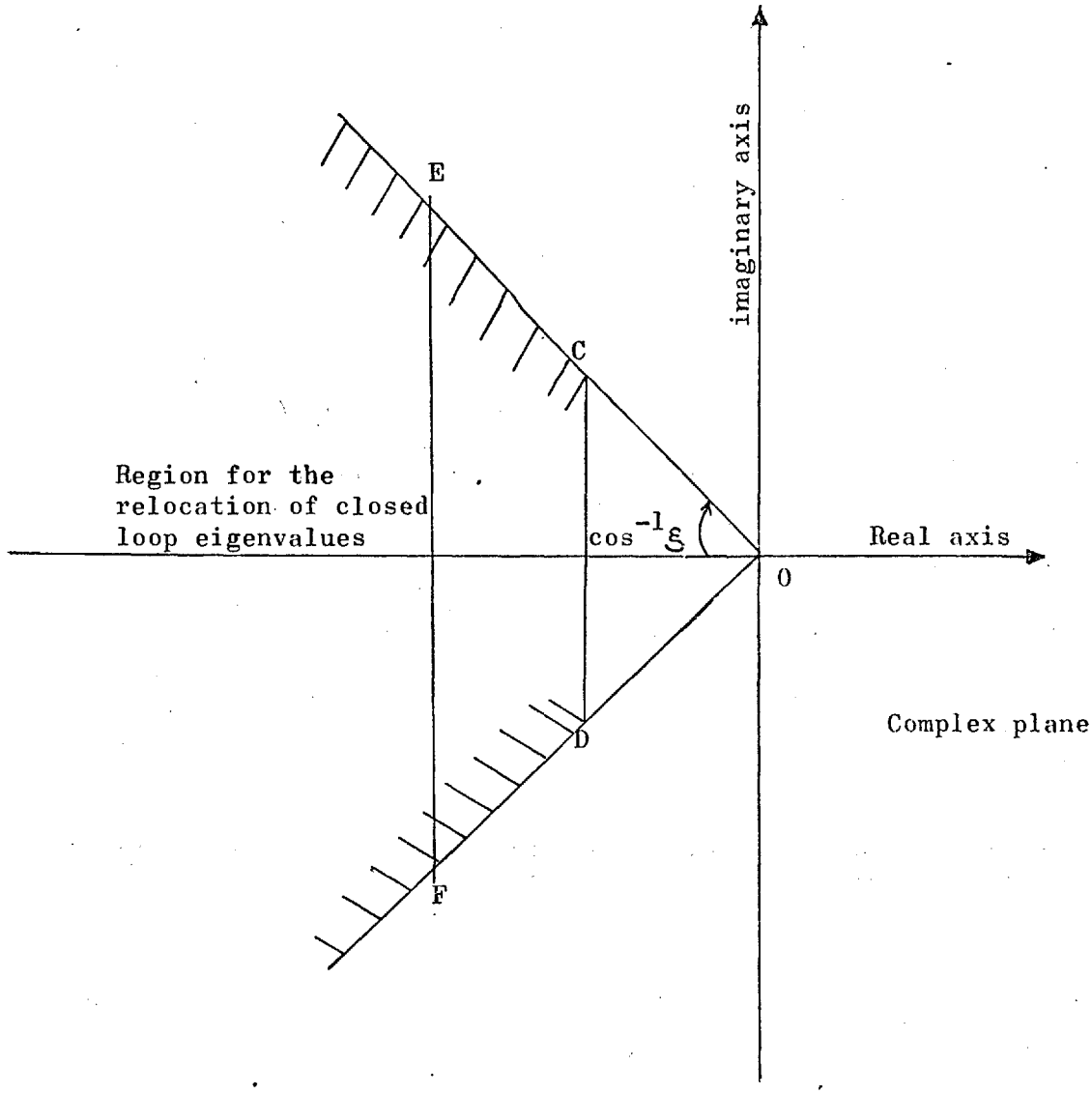

Figure 5.6: Criterion for the selection of new locations for the closed loop eigenvalues.

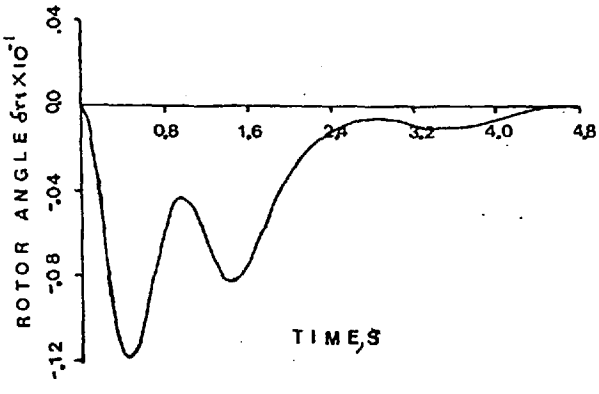

a) Rotor angle machine no. 1.

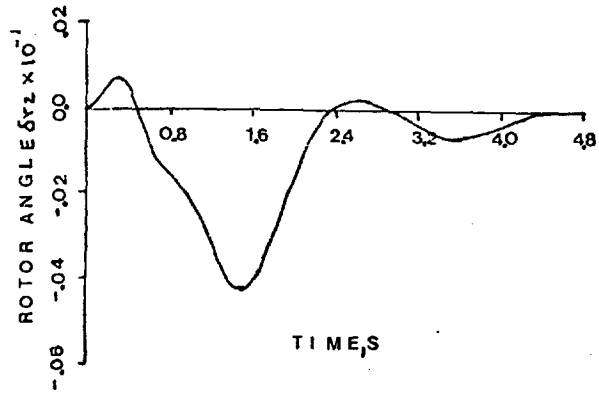

b) Rotor angle machine no. 2.

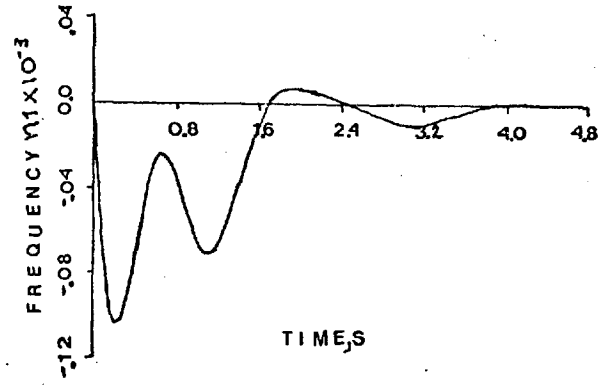

c) Frequency machine no. 1.

Figure 5.7: Rotor angles and frequency response to a small disturbance ($\Delta\psi_{fd_1}$ = 0.1 p.u.) local control.

Load Characteristics				Performance Index
Bus no. 2		Bus. no. 3		
K_p	K_q	K_p	K_q	
2	2	2	2	5055
1	2	1	2	5120
2	1	2	1	5012
1.5	1.5	0.5	0.5	5014
2	1.8	0.8	1.3	4996
combined load 12% induction motor		combined load 8% induction motor		10993

Table 5.6: Performance index for different load characteristics. Local control.

stabilize the system sending it from machine no. 2 to machine no. 3 excitation and speed governor setting reference points. The dominant signal was found to be the rotor speed of machine no. 2, which is an observable state variable. This gave the system a good transient response, as indicated by the eigenvalues in the last column of Table 5.5.

Figure 5.7 shows the response of the system when a small disturbance is applied for a local controller, designed by Method 2.

In this case, different load characteristics were also considered. Table 5.6 gives the performance index for different types of load representation at each bus bar.

5.5 CONCLUSION

Modal control techniques have been applied in order to design a global modal controller for a multi-machine system. A local modal controller at each machine without any feedback of state variables from other machines has been synthesized. In both cases the effect of load characteristics was investigated. Results indicate that the optimal feedback gains are very sensitive to load characteristics. Thus any global or local modal controller is far from optimal if these effects are not considered in the analysis. Combined load in this particular case appears to decrease the damping of the system and therefore the feedback gains required are higher than with the non-linear passive load representation. Global control control design for suitable eigenvalues relocation gives good

transient response, with low feedback gains, and a local control can be derived from it using the Method 2, whereas a local control with Method 1 can be suboptimal. However, both can improve the dynamic response of the system.

CHAPTER 6

CONCLUSIONS

6.1 MULTI-MACHINE DYNAMIC STABILITY MODEL AND SYNTHESIS OF FEEDBACK CONTROLLERS, INCLUDING THE EFFECT OF LOAD CHARACTERISTICS

The development of a mathematical model of the small signal dynamic performance of a multi-machine electric power system has been presented. For multi-input systems the algebraic manipulations required to derive a model would normally be difficult and would in any case be excessively time-consuming. Careful consideration of the system structure allows an efficient formulation that reduces significantly the time to compute the [A] and [B] matrices.

The recommended procedure of earlier systematic methods requires the inversion of ill-conditioned matrices[1,5,14,29]. The present procedure does not need the inversion of any matrix. An additional feature of the present model is that an open or closed loop model may be obtained and the system control inputs appear explicitly in the state space form for either situation. This is an essential requirement if modern control techniques are to be utilised to drive novel types of control systems. The structure of the model also gives the facility to apply eigenvalue sensitivities and state variable reduction techniques in order to identify how modes of oscillation are associated with each state variable.

It is shown that the application of modal control theory provides a direct non-iterative technique to design the feedback control law for a system. Its application to a power system problem

has shown that the system performance can be improved considerably without the trial and error involved in selecting the weighting matrices in the performance index for optimal control. Global control for suitable location of eigenvalues gives good performance with low feedback gains, whereas the local control derived from it can be suboptimal. Improvement was obtained when some machines drew additional signals from others.

In the dynamic stability studies of multi-machine systems reported previously[5,29,59,61,72] the system loads have been presented by rather crude models. In this mathematical model the effect of different load characteristics has been represented in the analysis of the dynamic stability and the synthesis of feedback controllers.

6.2 THE EFFECT OF LOAD CHARACTERISTICS ON DYNAMIC STABILITY CALCULATIONS

It is shown how state space theory can be applied to both multi-machine or single-machine systems including the effect of load characteristics in small-sized stability studies. In both cases it is shown that a crude load representation in the system model can lead to wrong results. In a single-machine system connected to an infinite bus-bar it is shown that the effect of the load characteristics upon the stability limit is dependent on the magnitude of the load and also the operating point. A non-linear passive load may be either stabilizing or unstabilizing, depending on the values of K_p and K_q. In the particular case of a big isolated load considered as an equivalent induction motor, it has

been shown that the critical condition is obtained only when the motor is considered to operate near pull out torque ($\tilde{T}_{max}$). This is one of the cases where an approximate load representation becomes necessary. A combined load representation gives a better load simulation for small disturbances, but it does not represent the dynamics of the induction motor.

In a multi-machine system the effect of load characteristics becomes difficult to evaluate in some circumstances. The IEEE Working Group[38] has mentioned some of these problems in discussing transient stability. Here it was found that the effect of load characteristics is on the oscillating modes associated with the transient stator and network terms that are usually neglected in multi-machine system models. When load is represented as non-linear and passive with $K_p \approx 0$ (approaching constant power), these modes of oscillation become highly undamped. However, if the reference machine is considered as an infinite bus-bar these oscillations are not present in the system even for a constant power load. Similarly with a combined load, in the absence of an infinite bus-bar, when the induction motor load is dominant a real mode $\lambda > 0$ can arise; this does not occur when the constant impedance load is dominant.

In Chapter 3 an eigenvalue was found associated with stator transient terms which varied dramatically with load conditions. As K_p and $K_q \longrightarrow 0$ the high frequency fell to zero and $\alpha > 0$. Both in this study and in one of the studies of Ludington (Chapter 4) system transient terms were ignored. When they were included (Chapter 4), this eigenvalue assumed supply frequency.

It is doubtful whether this eigenvalue represents the real performance of the system. The absence of network transient terms clearly distorts its frequency and damping.

The significance of such terms and the reason for their dependence on load characteristics is not clear. There must be a suspicion that the eigenvalue is spurious.

6.3 THE EFFECT OF LOAD CHARACTERISTICS ON THE DESIGN OF FEEDBACK CONTROLLERS OF GENERATORS

The effects of load representation on modal excitation and speed governor control, both in a single-machine system and a multi-machine power system, have been investigated. Non-linear passive load of different active and reactive power-voltage characteristics, as well as the combined load composed of constant impedance in parallel with the load of a group of induction motors, has been considered.

The effect of load characteristics on the design of the feedback controllers has been investigated using first a single infinite bus-bar system similar to that at Ludington (U.S.A.) which had steady-state stability problems. It has been found that the optimal feedback gains required for particular position of the eigenvalue depend upon the magnitude and characteristics of the load. An accurate network representation is important in the controller design.

A study of the effect of load characteristics in the design of feedback controllers for a multi-machine system was made. Modal

control technique was used to design such a controller. Many recent papers on optimal control[59,61,62] have used similar methods of modal design but none have taken the load characteristics into account. Here it has been shown that different load characteristics required different feedback gains to give the best response.

The results indicate that any global or local modal controller are far from optimal if load effects are not considered in the analysis.

6.4 SUGGESTIONS FOR FURTHER WORK

Load characteristics should be regarded as equally important as the other system parameters, and every effort should be made to determine them in a realistic way. Representative tests for every particular power system are required to guide in the formulation of a complete dynamic or a combined load, and ultimately to provide data for every stability study.

All the publications about small disturbance analyses have considered loads with static non-linear characteristics as dependent on voltage[14,34,35,38,56]. Moreover, load variation due to frequency changes is difficult to separate from that caused by accompanying voltage changes. The formulation presented in this thesis should be modified to introduce the variation of load with frequency at eacb load bus. Model reduction techniques can lead to the inclusion of better induction motor representations in a multi-machine system. The network representation has to be investigated for a multi-machine dynamic stability analysis including different load characteristics.

If the state vector of the system concerned is not accessible to direct measurement for the design of a modal controller, it is nevertheless possible to implement modal control by using an additional dynamic system known as an observer or state estimator. It would then be necessary to compare the designs for different load characteristics and select an appropriate one. Also, the feedback controller has to be tested in the non-linear system for large disturbances. This, and the use of decoupling control techniques, are large areas for future investigation.

REFERENCES

1. M.A. Laughton, "Matrix analysis of dynamic stability in synchronous multimachine systems", Proc. IEE, Vol. 113, p. 325, February 1966.

2. F.P. De Mello and C. Concordia, "Concepts of synchronous machine stability as affected by excitation control", Trans. IEEE on Power Apparatus and Systems, Vol. PAS-88, pp. 316-329, April 1969.

3. K. Prabhashankar and W. Janschewskyj, "Digital simulation of multimachine power system for stability studies", Trans. IEEE on Power Apparatus and Systems, Vol. PAS-88, pp. 73-80, May 1969.

4. J.M. Undrill, "Power system stability - studies by method of Lyapunov I, II", Trans. IEEE on Power Apparatus and Systems, Vol. PAS-86, pp. 791-811, July 1967.

5. J.M. Undrill, "Dynamic stability calculations for an arbitrary number of interconnected synchronous machines", Trans. IEEE on Power Apparatus and Systems, Vol. PAS-87, pp. 835-844, March 1968.

6. D.W. Olive, "New techniques for the calculations of dynamic stability", Trans. IEEE on Power Apparatus and Systems, Vol. PAS-85, pp. 767-777, 1966.

7. D.N. Ewart and F.P. De Mello, "A digital computer program for the automatic determination of dynamic stability limits", Trans. IEEE on Power Apparatus and Systems, Vol. PAS-86, No. 7, pp. 867-875, 1967.

8. D.S. Brereton, D.G. Lewis and C.C. Young, "Representation of Induction-Motor Loads during power system stability studies", Trans. AIEE, Vol. 76, Part III, pp. 451-461, 1957.

9. J.L. Gabbard Jr. and J.E. Rowe, "Digital computation of induction motor transient stability", Trans. AIEE, Vol. 76, Part III, pp. 970-977, 1957.

10. S.S. Kalsi, "Transient phenomena in large induction motors in a power system", Ph.D. Thesis, University of London, 1970.

11. S.S. Kalsi and B. Adkins, "Transient stability of power systems containing both synchronous and induction machines", Proc. IEE, Vol. 118, No, 10, pp. 1467-1474, 1971.

12. R.J. Alford, "Stability of synchronous generator associated with an induction motor load", Ph.D. Thesis, University of London, 1964.

13. IEEE Rotating Machinery Committee, "Recommended phasor diagram for synchronous machines", Trans. IEEE on Power Apparatus and Systems, Vol. PAS-88, pp. 1593-1610.

14. W. Mauricio and A. Semlyen, "Effect of load characteristics on the dynamic stability of power systems", Trans. IEEE on Power Apparatus and Systems, Vol. PAS-91, pp. 2295-2304, 1972.

15. E. Arriola Valdes, "Static economic dispatch in power systems", M.Sc. Thesis, University of London.

16. IEEE Committee Report, Computer representation of excitation systems, Paper 31, TP 67-424 IEEE Summer Power Meeting, 1967.

17. F.P. De Mello and T.F. Laskowski, "Concepts of power system dynamic stability", Trans. IEEE, Vol. PAS-94, pp. 827-833, 1975.

18. C. Concordia, "Representation of loads", IEEE Special Publication 75-CHO-970-4-PWR, pp. 41-45. Presented at the Power Engineering Society Winter Meeting, New York, 1975.

19. P.L. Dandeno and P. Kundur, "A non-iterative transient stability program including the effects of variable load-voltage characteristics", Trans. IEEE, Vol. PAS-92, pp. 1478-1484, 1973.

20. D.L. Neasham, K. Jenckins and J.F. Bashier, "Simulation of site tests on a 120 MW turbogenerator", Proc. IEE, Vol. 121, pp. 457-463, 1974.

21. J.H. Wilkinson, "The algebraic eigenvalue problem", Oxford University Press, 1965.

22. B. Adkins and R.G. Harley, "The general theory of alternating current machines", Chapman and Hall, London, 1975.

23. D.F. Shankle, C.M. Murphy, R.W. Long and E.L. Harder, "Transient stability studies - I: Synchronous and induction machines", Trans. AIEE, Vol. 73, Part III-B, 1954 (February 1955 section), pp. 1563-1577, Discussions by C. Concordia, pp. 1578-1579, and C.C. Young, p. 1579.

24. K. Prabhashankar and P.L. Dandeno, "Practical application of eigenvalue techniques in the analysis of power system dynamics", 5th Power Systems Computation Conference, Vol. 2, Cambridge, 1-5 September 1975.

25. J.H. Anderson, "Matrix methods for the study of a regulated synchronous machine", Proc. IEEE, Vol. 57, pp. 2122-2136, December 1969.

26. W.G. Heffron, Jr., "A simplified approach to steady state stability limits", Trans. AIEE, pp. 39-44, February 1954.

27. S.B. Crary, "Steady state stability of composite systems", Trans. AIEE, pp. 787-792, November 1933.

28. R.T.H. Alden and P.J. Nolan, "Evaluating alternative models for power system dynamic stability studies", Trans. IEEE, Vol. PAS-95, No. 2, pp. 433-440, March/April 1976.

29. R.T.H. Alden and H.M. Zein El Din, "Multimachine dynamic stability calculations", Trans. IEEE on Power Apparatus and Systems, Vol. PAS-95, No. 5, pp. 1529-1534, September/October 1976.

30. P.J. Nolan, N.K. Sinha and R.T.H. Alden, "Eigenvalue sensitivities of power systems including network and shaft dynamics", Trans. IEEE on Power Apparatus and Systems, Vol. PAS-95, No. 4, July/August 1976, pp. 1318-1324.

31. Nottingham Algorithms Group ICL 1900 System, N.A.G. Library Manual.

32. E.W. Kimbark, "Power system stability", Vol. I, Elements of Stability Calculations.

33. J.M. Stephenson and A.H.M.S. Vla, "Dynamic stability analysis of synchronous machines including damper circuits, automatic voltage regulator and governor", Proc. IEE, Vol. 124, No. 8, pp. 681-688, 1977.

34. R.T.H. Alden and H.M. Zein El Din, "Effect of load characteristics on power system dynamic stability", IEEE Paper A-76-363-2 presented at the Power Engineering Society Summer Meeting 1976.

35. N.D. Rao and S.C. Tripathy, "Effect of load characteristics and voltage regulator speed stabilizing signal on power system dynamic stability", Proc. IEE, Vol. 124, No. 7, pp. 613-618, 1977.

36. P. Subramaniam and G.J. Berg, "Effects of system load on optimal excitation control", Paper A-78-248-7 presented at the Power Engineering Society Winter Meeting, New York, 1978.

37. G.J. Berg and A.K. Kar, "Model representation of power system loads", Proc. PICA Conference, pp. 153-162, 1971.

38. IEEE Group Report, "System load dynamics simulation effects and determination of load constants", Trans. IEEE, Vol. PAS-92, pp. 600-609, 1973.

39. G. Shackshaft, O.C. Symons and J.G. Hadwick, "General purpose model of power system loads", Proc. IEE, Vol. 124, No. 8, pp. 715-723, August 1977.

40. M.H. Kent, W.R. Schmus, F.A. McCrakin and L.M. Wheeler, "Dynamic modelling of loads in stability studies", Trans. IEEE on Power Apparatus and Systems, Vol. PAS-88, pp. 756-763, May 1969.

41. G.R. Quan and M.Z. Tarnawecky, "Load representation for transient stability studies - digital modelling", Paper A-76-363-2 presented at the Power Engineering Society Summer Meeting 1976.

42. R.H. Nelson, T.A. Lipo and P.C. Krause, "Stability analysis of a symmetrical induction machine", Trans. IEEE, Vol. PAS-88, No. 11, pp. 1710-1717, 1969.

43. P.N. Bapast, "Frequency response of induction motors under forced oscillations", Proc. IEE, Vol. 117, No. 3, pp. 561-566, 1970.

44. J.J. Cathy, R.K. Cavin III and A.K. Ayoub, "Transient load model of an induction motor", Paper T-73-197-1 presented at the Power Engineering Society Winter Meeting, New York, 1973.

45. R. Stern and D.W. Novotny, "A simplified approach to the determination of induction machine dynamic response", Paper A-77-123-3 presented at the Power Engineering Society Winter Meeting, New York, 1977.

46. M.M. Abdel Haking and G.J. Berg, "Dynamic single unit representation of induction motor groups", Trans. IEEE, Vol. PAS-95, pp. 155-165, 1976.

47. D.H. Baker and P.C. Krause, "Low frequency rotor oscillations introduced by the excitation system", Paper C-74-510-5 presented at the Power Engineering Society Summer Meeting, July 1974.

48. D.H. Baker, P.C. Krause and P.A. Rauche, "An investigation of investigation system interaction", Paper C-74-105-3 presented at the Power Engineering Society Winter Meeting, January 1974.

49. D.H. Baker, P.C. Krause, P.A. Rauche and D.L. Kackett, "Dynamic stability analysis of a three-machine infinite bus system", Paper C-75-035-1 presented at the Power Engineering Society Winter Meeting, January 1975.

50. J.E. Van Ness, J.M. Boyle and F.P. Imad, "Sensitivities of a large multiple loop control system", Trans. IEEE on Automatic Control, Vol. AC-10, pp. 308-315, July 1965.

51. I.A. Edelstein, "Improvement in transient stability of a turbogenerator by rotation of field magnetomotive forces", Ph.D. Thesis, London University, 1976.

52. J.H. Anderson, "The control of synchronous machines using optimal control theory", Proc. IEEE, Vol. 59, No. 1, pp. 25-35, 1971.

53. E.J. Davison amd N.S. Rav, "The optimal output feedback control of a synchronous machine", Trans. IEEE on Power Apparatus and Systems, Vol. PAS-90, pp. 2123-2134, 1971.

54. P.A. Rusche, D.L. Hackett, D.H. Baker, G.E. Gareis and P.C. Krause, "Investigation of the dynamic oscillations of the Ludington pumped storage plant", Trans. IEEE on Power Apparatus and Systems, Vol. PAS-95, No. 6, pp. 1854-1862, 1976.

55. Yao-Nan Yu, K. Vonsuriya and L.N. Wedman, "Application of an optimal control theory to a power system", Trans. IEEE on Power Apparatus and Systems, Vol. PAS-89, No. 1, pp. 55-62, 1970.

56. D. Olguin Salinas and D.C. Macdonald, "The effect of load characteristics on the design of feedback controllers of generators", Proc. 14th Universities Power Engineering Conference, Loughborough University of Technology, 3-5 April 1979.

57. B. Porter and R. Crosby, "Modal control theory and applications", Book 1972, University of Salford.

58. M.A. Pai, S.S. Prabhu and I.V. Ramana, "Modal control of a power system", Int. J. Systems Sci., Vol. 6, No. 1, pp. 87-100, 1975.

59. E.J. Davison, N.S. Rau and F.V. Palmay, "The optimal decentralized control of a power system consisting of a number of interconnected synchronous machines", Int. J. Control, Vol. 18, No. 6, pp. 1313-1328, 1973.

60. J.H. Anderson, D.J. Leffen and V.M. Paina, "Dynamic modelling of an arbitrary number of interconnected power generating units in state space form", Paper C-73-093-2 presented at the Power Engineering Society Winter Meeting, New York, 1973.

61. M.A. Pai, K.R. Padiyar and P.S. Shetty, "Decentralized modal control of multimachine power systems", Paper A-78-255-2 presented at the Power Engineering Society Winter Meeting, 1978.

62. Yao Nan-Yu and H.A.M. Moussa, "Optimal stabilization of a multimachine system", IEEE Trans. on Power Apparatus and Systems, Vol. PAS-91, No. 3, pp. 1174-1182.

63. A.R. Fragg and R.B. Whorrod, "A comparative analogue simulation study of conventional and divided winding rotor 500 MW turbogenerators", Research Report of the CEGB, January 1969.

APPENDIX A.1

LINEAR SYNCHRONOUS MACHINE EQUATIONS

Using the sample procedure of considering only the first terms of a Taylor series expansion of the equations, about any operating point, suitable for linear analysis as shown below.

Direct-axis flux linkage:

$$\Delta\psi_{fd} = X_{ffd}\,\Delta i_{fd} + X_{afd}\,\Delta i_{d} + X_{fkd}\,\Delta i_{kd} \qquad (A.1.1)$$

$$\Delta\psi_{d} = X_{afd}\,\Delta i_{fd} + X_{d}\,\Delta i_{d} + X_{akd}\,\Delta i_{kd} \qquad (A.1.2)$$

$$\Delta\psi_{kd} = X_{fkd}\,\Delta i_{fd} + X_{akd}\,\Delta i_{d} + X_{kkd}\,\Delta i_{kd} \qquad (A.1.3)$$

Quadrature-axis flux linkage:

$$\Delta\psi_{q} = X_{q}\,\Delta i_{q} + X_{akq}\,\Delta i_{kq} \qquad (A.1.4)$$

$$\Delta\psi_{kq} = X_{akq}\,\Delta i_{q} + X_{kkq}\,\Delta i_{kq} \qquad (A.1.5)$$

In a matrix compact form:

$$[\Delta\psi_{g}] = [X][\Delta i_{g}] \qquad (A.1.6)$$

$$\Delta\psi_{g} = \mathrm{col}(\Delta\psi_{fd}, \Delta\psi_{d}, \Delta\psi_{kd}, \Delta\psi_{q}, \Delta\psi_{kq}) \qquad (A.1.7)$$

$$\Delta i_{g} = \mathrm{col}(\Delta i_{fd}, \Delta i_{d}, \Delta i_{kd}, \Delta i_{q}, \Delta i_{kq}) \qquad (A.1.8)$$

Direct-axis voltages:

$$\frac{1}{\omega_o}\,p\,\Delta\psi_{fd} = \frac{r_{fd}}{X_{afd}}\,\Delta E_{fd} - r_{fd}\,\Delta i_{fd} \qquad (A.1.9)$$

$$\frac{1}{\omega_o}\,p\Delta\psi_{d} = -\Delta v_{d} - r_{s}\,\Delta i_{d} - \Delta\psi_{q} - \psi_{q}\,\Delta n \qquad (A.1.10)$$

$$\frac{1}{\omega_o}\,p\Delta\psi_{kd} = -r_{kd}\,\Delta i_{kd} \qquad (A.1.11)$$

Quadrature-axis voltages:

$$\frac{1}{\omega_o} p\Delta\psi_q = - \Delta v_q - r_s \Delta i_q + \Delta\psi_d + \psi_d \Delta n \qquad \text{(A.1.12)}$$

$$\frac{1}{\omega_o} p\Delta\psi_{kq} = - r_{kq} \Delta i_{kq} \qquad \text{(A.1.13)}$$

In a matrix compact form:

$$[\Delta V] = [R][\Delta i_g] + \left\{\frac{p}{\omega_o}[I] - [I^*]\right\}[\Delta\psi_g] + [\psi_g^*]\, n \qquad \text{(A.1.14)}$$

$[I]$ = unit matrix

$$[\Delta V] = \text{col}\left(\frac{r_{fd}}{X_{afd}}\Delta E_{fd},\ -\Delta v_d,\ 0,\ -\Delta v_q,\ 0\right)$$

$$[R] = \text{diag}(r_{fd},\ r_s,\ r_{kd},\ r_s,\ r_{kq})$$

$$[I^*] = \begin{bmatrix} 0 & 0 & 0 & 0 & 0 \\ 0 & 0 & 0 & 1 & 0 \\ 0 & 0 & 0 & 0 & 0 \\ 0 & -1 & 0 & 0 & 0 \\ 0 & 0 & 0 & 0 & 0 \end{bmatrix}$$

$$[\Delta\psi_g^*] = \text{col}(0,\ \psi_q,\ 0,\ -\psi_d,\ 0)$$

Torque at the air gap:

$$\Delta T_g = \psi_d \Delta i_q + i_q \Delta\psi_d - \psi_q \Delta i_d - i_d \Delta\psi_q \qquad \text{(A.1.15)}$$

Mechanical equations:

$$T_m\, p\, \Delta n = \Delta T_{mech} - \Delta T_g \qquad \text{(A.1.16)}$$

$$p\, \Delta\delta r = \omega_o \Delta n \qquad \text{(A.1.17)}$$

Voltage regulator:

$$\Delta E_{fd} = \frac{K_r}{1 + T_{rg} p}\, \Delta V \qquad \text{(A.1.18)}$$

Speed Governor

Turbine:

$$\Delta T_{mech} = A_t \Delta g - D_{nom} B \Delta n + 1.5\, A_t B \Delta h \qquad \text{(A.1.19)}$$

Governor:

$$p\Delta c = - p\Delta n - \delta_t p\Delta g - \frac{1}{T_R}(\Delta C + \Delta n) \qquad \text{(A.1.20)}$$

Gate servomotor:

$$p\Delta g = Q_g(\Delta C - \delta p\Delta g - W_s p\Delta n) \qquad \text{(A.1.21)}$$

Water column:

$$p\Delta h = - 2p\Delta g - \frac{2}{T_w}\Delta h \qquad \text{(A.1.22)}$$

Transformation equations:

$$\Delta P_2 = i_d \Delta v_d + i_q \Delta v_q + v_d \Delta i_d + v_q \Delta i_q \qquad \text{(A.1.23)}$$

$$\Delta Q_2 = i_q \Delta v_d - i_d \Delta v_q + v_d \Delta i_q - v_q \Delta i_d \qquad \text{(A.1.24)}$$

$$\Delta v_2 = \frac{v_d}{V_2}\Delta v_d + \frac{v_q}{V_2}\Delta v_q \qquad \text{(A.1.25)}$$

$$\Delta \delta m = \frac{v_q}{V_2^2}\Delta v_d - \frac{v_d}{V_2^2}\Delta v_q \qquad \text{(A.1.26)}$$

$$\Delta \delta r = \Delta \delta_2 - \Delta \delta_m \qquad \text{(A.1.27)}$$

NON-SYNCHRONOUS LOAD REPRESENTATION

Induction Motor:

The equations below are obtained directly from the synchronous machine equations with the following simplifications:

(i) The terms and equations related to the field circuit can be eliminated.

(ii) The induction motor has round and symmetrical rotor windings.

$$X_d = X_q = X_s = X_{\ell_1} + X_m$$

$$X_{kkd} = X_{kkq} = X_r = X_{\ell_2} + X_m$$

$$X_{akd} = X_{akq} = X_m$$

$$r_d = r_q = R_s$$

$$r_{kd} = r_{kq} = R_r$$

(iii) In the induction motor the magnetic fields rotate at different speeds from the rotor. Therefore the reference frame for the induction motor should not be connected to the rotor. The most convenient reference frame in this case is the network frame which rotates at synchronous speed ω_0.

Machine Equations:

Flux linkage:

$$\psi_{sd} = X_s i_{sd} + X_m i_{rd} \quad \text{(A.1.28)}$$

$$\psi_{rd} = X_m i_{sd} + X_r i_{rd} \quad \text{(A.1.29)}$$

$$\psi_{sq} = X_s i_{sq} + X_m i_{rq} \quad \text{(A.1.30)}$$

$$\psi_{rq} = X_m i_{sq} + X_r i_{rq} \quad \text{(A.1.31)}$$

Voltages:

$$-v_d = R_s i_{sd} + \frac{1}{\omega_o} p\psi_{sd} + \psi_{sq} \quad \text{(A.1.32)}$$

$$0 = R_r i_{rd} + \frac{1}{\omega_o} p\psi_{rd} + S\psi_{rq} \quad \text{(A.1.33)}$$

$$-v_q = R_s i_{sq} + \frac{1}{\omega_o} p\psi_{sq} - \psi_{sq} \quad \text{(A.1.34)}$$

$$0 = R_s i_{rq} + \frac{1}{\omega_o} p\psi_{rq} - S\psi_{rd} \quad \text{(A.1.35)}$$

Electrical torque:

$$T_g = \psi_{sd} i_{sq} - \psi_{sq} i_{sd} \quad \text{(A.1.36)}$$

Mechanical equation:

$$T_m pn = T_{mech} - T_g \quad \text{(A.1.37)}$$

In the same way as the the synchronous machine, the above equations can be linearized for small perturbance analysis.

Flux linkage:

$$[\Delta\psi_M] = [X][\Delta i_M] \tag{A.1.38}$$

$$[\Delta\psi_M] = \text{col}(\Delta\psi_{sd}, \Delta\psi_{rd}, \Delta\psi_{sq}, \Delta\psi_{rq}) \tag{A.1.39}$$

$$[\Delta i_M] = \text{col}(\Delta i_{sd}, \Delta i_{rd}, \Delta i_{sq}, \Delta i_{rd}) \tag{A.1.40}$$

$$[X] = \begin{bmatrix} X_s & X_m & & \\ X_m & X_r & & \\ & & X_s & X_m \\ & & X_m & X_r \end{bmatrix} \tag{A.1.41}$$

Voltages:

$$[\Delta V] = [R][\Delta i_M] + \left\{\frac{p}{\omega_o}[I] + [S]\right\}[\Delta\psi_M] + [\psi_M^*]\Delta n \tag{A.1.42}$$

$$[\Delta V] = \text{col}(-\Delta v_{sd}, 0, -\Delta v_{sq}, 0) \tag{A.1.43}$$

$$[\Delta i_M] = \text{col}(\Delta i_{sd}, \Delta i_{rd}, \Delta i_{sq}, \Delta i_{rq}) \tag{A.1.44}$$

$$[R] = \text{diag}(R_s, R_r, R_s, R_r) \tag{A.1.45}$$

$$[\psi_M^*] = \text{col}(0, -\psi_{rq}, 0, \psi_{rd}) \tag{A.1.46}$$

$$[S] = \begin{bmatrix} 0 & 0 & 1 & 0 \\ 0 & 0 & 0 & S \\ -1 & 0 & 0 & 0 \\ 0 & -S & 0 & 0 \end{bmatrix} \tag{A.1.47}$$

Transformation equations:

For the induction motor only the transformation from the rectangular to polar form is necessary. Here the reference frame is the network reference, which rotated at ω_o.

$$P_3 = v_{sd} i_{sd} + v_{sq} i_{sq} \tag{A.1.48}$$

$$Q_3 = v_{sd} i_{sq} - v_{sq} i_{sd} \tag{A.1.49}$$

$$V_3 = v_{sd}^2 + v_{sq}^2 \tag{A.1.50}$$

$$\delta_3 = t_g^{-1} \left(\frac{v_{sd}}{v_{sq}}\right) \tag{A.1.51}$$

Equations (A.1.48) - (A.1.51) in linearized form are obtained in a straightforward manner:

$$\Delta P_3 = i_{sd} \Delta v_{sd} + i_{sq} \Delta v_{sq} + v_{sd} \Delta i_{sd} + v_{sq} \Delta i_{sq} \tag{A.1.52}$$

$$\Delta Q_3 = i_{sq} \Delta v_{sd} - i_{sd} \Delta v_{sq} + v_{sd} \Delta i_{sq} - v_{sq} \Delta i_{sd} \tag{A.1.53}$$

$$\Delta V_3 = \frac{v_{sd}}{V_3} \Delta v_{sd} + \frac{v_{sq}}{V_3} \Delta v_{sq} \tag{A.1.54}$$

$$\Delta \delta_3 = \frac{v_{sq}}{V_3^2} \Delta v_{sd} - \frac{v_{sd}}{V_3^2} \Delta v_{sq} \tag{A.1.55}$$

Non-linear passive loads:

For a non-linear admittance, active and reactive powers are:

$$P_L = G(V, \omega) V^2 \tag{A.1.56}$$

$$Q_L = B(V, \omega) V^2 \tag{A.1.57}$$

$$VA = Vi^*$$

$$i = YV \qquad Y = G - jB$$

$$i^* = Y^*V^*$$

$$VA = V(G + jB)V^* \tag{A.1.58}$$

$$VA = (G + jB)V^2 \tag{A.1.59}$$

If frequency dependence of G and B is ignored:

$$P_L = GV^2 \tag{A.1.60}$$

$$Q_L = BV^2 \tag{A.1.61}$$

The linearized form of equations (A.1.60) and (A.1.61) is:

$$\Delta P_L = (V^2 \frac{\partial G}{\partial V} + 2GV)\Delta V \tag{A.1.62}$$

$$\Delta P_L = (\frac{V^2 G}{G} \frac{\partial G}{\partial V} + 2G \frac{VV}{V})\Delta V \tag{A.1.63}$$

$$\Delta P_L = \frac{P_L}{V}(2 + \frac{V}{G} \frac{\partial G}{\partial V})\Delta V \tag{A.1.64}$$

In a similar way:

$$\Delta Q_L = \frac{Q_L}{V}(2 + \frac{V}{B} \frac{\partial B}{\partial V})\Delta V \tag{A.1.65}$$

A type of relationship widely used to represent non-linear passive loads is:

$$P_L = C_1 V^{KP} \tag{A.1.66}$$

$$Q_L = C_2 V^{KQ} \tag{A.1.67}$$

The linearized form of equations (A.1.66) and (A.1.67) is:

$$\Delta P_L = C_1 \frac{\partial V^{KP}}{\partial V}\Delta V = C_1 K_p V^{(K_p - 1)}\Delta V$$

$$\Delta P_L = K_p C_i V^{K_p} V^{-1}\Delta V$$

$$\Delta P_L = K_p \frac{P_L}{V} \Delta V \qquad (A.1.68)$$

In a similar way:

$$\Delta Q_L = K_q \frac{Q_L}{V} \Delta V \qquad (A.1.69)$$

Combined Load:

It is assumed that the load group can be simulated by the simple equivalent circuit shown in Figure A.1.3, in which a constant shunt admittance reoresents the static load and a voltage behind a constant admittance represents an equivalent induction motor.

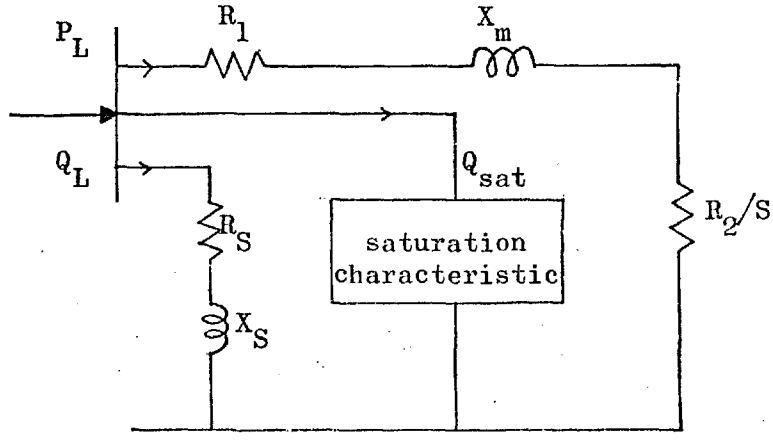

Figure A.1.2: Model to represent the combined load.

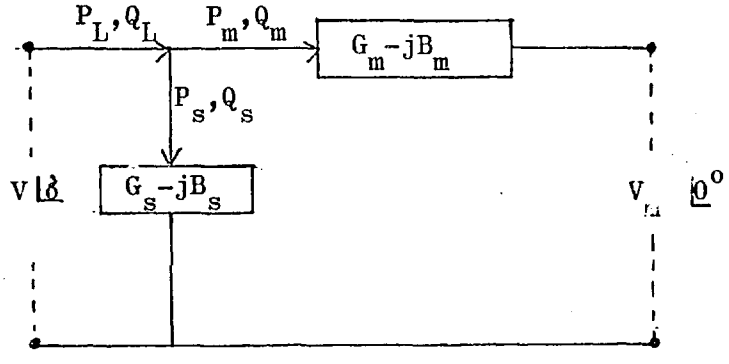

Figure A.1.3: Simple equivalent circuit.

The real and reactive powers taken by the equivalent motor are:

$$P_m = V^2 G_m - V V_m Y_m \cos(\phi'_m + \delta) \quad \text{(A.1.70)}$$

$$Q_m = V^2 B_m - V V_m Y_m \sin(\phi'_m + \delta) \quad \text{(A.1.71)}$$

and those taken by the static load are:

$$P_s = V^2 G_s \quad \text{(A.1.72)}$$

$$Q_s = V^2 B_s \quad \text{(A.1.73)}$$

giving group demand of:

$$P_L = V^2(G_m+G_s) - V V_m Y_m \cos(\phi'_m+\delta) \quad \text{(A.1.74)}$$

$$Q_L = V^2(B_m+B_s) - V V_m Y_m \sin(\phi'_m+\delta) \quad \text{(A.1.75)}$$

$$Y_m = (G_m^{\,2} + B_m^{\,2})^{\frac{1}{2}} \quad \text{(A.1.76)}$$

$$\phi'_m = T_g^{-1} \frac{B_m}{G_m} \quad \text{(A.1.77)}$$

$$Y_s = (G_s^{\,2} + B_s^{\,2})^{\frac{1}{2}} \quad \text{(A.1.78)}$$

$$\phi'_s = t_g^{-1} \frac{B_s}{G_s} \quad \text{(A.1.79)}$$

These equations above can be linearized in order to have the power variations against voltage and phase angle:

$$\Delta P_L = \left[2V(G_m+G_s) - V_m Y_m \cos(\phi'_m+\delta)\right] \Delta V + \left[V V_m Y_m \sin(\phi'_m+\delta)\right] \Delta\delta \quad \text{(A.1.80)}$$

$$\Delta Q_L = \left[2V(B_m+B_s) - V_m Y_m \sin(\phi'_m+\delta)\right] \Delta V - \left[V V_m Y_m \cos(\phi'_m+\delta)\right] \Delta\delta \quad \text{(A.1.81)}$$

For the sake of facility, equations (A.1.80) and (A.1.81) are written in condensed form, to be used in the program as:

$$\begin{bmatrix} \Delta P_L \\ \Delta Q_L \end{bmatrix} = \begin{bmatrix} PART_3 & PART_4 \\ QART_3 & QART_4 \end{bmatrix} \begin{bmatrix} \Delta V \\ \Delta \delta \end{bmatrix} \qquad (A.1.82)$$

APPENDIX A.2

EQUATION SYSTEM TO FORM [K] MATRIX

The equations (2.62) and (2.63) described in Chapter 2 are obtained after the linearized equations of each element are known. The set of these equations depends on the load representation. The matrices $[K_1, \ldots, K_5]$ can be formed by inspection (Figures 2.3 and 2.4). According to Figures 2.3 and 2.4 the vector elements should first be specified in the following sequence: derivatives of state variables, state variables, and algebraic variables, as follows:

1) Equations considering the load as an induction motor ($T_{mech} \propto n$):

$$\frac{1}{\omega_o} p \Delta\psi_{fd} - \frac{r_{fd}}{X_{afd}} \Delta E_{fd} + r_{fd} \Delta i_{fd} = 0 \qquad (A.2.1)$$

$$\frac{1}{\omega_o} p \Delta\psi_d + \Delta\psi_q + \Delta\psi_q \Delta n + \Delta v_d + r_s \Delta i_d = 0 \qquad (A.2.2)$$

$$\frac{1}{\omega_o} p \Delta\psi_{kd} + r_{kd} \Delta i_{kd} = 0 \qquad (A.2.3)$$

$$\frac{1}{\omega_o} p \Delta\psi_q - \Delta\psi_d - \psi_d \Delta n + \Delta v_q + r_s \Delta i_q = 0 \qquad (A.2.4)$$

$$\frac{1}{\omega_o} p \Delta\psi_{kq} + r_{kq} \Delta i_{kq} = 0 \qquad (A.2.5)$$

$$T_{rg} p \Delta E_{fd} + \Delta E_{fd} - K_r \Delta v_2 = 0 \qquad (A.2.6)$$

$$- p \Delta\delta r + \omega_o \Delta n = 0 \qquad (A.2.7)$$

$$-T_m p \Delta n - i_q \Delta\psi_d + i_d \Delta\psi_q - D_{nom}{}^B \Delta n + A_t \Delta g + 1.5 A_t{}^B \Delta h + \psi_q \Delta i_d - \psi_d \Delta i_q = 0 \qquad (A.2.8)$$

$$- p \Delta g - Q_g W_s p \Delta n - Q_g \delta_p \Delta g + Q_g \Delta C = 0 \qquad (A.2.9)$$

$$- p\Delta C - p\Delta n - \delta_t p\Delta g - \frac{1}{T_R}\Delta n - \frac{1}{T_R}\Delta C = 0 \qquad (A.2.10)$$

$$- p\Delta h - 2p\Delta g - \frac{2}{T_w}\Delta h = 0 \qquad (A.2.11)$$

$$\frac{1}{\omega_o} p\Delta\psi_{sd} + \psi_{sq} + \Delta v_{sd} + R_s \Delta i_{sd} = 0 \qquad (A.2.12)$$

$$\frac{1}{\omega_o} p\Delta\psi_{rd} + S\psi_{rq} - \Delta n\ \psi_{rq} + R_r \Delta i_{rd} = 0 \qquad (A.2.13)$$

$$\frac{1}{\omega_o} p\Delta\psi_{sq} - \Delta\psi_{sd} + \Delta v_{sq} + R_s \Delta i_{sq} = 0 \qquad (A.2.14)$$

$$\frac{1}{\omega_o} p\Delta\psi_{rq} - S\Delta\psi_{rd} + \Delta n\ \psi_{rd} + R_r \Delta i_{rq} = 0 \qquad (A.2.15)$$

$$-T_m p\Delta n + P_{ROT}\Delta n - i_{sq}\Delta\psi_{sd} + i_{sd}\Delta\psi_{sq} + \psi_{sq}\Delta i_{sd} - \psi_{sd}\Delta i_{sq} = 0 \qquad (A.2.16)$$

$$- \Delta P_2 + \frac{\partial P_2}{\partial \delta_2}\Delta\delta_2 + \frac{\partial P_2}{\partial V_2}\Delta V_2 + \frac{\partial P_2}{\partial \delta_3}\Delta\delta_3 + \frac{\partial P_2}{\partial V_3}\Delta V_3 = 0 \qquad (A.2.17)$$

$$- \Delta Q_2 + \frac{\partial Q_2}{\partial \delta_2}\Delta\delta_2 + \frac{\partial Q_2}{\partial V_2}\Delta V_2 + \frac{\partial Q_2}{\partial \delta_3}\Delta\delta_3 + \frac{\partial Q_2}{\partial V_3}\Delta V_3 = 0 \qquad (A.2.18)$$

$$- \Delta\delta_2 + \Delta\delta r + \frac{v_q}{V_2^2}\Delta v_d - \frac{v_d}{V_2^2}\Delta v_q = 0 \qquad (A.2.19)$$

$$- \Delta V_2 + \frac{v_d}{V_2}\Delta v_d + \frac{v_q}{V_2}\Delta v_q = 0 \qquad (A.2.20)$$

$$- \Delta P_2 + i_d \Delta v_d + i_q \Delta v_q + v_d \Delta i_d + v_q \Delta i_q = 0 \qquad (A.2.21)$$

$$- \Delta Q_2 + i_q \Delta v_d - i_d \Delta v_q - v_q \Delta i_d + v_d \Delta i_q = 0 \qquad (A.2.22)$$

$$- \Delta\psi_{fd} + X_{ffd}\Delta i_{fd} + X_{afd}\Delta i_d + X_{fkd}\Delta i_{kd} = 0 \qquad (A.2.23)$$

$$- \Delta\psi_d + X_{afd}\Delta i_{fd} + X_d \Delta i_d + X_{akd}\Delta i_{kd} = 0 \qquad (A.2.24)$$

$$- \Delta\psi_{kd} + X_{fkd}\Delta i_{fd} + X_{akd}\Delta i_d + X_{kkd}\Delta i_{kd} = 0 \qquad (A.2.25)$$

$$- \Delta\psi_q + X_q \Delta i_q + X_{akq}\Delta i_{kq} = 0 \qquad (A.2.26)$$

$$- \Delta\psi_{kq} + X_{akq}\Delta i_q + X_{kkq}\Delta i_{kq} = 0 \qquad (A.2.27)$$

$$-\Delta P_3 + \frac{\partial P_3}{\partial \delta_2}\Delta\delta_2 + \frac{\partial P_3}{\partial V_2}\Delta V_2 + \frac{\partial P_3}{\partial \delta_3}\Delta\delta_3 + \frac{\partial P_3}{\partial V_3}\Delta V_3 = 0 \qquad \text{(A.2.28)}$$

$$-\Delta Q_3 + \frac{\partial Q_3}{\partial \delta_2}\Delta\delta_2 + \frac{\partial Q_3}{\partial V_2}\Delta V_2 + \frac{\partial Q_3}{\partial \delta_3}\Delta\delta_3 + \frac{\partial Q_3}{\partial V_3}\Delta V_3 = 0 \qquad \text{(A.2.29)}$$

$$-\Delta\delta_3 + \frac{v_{sq}}{v_3^2}\Delta v_{sd} - \frac{v_{sd}}{v_3^2}\Delta v_{sq} = 0 \qquad \text{(A.2.30)}$$

$$-\Delta v_3 + \frac{v_{sd}}{v_3}\Delta v_{sd} + \frac{v_{sq}}{v_3}\Delta v_{sq} = 0 \qquad \text{(A.2.31)}$$

$$-\Delta P_3 + i_{sd}\Delta v_{sd} + i_{sq}\Delta v_{sq} + v_{sd}\Delta i_{sd} + v_{sq}\Delta i_{sq} = 0 \qquad \text{(A.2.32)}$$

$$-\Delta Q_3 + i_{sq}\Delta v_{sd} - i_{sd}\Delta v_{sq} + v_{sd}\Delta i_{sq} - v_{sq}\Delta i_{sd} = 0 \qquad \text{(A.2.33)}$$

$$-\Delta\psi_{sd} + X_s\Delta i_{sd} + X_m\Delta i_{rd} = 0 \qquad \text{(A.2.34)}$$

$$-\Delta\psi_{rd} + X_m\Delta i_{sd} + X_r\Delta i_{rd} = 0 \qquad \text{(A.2.35)}$$

$$-\Delta\psi_{sq} + X_s\Delta i_{sq} + X_m\Delta i_{rq} = 0 \qquad \text{(A.2.36)}$$

$$-\Delta\psi_{rq} + X_m\Delta i_{sq} + X_r\Delta i_{rq} = 0 \qquad \text{(A.2.37)}$$

2) Equations considering the non-linear passive load representation:

$$\frac{1}{\omega_o} p\,\Delta\psi_{fd} - \frac{r_{fd}}{X_{afd}}\Delta E_{fd} + r_{fd}\Delta i_{fd} = 0 \qquad \text{(A.2.38)}$$

$$\frac{1}{\omega_o} p\,\Delta\psi_d + \Delta\psi_q + \psi_q\Delta n + \Delta v_d + r_d\Delta i_d = 0 \qquad \text{(A.2.39)}$$

$$\frac{1}{\omega_o} p\,\Delta\psi_{kd} + r_{kd}\Delta i_{kd} = 0 \qquad \text{(A.2.40)}$$

$$\frac{1}{\omega_o} p\,\Delta\psi_q - \Delta\psi_d - \psi_d\Delta n + \Delta v_q + r_s\Delta i_q = 0 \qquad \text{(A.2.41)}$$

$$\frac{1}{\omega_o} p\,\Delta\psi_{kq} + r_{kq}\Delta i_{kq} = 0 \qquad \text{(A.2.42)}$$

$$T_{rg}p\Delta E_{fd} + \Delta E_{fd} - k_r \Delta v_2 = 0 \qquad (A.2.43)$$

$$- p\Delta\delta r + \omega_o \Delta n = 0 \qquad (A.2.44)$$

$$-T_m p\Delta n - i_q\Delta\psi_d + i_d\Delta\psi_q - D_{nom}B\Delta n + A_t\Delta g + 1.5A_tB\Delta h + \\ + \psi_q\Delta i_d - \psi_d\Delta i_q = 0 \qquad (A.2.45)$$

$$-p\Delta g - Q_g W_s p\Delta n - Q_g\delta p\Delta g + Q_g\Delta C = 0 \qquad (A.2.46)$$

$$-p\Delta C - p\Delta n - \delta tp\Delta g - \frac{1}{T_R}\Delta n - \frac{1}{T_R}\Delta C = 0 \qquad (A.2.47)$$

$$-p\Delta h - 2p\Delta g - \frac{2}{T_w}\Delta h = 0 \qquad (A.2.48)$$

$$-\Delta P_2 + \frac{\partial P_2}{\partial\delta_2}\Delta\delta_2 + \frac{\partial P_2}{\partial V_2}\Delta V_2 + \frac{\partial P_2}{\partial\delta_3}\Delta\delta_3 + \frac{\partial P_2}{\partial V_3}\Delta V_3 = 0 \qquad (A.2.49)$$

$$-\Delta Q_2 + \frac{\partial Q_2}{\partial\delta_2}\Delta\delta_2 + \frac{\partial Q_2}{\partial V_2}\Delta V_2 + \frac{\partial Q_2}{\partial\delta_3}\Delta\delta_3 + \frac{\partial Q_2}{\partial V_3}\Delta V_3 = 0 \qquad (A.2.50)$$

$$-\Delta\delta_2 + \Delta\delta r + \frac{v_q}{V_2^2}\Delta v_d - \frac{v_d}{V_2^2}\Delta v_q = 0 \qquad (A.2.51)$$

$$-\Delta v_2 + \frac{v_d}{V_2}\Delta v_d + \frac{v_q}{V_2}\Delta v_q = 0 \qquad (A.2.52)$$

$$-\Delta P_2 + i_d\Delta v_d + i_q\Delta v_q + v_d\Delta i_d + v_q\Delta i_q = 0 \qquad (A.2.53)$$

$$-\Delta Q_2 + i_q\Delta v_d - i_d\Delta v_q - v_q\Delta i_d + v_d\Delta i_q = 0 \qquad (A.2.54)$$

$$-\Delta\psi_{fd} + X_{ffd}\Delta i_{fd} + X_{afd}\Delta i_d + X_{fkd}\Delta i_{kd} = 0 \qquad (A.2.55)$$

$$-\Delta\psi_d + X_{afd}\Delta i_{fd} + X_d\Delta i_d + X_{akd}\Delta i_{kd} = 0 \qquad (A.2.56)$$

$$-\Delta\psi_{kd} + X_{fkd}\Delta i_{fd} + X_{akd}\Delta i_d + X_{kkd}\Delta i_{kd} = 0 \qquad (A.2.57)$$

$$-\Delta\psi_q + X_q\Delta i_q + X_{akq}\Delta i_{kq} = 0 \qquad (A.2.58)$$

$$-\Delta\psi_{kq} + X_{akq}\Delta i_q + X_{kkq}\Delta i_{kq} = 0 \qquad (A.2.59)$$

$$-\Delta P_3 + \frac{K_p P_3}{V_3}\Delta V_3 = 0 \qquad \text{(A.2.60)}$$

$$-\Delta Q_3 + \frac{K_q Q_3}{V_3}\Delta V_3 = 0 \qquad \text{(A.2.61)}$$

$$-\Delta P_3 + \frac{\partial P_3}{\partial \delta_2}\Delta\delta_2 + \frac{\partial P_3}{\partial V_2}\Delta V_2 + \frac{\partial P_3}{\partial \delta_3}\Delta\delta_3 + \frac{\partial P_3}{\partial V_3}\Delta V_3 = 0 \qquad \text{(A.2.62)}$$

$$-\Delta Q_3 + \frac{\partial Q_3}{\partial \delta_2}\Delta\delta_2 + \frac{\partial Q_3}{\partial V_2}\Delta V_2 + \frac{\partial Q_3}{\partial \delta_3}\Delta\delta_3 + \frac{\partial Q_3}{\partial V_3}\Delta V_3 = 0 \qquad \text{(A.2.63)}$$

3) Equations considering a combined load:

In this case, equations (A.2.38)-(A.2.63) are the same, except that equations (A.2.60) and (A.2.61) are substituted by:

$$-\Delta P_3 + PART_3\,\Delta V_3 + PART_4\,\Delta\delta_3 = 0 \qquad \text{(A.2.64)}$$

$$-\Delta Q_3 + QART_3\,\Delta V_3 + QART_4\,\Delta\delta_3 = 0 \qquad \text{(A.2.65)}$$

APPENDIX A.3

HAKING AND BERG[16] APPROACH FOR A SINGLE EQUIVALENT INDUCTION MOTOR

The single model representing a group of motors is assumed to have an electrical circuit structure identical to the conventional approximate circuit of a symmetrical three-phase induction motor. The procedure for obtaining the single unit equivalent parameters is discussed for a two motor group. Considering that generalization to more than two motors can be considered:

Electrical parameters:

Consider two motors driving separate loads and supplied from the same bus. At standstill the two motors may be represented by:

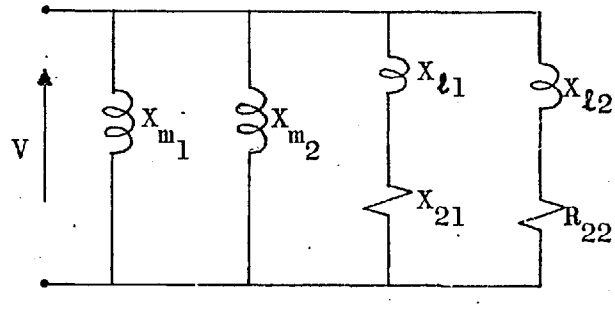

Figure A.3.1

In order to maintain the electrical power invariance, we let:

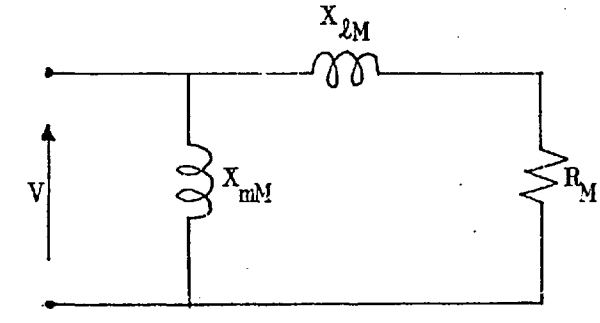

Figure A.3.2

$$X_{mM} = \frac{X_{m_1} X_{m_2}}{X_{m_1} + X_{m_2}}$$

$$Z_{mM} = \frac{(R_{21} + jX_{\ell_1})(R_{22} + jX_{\ell_2})}{(R_{21}+jX_{\ell_1}) + (R_{22}+jX_{\ell_2})}$$

$$R_M = \frac{R_{21}(R_{22}^2 + X_{\ell_2}^2) + R_{22}(R_{21}^2 + X_{\ell_1}^2)}{(R_{21} + R_{22})^2 + (X_{\ell_1} + X_{\ell_2})^2}$$

$$X_{\ell_M} = \frac{X_{\ell_1}(X_{\ell_2}^2 + R_{22}^2) + X_{\ell_2}(X_{\ell_1}^2 + R_{21}^2)}{(R_{21} + R_{22})^2 + (X_{\ell_1} + X_{\ell_2})^2}$$

Equivalent slip:

If two motors are running at constant slips, S_1 and S_2, the corresponding slip of the equivalent single motor is S_M, by equating the real parts of the input impedances of the two equivalent circuits:

$$\frac{R_M}{S_M} = \frac{(R_{21}/S_1)\left[X_{\ell_2}^2 + (R_{22}/S_2)^2\right] + R_{22}/S_2\left[(R_{21}/S)^2 + (X_{\ell_1})^2\right]}{\left[(R_{21}/S_1 + R_{22}/S_2)^2 + (X_{\ell_1} + X_{\ell_2})^2\right]}$$

Let $\frac{R_{21}}{S_1} = R'_{21}$, $\frac{R_{22}}{S_2} = R'_{22}$, the equivalent slip is found to be:

$$S_M = \frac{\left[R_{21}(R_{22}^2+X_{\ell_2}^2)+R_{22}(R_{21}^2+X_{\ell_1}^2)\right]\left[(R'_{21}+R'_{22})^2+(X_{\ell_1}+X_{\ell_2})^2\right]}{\left[R'_{21}(X_{\ell_2}^2+R'^2_{22}) + R'_{22}(R'^2_{21}+X_{\ell_1}^2)\right]\left[(R_{21}+R_{22})^2+(X_{\ell_1}+X_{\ell_2})^2\right]}$$

Equivalent inertia constant:

In order to find the moment of inertia for the equivalent motor, this motor is assumed to retain an amount of kinetic energy at synchronous speed equal to the sum of the kinetic energies of the

individual motors at synchronous speed. Using the definition of H as the amount of kinetic energy at synchronous speed divided by the rated voltamperes:

$$H_M(VA_M) = H_1(VA_1) + H_2(VA_2)$$

$$VA_M = VA_1 + VA_2$$

$$H_M = \frac{H_1(VA_1) + H_2(V_2)}{VA_M}$$

Composite load torque characteristics:

The composite mechanical load torque-speed function is then expressed as:

$$T_{\ell_m} = T_{oM}\omega_M^{\beta_M}$$

Single unit equivalent motor:

The procedure used for the case of two motor group can be extended to obtain the parameters of a single-unit equivalent of more than two motors supplied from the same bus.

APPENDIX B.1

LINEARIZED DIFFERENTIAL AND ALGEBRAIC EQUATIONS FOR A MULTI-MACHINE SYSTEM

The equations are written for a two-machine and three-node system (Figure 3.5) by way of an example, but the extension to n machines and m nodes is executed automatically by the computer program. The order in which these equations are written is maintained in the program; thermoelectric machines first, followed by hydroelectric machines. Synchronous machines are represented by Park's equations[14] using the convention given in Reference 13.

Thermoelectric machine:

$$\frac{1}{\omega_o} p \Delta\psi_{fd_1} - \frac{r_{fd_1}}{X_{afd_1}} \Delta E_{fd_1} + r_{fd_1} \Delta i_{fd_1} = 0 \qquad \text{(B.1.1)}$$

$$\frac{1}{\omega_o} p\Delta\psi_{d_1} + \Delta\psi_{q_1} + \psi_{q_1} \Delta n_1 + \Delta v_{d_1} + r_{s_1} \Delta i_{d_1} = 0 \qquad \text{(B.1.2)}$$

$$\frac{1}{\omega_o} p\Delta\psi_{kd_1} + r_{kd_1} \Delta i_{kd_1} = 0 \qquad \text{(B.1.3)}$$

$$\frac{1}{\omega_o} p\Delta\psi_{q_1} - \Delta\psi_{d_1} - \psi_{d_1} \Delta n + \Delta v_{q_1} + r_{s_1} \Delta i_{q_1} = 0 \qquad \text{(B.1.4)}$$

$$\frac{1}{\omega_o} p\Delta\psi_{kq_1} + r_{kq_1} \Delta i_{kq_1} = 0 \qquad \text{(B.1.5)}$$

$$T_{rg_1} p \Delta E_{fd_1} + \Delta E_{fd_1} - K_{r_1} \Delta V_1 = - K_{r_1} \Delta V_{ref} \qquad \text{(B.1.6)}$$

$$-p\Delta\delta r_1 - \omega_o \Delta n_1 = 0 \qquad \text{(B.1.7)}$$

$$-T_{m_1}p\Delta n_1 - i_{q_1}\Delta\psi_{d_1} + i_{d_1}\Delta\psi_{q_1} + \psi_{q_1}\Delta i_{d_1} - \psi_{d_1}\Delta i_{q_1} + 0.28\Delta\omega h_2' + 0.72\Delta\omega i_2' = 0 \quad \text{(B.1.8)}$$

$$p\Delta\omega h_1' + \frac{G_1}{T_1'}\Delta n_1 + \frac{1}{T_1}\Delta\omega h_1' = \frac{1}{T_1}\Delta Y_o \quad \text{(B.1.9)}$$

$$p\Delta\omega h_2' - \frac{1}{T_2'}\Delta\omega h_1' + \frac{1}{T_2'}\Delta\omega h_2' = 0 \quad \text{(B.1.10)}$$

$$p\Delta\omega i_2' - \frac{1}{T_3'}\Delta\omega h_2' + \frac{1}{T_3'}\Delta\omega i_2' = 0 \quad \text{(B.1.11)}$$

Hydroelectric machine:

$$\frac{1}{\omega_o}p\Delta\psi_{fd_2} - \frac{r_{fd_2}}{X_{afd_2}}\Delta E_{fd_2} + r_{fd_2}\Delta i_{fd_2} = 0 \quad \text{(B.1.12)}$$

$$\frac{1}{\omega_o}p\Delta\psi_{d_2} + \Delta\psi_{q_2} + \psi_{q_2}\Delta n_2 + \Delta v_{d_2} + r_{s_2}\Delta i_{d_2} = 0 \quad \text{(B.1.13)}$$

$$\frac{1}{\omega_o}p\Delta\psi_{kd_2} + r_{kd_2}\Delta i_{kd_2} = 0 \quad \text{(B.1.14)}$$

$$\frac{1}{\omega_o}p\Delta\psi_{q_2} - \Delta\psi_{d_2} - \psi_{d_2}\Delta n_2 + \Delta v_{q_2} + r_{s_2}\Delta i_{q_2} = 0 \quad \text{(B.1.15)}$$

$$\frac{1}{\omega_o}p\Delta\psi_{kq_2} + r_{kq_2}\Delta i_{kq_2} = 0 \quad \text{(B.1.16)}$$

$$T_{rg_2}p\Delta E_{fd_2} + \Delta E_{fd_2} - K_{r_2}\Delta V_2 = -K_{r_2}\Delta V_{ref_2} \quad \text{(B.1.17)}$$

$$-p\Delta\delta r_2 - \omega_b\Delta n_2 = 0 \quad \text{(B.1.18)}$$

$$-T_{m_2}p\Delta n_2 - i_{q_2}\Delta\psi_{d_2} + i_{d_2}\Delta\psi_{q_2} + \psi_{q_2}\Delta i_{d_2} - \psi_{d_2}\Delta i_{q_2} - D\Delta n_2 + A_{t_2}\Delta g_2 + 1.5A_{t_2}B_2\Delta h_2 = 0 \quad \text{(B.1.19)}$$

$$-p\Delta g_{f_1} - \frac{1}{T_{a_1}}\Delta g_{f_1} = -\frac{\mu_{a_1}}{T_{a_1}}\Delta\mu_{gov_1} \quad \text{(B.1.20)}$$

$$-p\Delta g_1 - \frac{\delta p_1}{T_{g_1}}\Delta g_1 - \frac{1}{T_{g_1}}\Delta n_2 - \frac{1}{T_{g_1}}\Delta gf_1 = 0 \qquad \text{(B.1.21)}$$

$$-p\Delta h_1 - 2p\Delta g_1 - \frac{2}{T_{w_1}}\Delta h_1 = 0 \qquad \text{(B.1.22)}$$

Algebraic equations:

Network equations:

$$\frac{\partial P_1}{\partial \delta_1}\Delta\delta_1 + \frac{\partial P_1}{\partial V_1}\Delta V_1 + \frac{\partial P_1}{\partial \delta_2}\Delta\delta_2 + \frac{\partial P_1}{\partial V_2}\Delta V_2 + \frac{\partial P_1}{\partial \delta_3}\Delta\delta_3 + \frac{\partial P_1}{\partial V_3}\Delta V_3 - \Delta P_1 = 0 \qquad \text{(B.1.23)}$$

$$\frac{\partial Q_1}{\partial \delta_1}\Delta\delta_1 + \frac{\partial Q_1}{\partial V_1}\Delta V_1 + \frac{\partial Q_1}{\partial \delta_2}\Delta\delta_2 + \frac{\partial Q_1}{\partial V_2}\Delta V_2 + \frac{\partial Q_1}{\partial \delta_3}\Delta\delta_3 + \frac{\partial Q_1}{\partial V_3}\Delta V_3 - \Delta Q_1 = 0 \qquad \text{(B.1.24)}$$

$$\frac{\partial P_2}{\partial \delta_1}\Delta\delta_1 + \frac{\partial P_2}{\partial V_1}\Delta V_1 + \frac{\partial P_2}{\partial \delta_2}\Delta\delta_2 + \frac{\partial P_2}{\partial V_2}\Delta V_2 + \frac{\partial P_2}{\partial \delta_3}\Delta\delta_3 + \frac{\partial P_2}{\partial V_3}\Delta V_3 - \Delta P_2 = 0 \qquad \text{(B.1.25)}$$

$$\frac{\partial Q_2}{\partial \delta_1}\Delta\delta_1 + \frac{\partial Q_2}{\partial V_1}\Delta V_1 + \frac{\partial Q_2}{\partial \delta_2}\Delta\delta_2 + \frac{\partial Q_2}{\partial V_2}\Delta V_2 + \frac{\partial Q_2}{\partial \delta_3}\Delta\delta_3 + \frac{\partial Q_2}{\partial V_3}\Delta V_3 - \Delta Q_2 = 0 \qquad \text{(B.1.26)}$$

$$\frac{\partial P_3}{\partial \delta_1}\Delta\delta_1 + \frac{\partial P_3}{\partial V_1}\Delta V_1 + \frac{\partial P_3}{\partial \delta_2}\Delta\delta_2 + \frac{\partial P_3}{\partial V_2}\Delta V_2 + \frac{\partial P_3}{\partial \delta_3}\Delta\delta_3 + \frac{\partial P_3}{\partial V_3}\Delta V_3 - \Delta P_3 = 0 \qquad \text{(B.1.27)}$$

$$\frac{\partial Q_3}{\partial \delta_1}\Delta\delta_1 + \frac{\partial Q_3}{\partial V_1}\Delta V_1 + \frac{\partial Q_3}{\partial \delta_2}\Delta\delta_2 + \frac{\partial Q_3}{\partial V_2}\Delta V_2 + \frac{\partial Q_3}{\partial \delta_3}\Delta\delta_3 + \frac{\partial Q_3}{\partial V_3}\Delta V_3 - \Delta Q_3 = 0 \qquad \text{(B.1.28)}$$

Power Transformation equations including non-linear passive load representation:

$$\Delta P_1 = \Delta P_{G_1} - \Delta P_{L_1} = i_{d_1}\Delta v_{d_1} + i_{q_1}\Delta v_{q_1} + v_{d_1}\Delta i_{d_1} + v_q\Delta i_{q_1} - K_{p_1}\frac{P_{L_1}}{V_1}\Delta V_1 \qquad \text{(B.1.29)}$$

$$\Delta Q_1 = \Delta Q_{G_1} - \Delta Q_{L_1} = i_{q_1}\Delta v_{d_1} - i_{d_1}\Delta v_{q_1} - v_{q_1}\Delta i_{d_1} + v_{d_1}\Delta i_{q_1} - K_{q_1}\frac{Q_{L_1}}{V_1}\Delta V_1 \quad \text{(B.1.30)}$$

$$\Delta P_2 = \Delta P_{G_2} - \Delta P_{L_2} = i_{q_2}\Delta v_{d_2} - i_{d_2}\Delta v_{q_2} - v_{q_2}\Delta i_{d_2} + v_{d_2}\Delta i_{q_2} - K_{p_2}\frac{P_{L_2}}{V_2}\Delta V_2 \quad \text{(B.1.31)}$$

$$\Delta Q_2 = \Delta Q_{G_2} - \Delta Q_{L_2} = i_{q_2}\Delta v_{d_2} - i_{d_2}\Delta v_{q_2} - v_{q_2}\Delta i_{d_2} + v_{d_2}\Delta i_{q_2} - K_{q_2}\frac{Q_{L_2}}{V_2}\Delta V_2 \quad \text{(B.1.32)}$$

$$\Delta P_3 = \Delta P_{G_3} - \Delta P_{L_3} = i_{q_3}\Delta v_{d_3} - i_{d_3}\Delta v_{q_3} - v_{q_3}\Delta i_{d_3} + v_{d_3}\Delta i_{q_3} - K_{p_3}\frac{P_{L_3}}{V_3}\Delta V_3 \quad \text{(B.1.33)}$$

$$\Delta Q_3 = \Delta Q_{G_3} - \Delta Q_{L_3} = i_{q_3}\Delta v_{d_3} - i_{d_3}\Delta v_{q_3} - v_{q_3}\Delta i_{d_3} + v_{d_3}\Delta i_{q_3} - K_{q_3}\frac{Q_{L_3}}{V_3}\Delta V_3 \quad \text{(B.1.34)}$$

Some of these algebraic equations have been solved analytically substituting equations (B.1.29)-(B.1.34) into equations (B.1.23) -(B.1.28) and a minimum number of algebraic variables are chosen in the present formulation.

Phase angle and voltage transformation equations:

In Chapter 2 details for the derivation of these equations are given in Appendix A.1 for a single-machine system. The equations for a multi-machine system are shown below, derived in a similar way.

$$\Delta\delta_1 + \Delta\delta r_1 + \frac{v_{q_1}}{V_1^2}\Delta v_{d_1} - \frac{v_{d_1}}{V_1^2}\Delta v_{q_1} = 0 \quad \text{(B.1.35)}$$

$$\Delta\delta_2 + \Delta\delta r_2 + \frac{v_{q_2}}{V_2^2}\Delta v_{d_2} - \frac{v_{d_2}}{V_2^2}\Delta v_{q_2} = 0 \quad \text{(B.1.36)}$$

$$-\Delta V_1 + \frac{v_{d_1}}{V_1}\Delta v_{d_1} + \frac{v_{q_1}}{V_1}\Delta v_{q_1} = 0 \qquad \text{(B.1.37)}$$

$$-\Delta V_2 + \frac{v_{d_2}}{V_2}\Delta v_{d_2} + \frac{v_{q_2}}{V_2}\Delta v_{q_2} = 0 \qquad \text{(B.1.38)}$$

Flux equations:

$$-\Delta\psi_{fd_1} + X_{ffd_1}\Delta i_{fd_1} + X_{afd_1}\Delta i_{d_1} + X_{fkd_1}\Delta i_{kd_1} = 0 \qquad \text{(B.1.39)}$$

$$-\Delta\psi_{d_1} + X_{afd_1}\Delta i_{fd_1} + X_{d_1}\Delta i_{d_1} + X_{akd_1}\Delta i_{kd_1} = 0 \qquad \text{(B.1.40)}$$

$$-\Delta\psi_{kd_1} + X_{fkd_1}\Delta i_{fd_1} + X_{akd_1}\Delta i_{d_1} + X_{kkd_1}\Delta i_{kd_1} = 0 \qquad \text{(B.1.41)}$$

$$-\Delta\psi_{q_1} + X_{q_1} i_{q_1} + X_{akq_1}\Delta i_{kq_1} = 0 \qquad \text{(B.1.42)}$$

$$-\Delta\psi_{kq_1} + X_{akq_1}\Delta i_{q_1} + X_{kkq_1}\Delta i_{kq_1} = 0 \qquad \text{(B.1.43)}$$

$$-\Delta\psi_{fd_2} + X_{ffd_2}\Delta i_{fd_2} + X_{afd_2}\Delta i_{d_2} + X_{fkd_2}\Delta i_{kd_2} = 0 \qquad \text{(B.1.44)}$$

$$-\Delta\psi_{d_2} + X_{afd_2}\Delta i_{fd_2} + X_{d_2}\Delta i_{d_2} + X_{akd_2}\Delta i_{kd_2} = 0 \qquad \text{(B.1.45)}$$

$$-\Delta\psi_{kd_2} + X_{fkd_2}\Delta i_{fd_2} + X_{akd_2}\Delta i_{d_2} + X_{kkd_2}\Delta i_{kd_2} = 0 \qquad \text{(B.1.46)}$$

$$-\Delta\psi_{q_2} + X_{q_2}\Delta i_{q_2} + X_{akq_2}\Delta i_{kq_2} = 0 \qquad \text{(B.1.47)}$$

$$-\Delta\psi_{kq_2} + X_{akq_2}\Delta i_{q_2} + X_{kkq_2}\Delta i_{kq_2} = 0 \qquad \text{(B.1.48)}$$

When one machine is taken as the reference, simplifications are made, as explained in Section 3.3.3.

Equations (B.1.1)-(B.1.48) can be arranged in a matrix form as equation (3.2), and all the $[K]$ submatrices are obtained straightforwardly. The general structure of the multi-machine system equations, is shown in Figure B.1.1

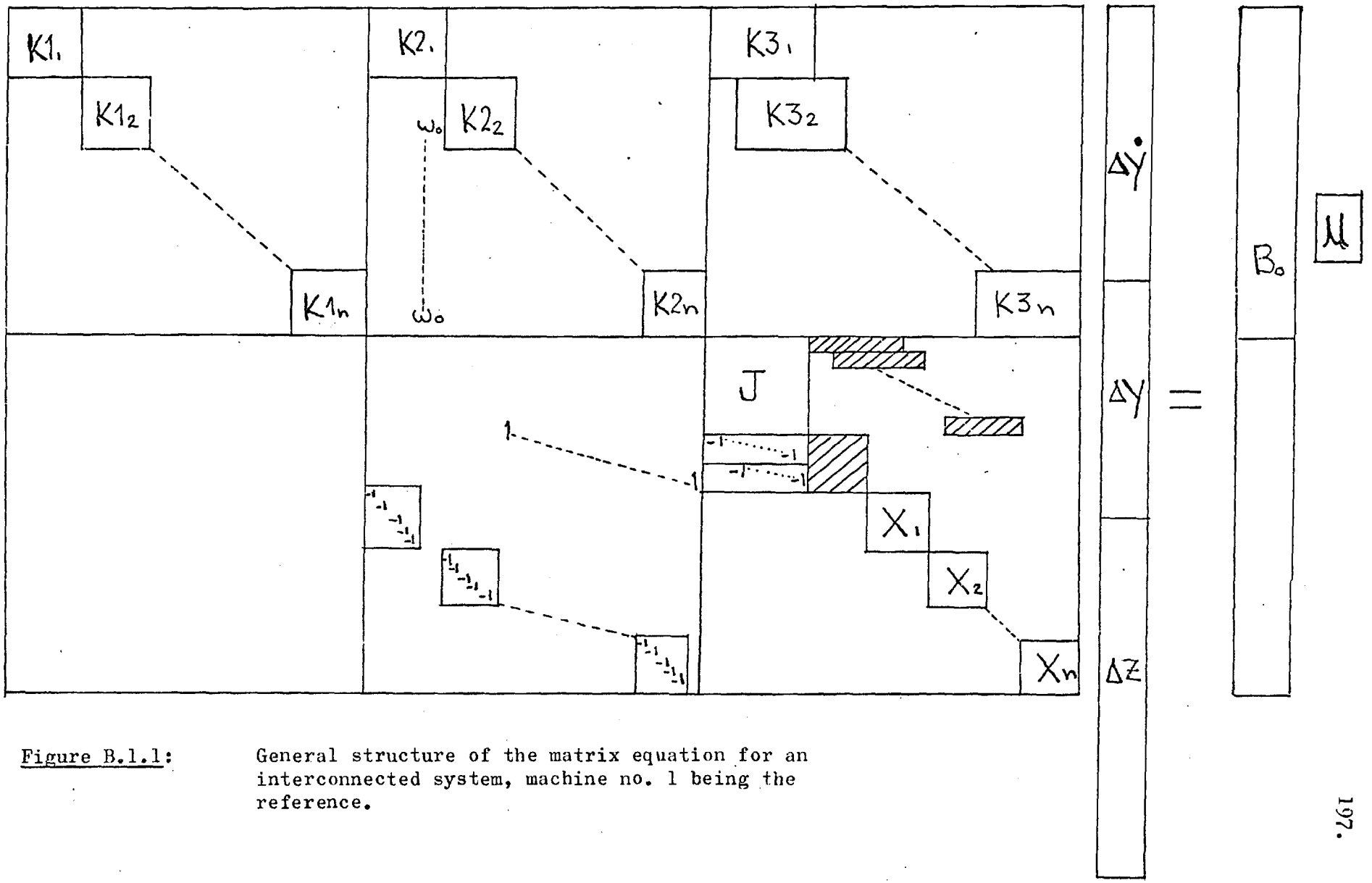

Figure B.1.1: General structure of the matrix equation for an interconnected system, machine no. 1 being the reference.

APPENDIX B.2

TURBINE-GOVERNOR MODEL AND DATA

Thermoelectric Machine:

The model of the governor and turbine is similar to that used in previous studies[51,63]. In order to maintain the same number of state variables as for hydroelectric machines, the system was reduced to a third order by the combination of time constants into a single equivalent time constant. The interceptor valve is also excluded, as in Reference 51. This reduction can be seen by comparing the full and simplified models of Figures B.1.1 and B.1.2, respectively. In Figure B.1.2 the reheater storage and I.P./L.P. storage time constants T_3 and T_4 are combined into a single time constant T_3'. The operational equations defining the turbine-governor and data are given.

Governor gain	G_1	0.00139 sec/deg.
Throttle valve opening time constant	T_{10}	1.0 seconds
Throttle valve closing time constant	T_{1C}	0.1 seconds
H.P. pipe storage time constant	T_2	0.1 seconds
Reheater storage time constant	T_3	14.4 seconds
IP/LP storage time constant	T_4	0.51 seconds

Table B.1.1: Turbine and governor parameters.

Linearized model equations

Turbine power:

$$\Delta P_{HP} = 0.28\,\Delta Wh_2 \qquad \text{(B.2.1)}$$

$$\Delta P_{ILP} = 0.72\,\Delta Wi_2 \qquad \text{(B.2.2)}$$

$$\Delta P_{in} = \Delta P_{HP} + \Delta P_{ILP} \qquad \text{(B.2.3)}$$

Main governing valve:

$$\Delta Y = G_1 \Delta \dot{\delta}_r = G_1 \Delta n \qquad \text{(B.2.4)}$$

$$\Delta Y_1 = \Delta Y_o - \Delta Y \qquad \text{(B.2.5)}$$

Valve relays:

$$p\,\Delta Wh_i + \frac{G_1}{T_1}\Delta n + \frac{1}{T_1}\Delta Wh_1 = \frac{1}{T_1}\Delta Y_o \qquad \text{(B.2.6)}$$

H.P. cylinder:

$$p\,\Delta Wh_2 - \frac{1}{T_2}Wh_1 + \frac{1}{T_2}\Delta Wh_2 = 0 \qquad \text{(B.2.7)}$$

L.P. and I.P. cylinder:

$$p\,\Delta Wi_2 - \frac{1}{T_3^1}\Delta Wh_2 + \frac{1}{T_3^1}\Delta Wi_2^1 = 0 \qquad \text{(B.2.8)}$$

Note: In this study the time constant T_3^1, i.e. H.P. exhaust and I.P. LP exhaust, was taken as 5.475 seconds in total, as Reference 20.

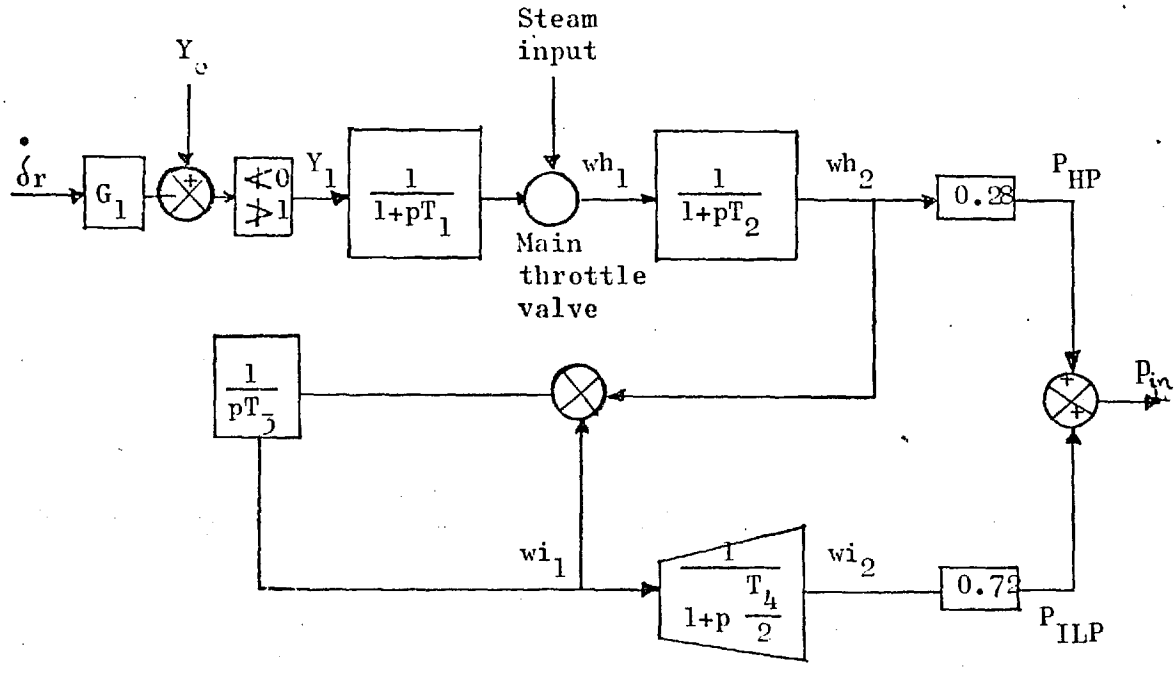

Figure B.2.1 Model of turbine and governor system excluding interceptor valve.

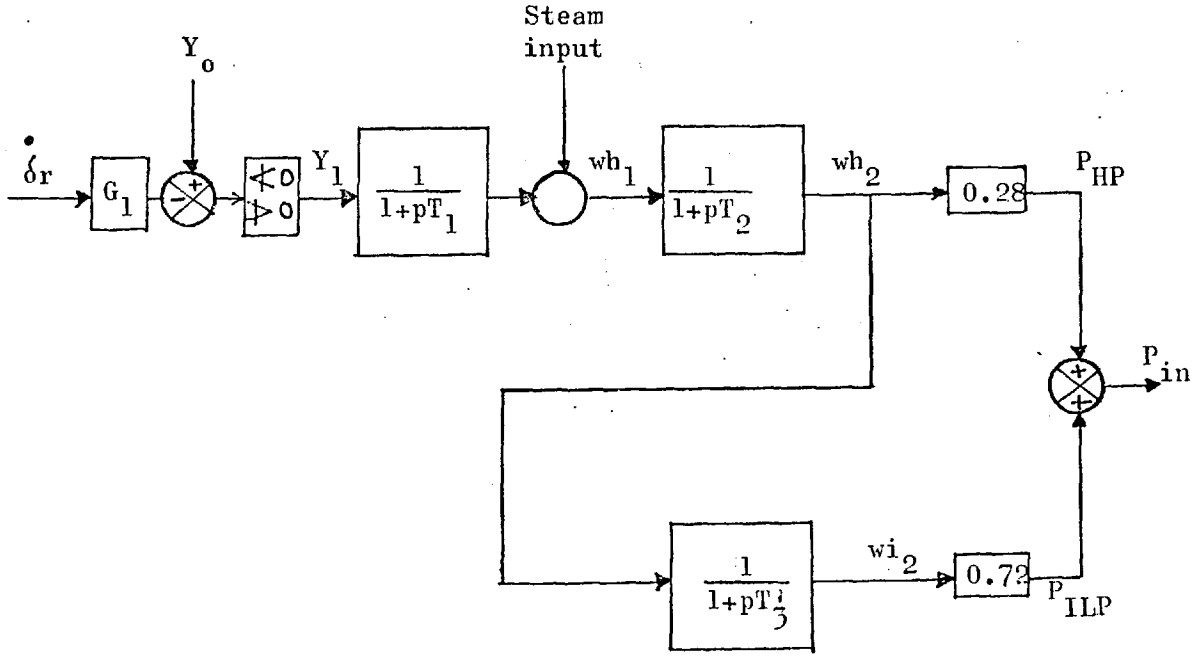

Figure B.2.2 Block diagram of reduced turbine and governor system model.

Hydroelectric machines:

Each primemover is controlled by a conventional dashpot-type hydrogovernor whose differential equations and data are given. The model is similar to that used by Yu et al[55].

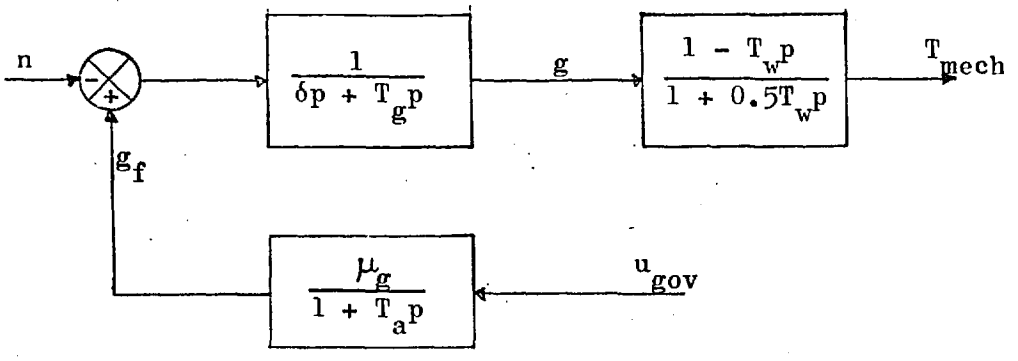

Figure B.2.3: Governor hydraulic system.

Parameter	Symbol	Valve
Gate time constant	T_g	0.1 sec.
Governor activator time constant	T_a	0.01 sec.
Water time constant	T_w	0.5 sec.
Permanent droop	δp	0.045
Governor activator gain	μ_a	1.0

Table B.2.2: Hydrospeed governor parameters.

Linearized equations:

Turbine:

$$\Delta T_{mech} = - D\Delta n + A_t \Delta g + 1.5 A_t B \Delta h \qquad (B.2.9)$$

Gate opening:

$$-p\Delta g - \frac{\delta p}{T_g}\Delta g - \frac{1}{T_g}\Delta n - \frac{1}{T_g}\Delta gf = 0 \qquad \text{(B.2.10)}$$

Governor feedback loop:

$$-p\Delta gf - \frac{1}{T_a}\Delta gf = -\frac{\mu_a}{T_a}\Delta u_{gov} \qquad \text{(B.2.11)}$$

Water head:

$$-p\Delta h - 2p\Delta g - \frac{2}{T_w}\Delta h = 0 \qquad \text{(B.2.12)}$$

APPENDIX C.1

FORMULATION OF SYSTEM EQUATIONS

The equations for the synchronous machine are written in per unit, using Park's transformation[14]. Three different network representations were used.

a) Line and transformer reactances coupled with the machine reactance, in the classical way:

$$v_q = -\frac{p}{\omega_o}\psi_q + \psi_d \frac{\omega_r}{\omega_o} - r_s i_q \qquad (C.1)$$

$$v_d = -\frac{p}{\omega_o}\psi_d - \psi_q \frac{\omega_r}{\omega_o} - r_s i_d \qquad (C.2)$$

$$0 = \frac{p}{\omega_o}\psi_{kq} + r_{kq} i_{kq} \qquad (C.3)$$

$$0 = \frac{p}{\omega_o}\psi_{kd} + r_{kd} i_{kd} \qquad (C.4)$$

$$\frac{r_{fd}}{X_{md}} E_{fd} = \frac{p}{\omega_o}\psi_{fd} + r_{fd} i_{fd} \qquad (C.5)$$

$$\psi_q = \psi_{mq} + X_{\ell_a} i_q \qquad (C.6)$$

$$\psi_d = \psi_{md} + X_{\ell_a} i_d \qquad (C.7)$$

$$\psi_{kq} = \psi_{mq} + X_{\ell_{kq}} i_{kq} \qquad (C.8)$$

$$\psi_{kd} = \psi_{md} + X_{\ell_{kd}} i_{kd} \qquad (C.9)$$

$$\psi_{mq} = X_{mq}(i_{kq} + i_q) \qquad (C.10)$$

$$\psi_{md} = X_{md}(i_{kd} + i_{fd} + i_d) \qquad (C.11)$$

$$T_g = \psi_d i_q - \psi_q i_d \qquad (C.12)$$

$$pn = \frac{1}{2H}(T_{mech} - T_g) \qquad (C.13)$$

$$p\delta_r = (\omega_r - \omega_o) \qquad (C.14)$$

Equations describing the transmission line in a frame of reference fixed to the rotor:

$$v_q = \frac{X_t}{\omega_o} p\, i_q - X_t i_d \frac{\omega_r}{\omega_o} + r_t i_q + V_{qB} \qquad (C.15)$$

$$v_d = \frac{X_t}{\omega_o} p\, i_d + X_t i_q \frac{\omega_r}{\omega_o} + r_t i_d + V_{dB} \qquad (C.16)$$

$$V_{qB} = V_B \cos \delta_r \qquad (C.17)$$

$$V_{dB} = -V_B \sin \delta_r \qquad (C.18)$$

The small displacement equation system was obtained in the same way as by Baker and Krause[47].

$$[V_m]\,\dot{y}(t) = [R_M]\,y(t) + bu(t) \qquad (C.19)$$

$$u(t) = V_{ref}$$

$$[V_M] = \begin{bmatrix}
-\frac{(X_t+X_q)}{\omega_o} & 0 & -\frac{1}{\omega_o}X_{mq} & 0 & 0 & 0 & 0 & 0 & 0 & 0 \\
0 & -\frac{(X_t+X_d)}{\omega_o} & \frac{1}{\omega_o}X_{md} & 0 & \frac{1}{\omega_o}X_{md} & 0 & 0 & 0 & 0 & 0 \\
\frac{1}{\omega_o}X_{mq} & 0 & \frac{1}{\omega_o}X_{kq} & 0 & 0 & 0 & 0 & 0 & 0 & 0 \\
0 & \frac{1}{\omega_o}X_{md} & 0 & \frac{1}{\omega_o}X_{kd} & \frac{1}{\omega_o}X_{md} & 0 & 0 & 0 & 0 & 0 \\
0 & \frac{X_{md}^2}{\omega_o r_{fd}} & 0 & \frac{X_{md}^2}{\omega_o r_{fd}} & \frac{X_{md}X_{fd}}{\omega_o r_{fd}} & 0 & 0 & 0 & 0 & 0 \\
0 & 0 & 0 & 0 & 0 & 1 & 0 & 0 & 0 & 0 \\
0 & 0 & 0 & 0 & 0 & 0 & 1 & 0 & 0 & 0 \\
0 & 0 & 0 & 0 & 0 & 0 & 0 & 1 & 0 & 0 \\
\frac{K_A V_q X_t}{T_A V_t \omega_o} & \frac{K_A V_d X_t}{T_A V_t \omega_o} & 0 & 0 & 0 & 0 & 0 & 0 & 1 & 0 \\
0 & 0 & 0 & 0 & 0 & 0 & 0 & 0 & 0 & 1
\end{bmatrix}$$

$$[R_M] = \begin{bmatrix}
(r_s+r_t) & -(X_t+X_d) & 0 & -X_{md} & -X_{md} & \psi_{do} & -V_B\sin\delta_r & 0 & 0 & 0 \\
(X_q+X_t) & (r_t+r_s) & X_{mq} & 0 & 0 & \psi_{qo} & -V_B\cos\delta_r & 0 & 0 & 0 \\
0 & 0 & -r_{kq} & 0 & 0 & 0 & 0 & 0 & 0 & 0 \\
0 & 0 & 0 & -r_{kd} & 0 & 0 & 0 & 0 & 0 & 0 \\
0 & 0 & 0 & 0 & -r_{kd} & 0 & 0 & 0 & 0 & 0 \\
0 & 0 & 0 & 0 & 0 & -X_{md} & 0 & 0 & 0 & 0 \\
T_1/2H & T_2/2H & T_3/2H & T_4/2H & T_5/2H & 0 & 0 & 0 & 0 & 0 \\
0 & 0 & 0 & 0 & 0 & \omega_o & 0 & 0 & 0 & 0 \\
0 & 0 & 0 & 0 & 0 & 0 & 0 & -\frac{K_E}{T_E} & 0 & 0 \\
P_1 & P_2 & 0 & 0 & 0 & P_3 & P_4 & 0 & -\frac{1}{T_A} & -\frac{K_A}{T_A} \\
0 & 0 & 0 & 0 & 0 & 0 & 0 & -\frac{K_f K_E}{T_f T_E} & \frac{K_f}{T_f T_e} & -\frac{1}{T_f}
\end{bmatrix}$$

$$b^T = \begin{bmatrix} 0 & 0 & 0 & 0 & 0 & 0 & 0 & 0 & \frac{K_A}{T_A} & 0 \end{bmatrix}$$

$$T_1 = (X_{mq} - X_{md})i_d - X_{md}i_{fd} \qquad (C.20)$$

$$T_2 = (X_{mq} - X_{md})i_q \qquad (C.21)$$

$$T_3 = X_{mq}i_d \qquad (C.22)$$

$$T_4 = -X_{md}i_q \qquad (C.23)$$

$$T_5 = -X_{md}i_q \qquad (C.24)$$

$$P_1 = -\frac{K_A}{T_A}\left(\frac{v_d}{v_t}X_t + \frac{v_q}{v_t}r_t\right) \qquad (C.25)$$

$$P_2 = -\frac{K_A}{T_A}\left(\frac{v_d}{v_t}r_t - \frac{v_q}{V_t}X_t\right) \qquad (C.26)$$

$$P_3 = -\frac{K_A}{T_A}\left(\frac{v_d}{v_t}X_t i_q - \frac{v_q}{V_t}X_t i_d\right) \qquad (C.27)$$

$$P_4 = -\frac{K_A}{T_A}\left[\frac{v_d}{v_t}(-V_B\cos\delta_r) + \frac{v_q}{V_t}(-V_B\sin\delta_r)\right] \qquad (C.28)$$

b) Algebraic Node equations of the form I = YV:

For this network representation the formulation for building up the 'A' matrix is similar to that given in Chapter 2, but with the equations corresponding with the network representation. The transformation matrix to refer individual machine quantities to the network is:

$$\begin{bmatrix} v_q \\ v_d \end{bmatrix} = \begin{bmatrix} \cos \delta_r & \text{sen } \delta_r \\ -\text{sen } \delta_r & \cos \delta_r \end{bmatrix} \begin{bmatrix} V_D \\ V_Q \end{bmatrix} \qquad (C.29)$$

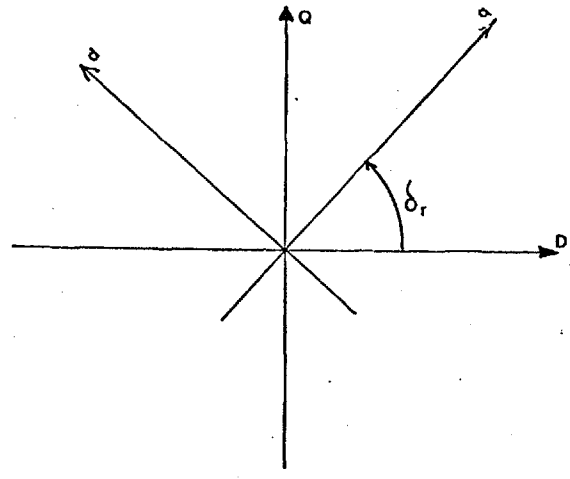

Figure C.1: Machine (d,q) and reference (D.Q) frames.

Applying this transformation to the nodal admittance matrix equation (I = YV) of the network representation as Alden and Zein El-Din[29], the linearized system equations in the matrix form of equation (C.30) are obtained, ready to form the characteristic A matrix and the control matrix, b.

c) Algebraic representation by Newton-Raphson:

The power equations are as in Chapter 2 including the input b matrix as is shown in equation (C.31).

[K] matrix when network is represented by algebraic node equations of the form I = YV.

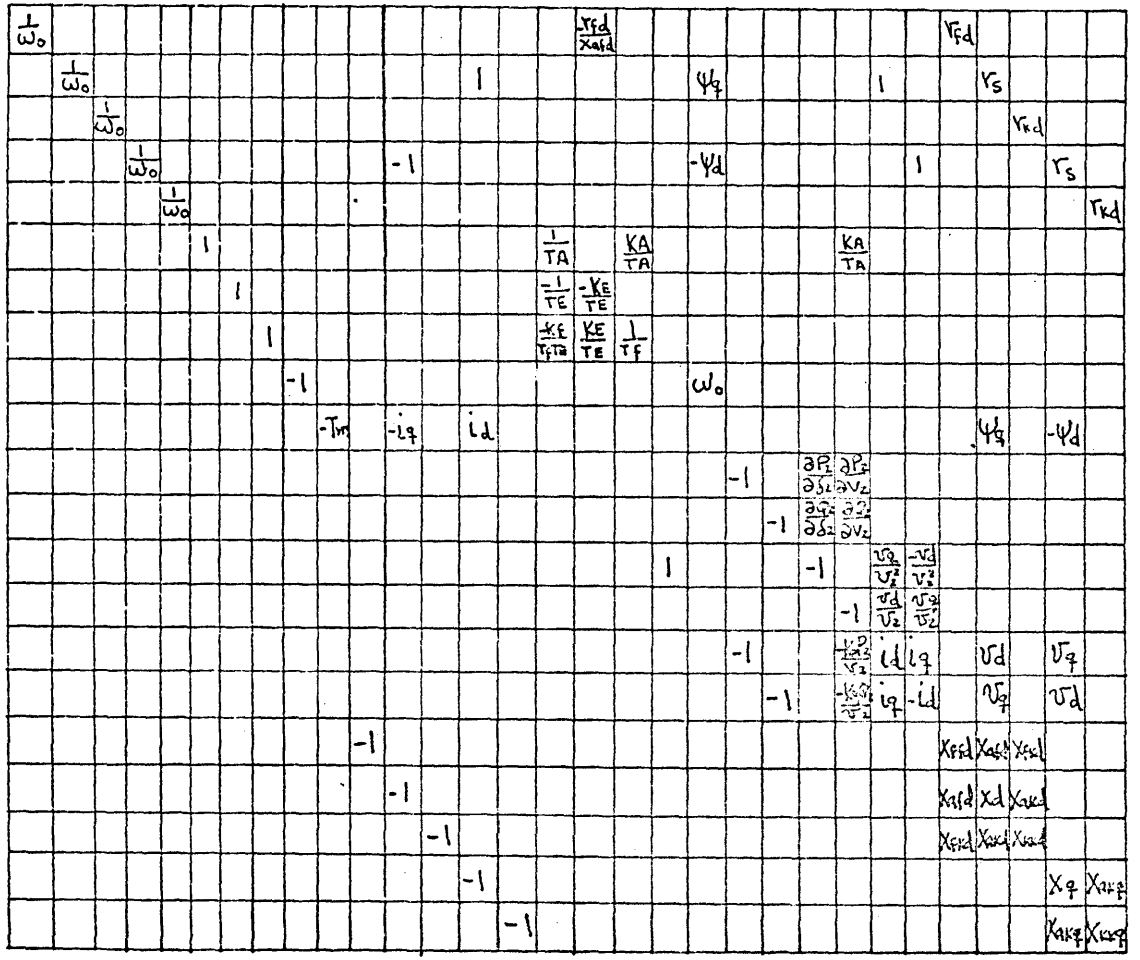

[K] matrix equation when network is represented by Newton-Raphson power equations.